

自旋量子精密测量及其应用

彭新华

中国科学技术大学近代物理系

2025年12月4日

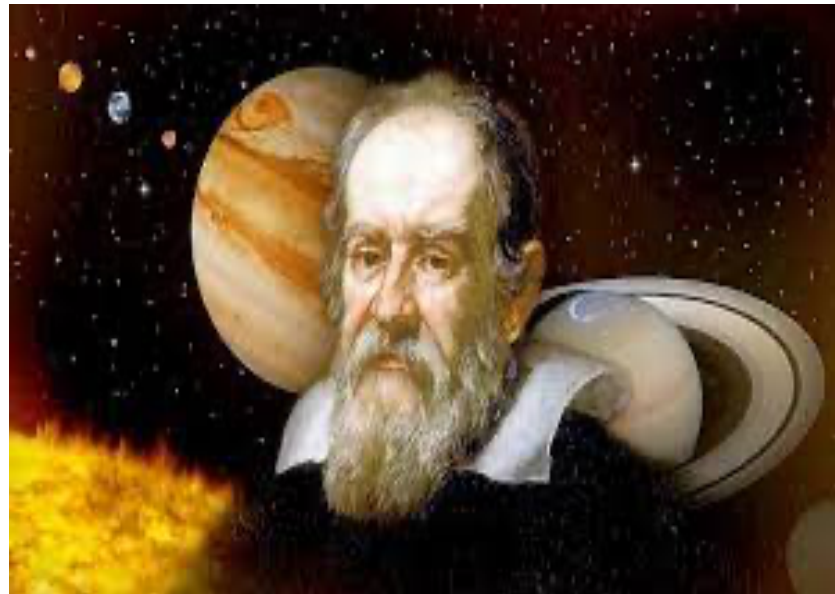


(1) 为什么需要测量极弱磁场？

(2) 如何实现高精度的极弱磁场测量？

(3) 有什么前沿科学应用？

测量是科学发展的第一推动力

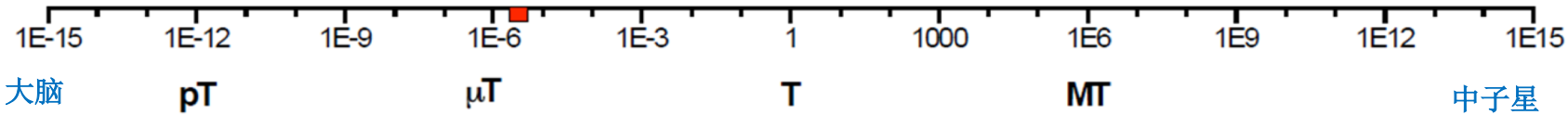


"测量是科学的眼睛和手段"
- 伽利略



"科学是从测量开始的"
- 门捷列夫

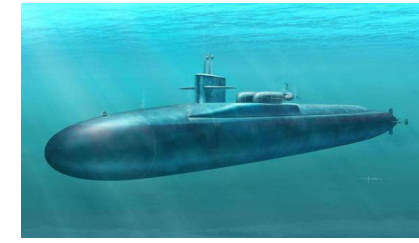
磁是普遍存在的自然属性



地磁场



飞行器磁信号



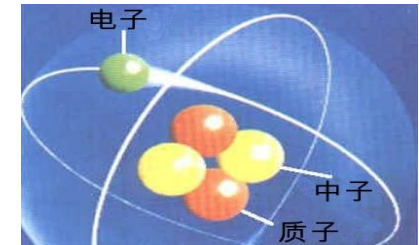
水下航行器磁信号



磁性材料



生物磁信号

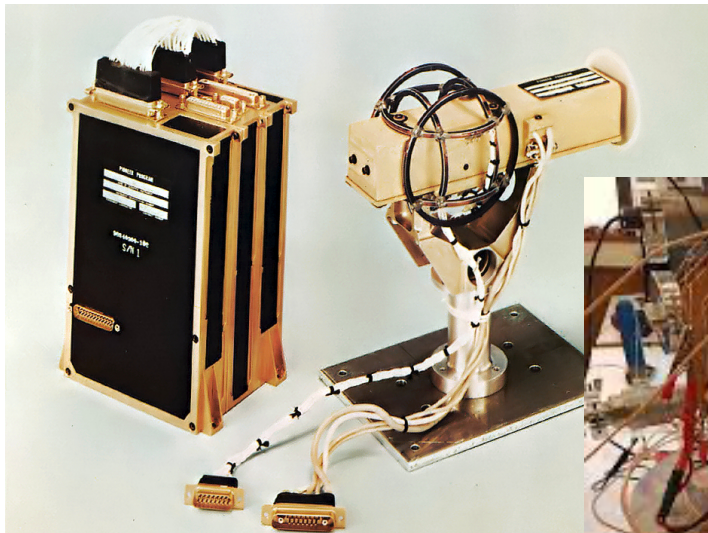


基本粒子磁矩

从基本粒子到宏观宇宙天体，磁场与磁现象无处不在

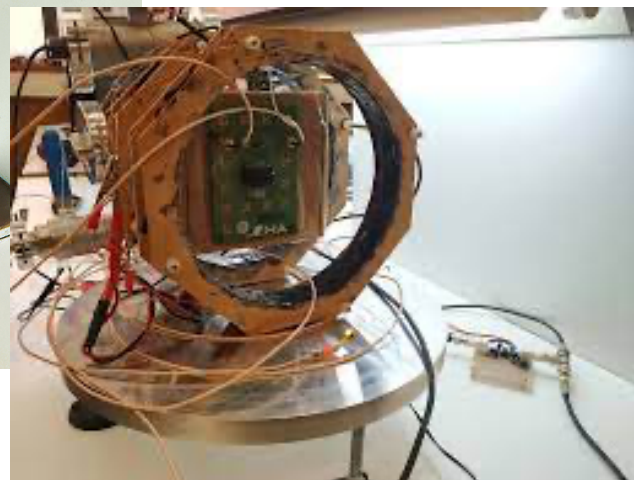
基于经典物理原理的磁力计

霍尔效应磁力计



精度 : $\mu\text{T}-\text{mT}$

洛伦兹力磁力计



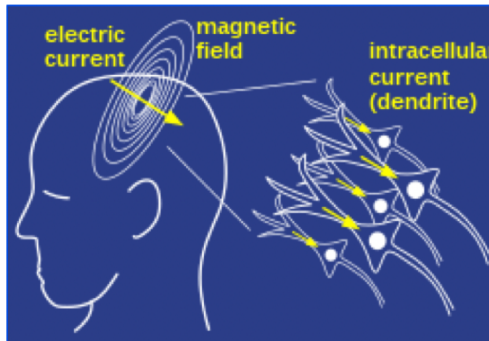
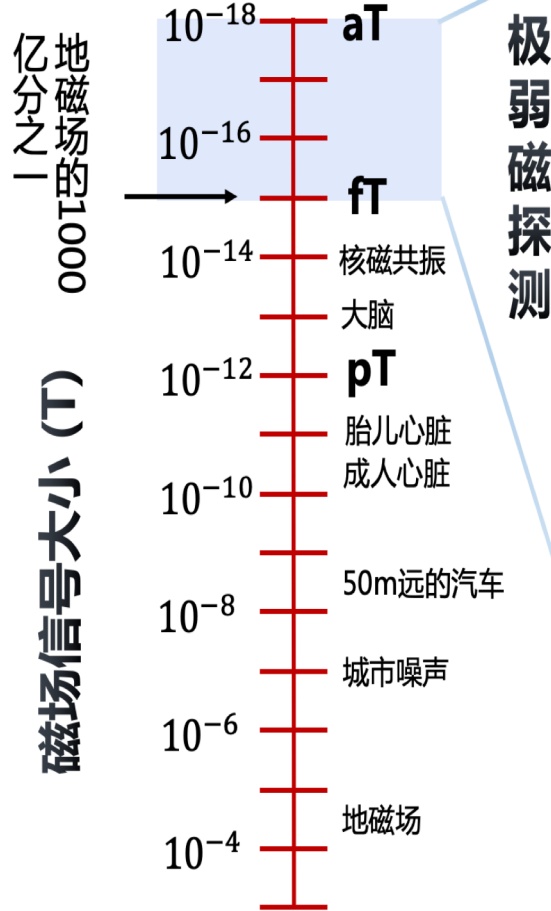
0.1-1 μT

磁通门磁力计



1 nT

极弱磁场探测具有重要科学意义



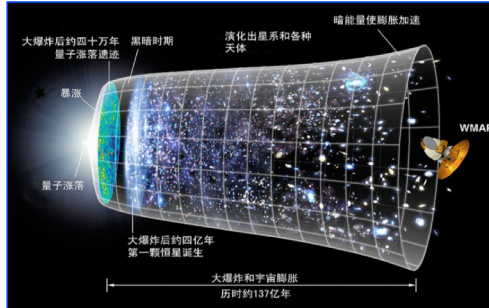
生物医学

心磁、脑磁、脑科学认知



地球和空间物理

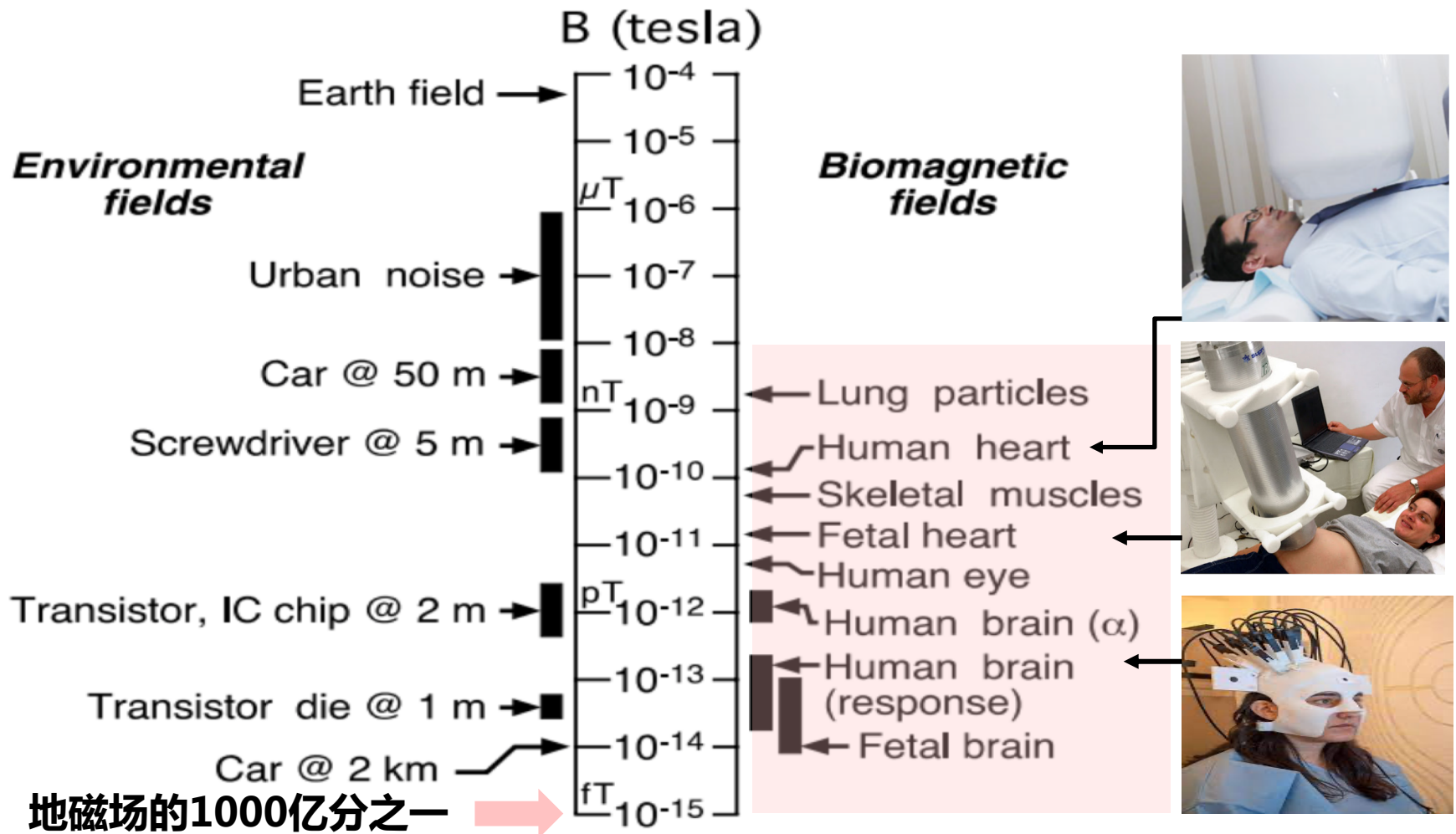
深空深地深海磁、古地磁



前沿基础物理

暗物质、EDM、磁单极子

人体磁场



核磁共振



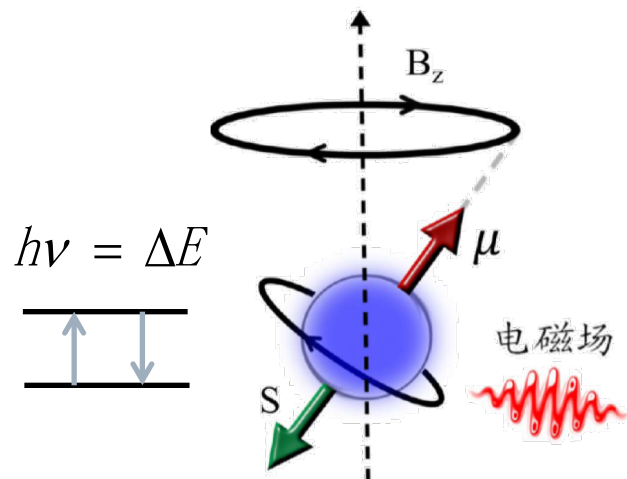
核磁共振成像



核磁共振谱仪

原子分子磁场

核磁共振 —— 最早的自旋精密测量



原理：原子核自旋处于外磁场中，能够吸收和放出对应频率的电磁辐射，发生磁共振现象

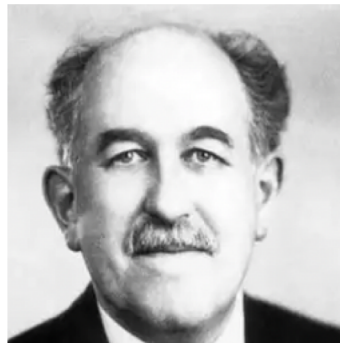
$$\text{Larmor进动} \quad \omega = \gamma B$$

Nuclear Magnetic Resonance Spectroscopy:

特点：能够用来准确、快速和无破坏性地获取物质的组成和结构上的信息

- **Nucleus with spin (核自旋)**
- **Magnetic field (磁场)**
- **Resonance perturbation (共振扰动)**

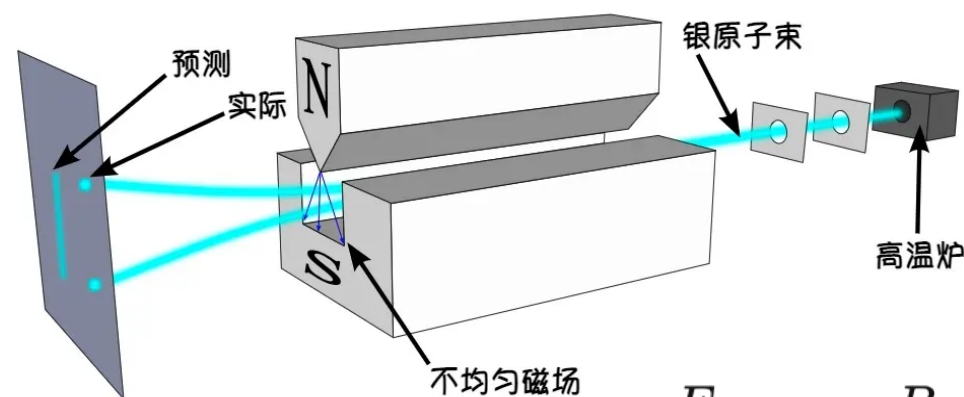
自旋磁共振的发现：斯特恩-格拉赫实验



斯特恩



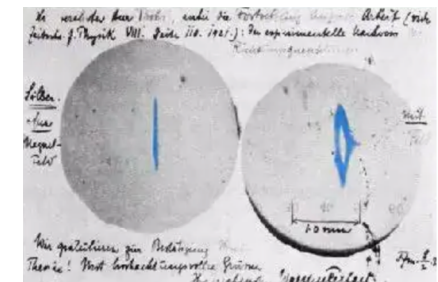
格拉赫



$$E = -\mu \cdot B$$

$$F = -\nabla(E)$$

- ✓ 分子束方法 (1911年 法国科学家丢努瓦耶提出)
- ✓ 索末菲的角动量量子化理论
- ✓ 银原子束实验：检验银原子束受到梯度力的作用效应
- ✓ 1922年首次**证实了角动量的量子化**：一种新的角动量
- ✓ **发现质子磁矩**，比电子磁矩小2000倍

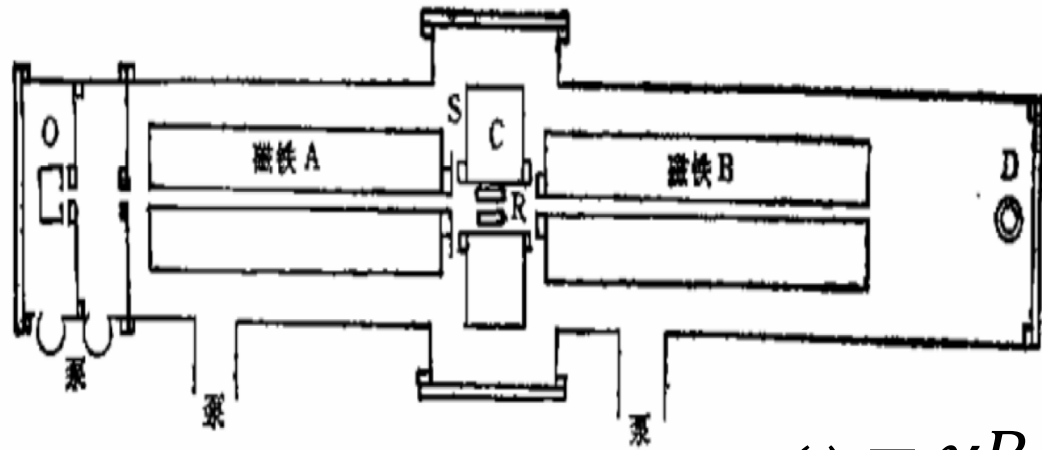


The Stern-Gerlach experiment at 100, Nature 4, 140 (2022)

自旋磁共振的发现：气态分子束共振法



拉比



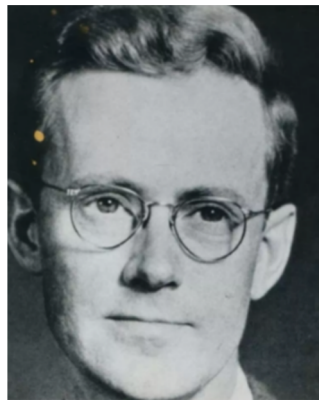
$$\omega = \gamma B$$

- ✓ 认识Stern实验室中会说英语的博士后：R. Fraser和J. B. Taylor
- ✓ 1936年 荷兰物理学家C.J.Gorter提出射频共振吸收，但未成功
- ✓ 斯特恩-格拉赫实验升级版本：引入均匀磁场和射频共振磁场
- ✓ 精确测量80多种原子核的磁矩和自旋（1944年 诺贝尔物理学奖）

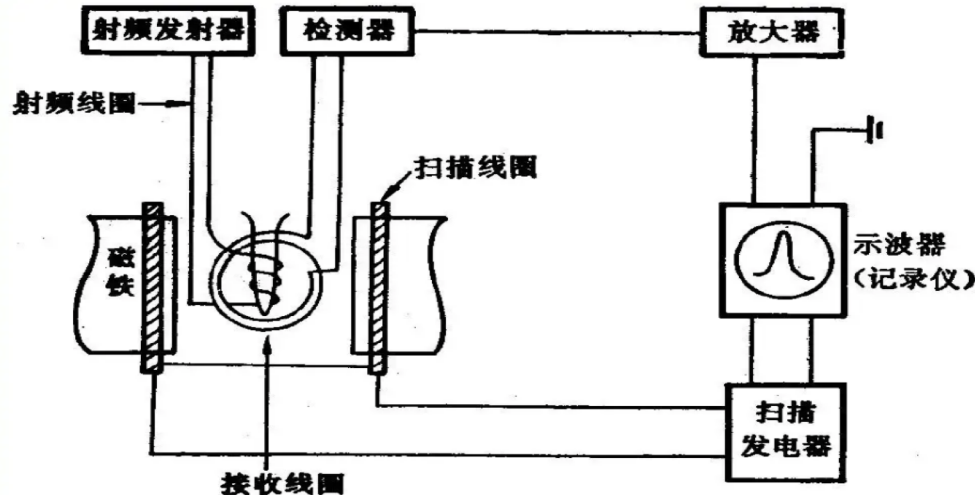
自旋磁共振的发现：凝聚态样品的核磁共振



布洛赫



珀塞尔



- ✓ 发明核磁共振感应法：首次扩展到凝聚态样品 $V = \frac{\partial \Phi}{\partial t} \quad \frac{N_1}{N_2} = e^{-\frac{hv}{kT}} \approx 10^{-6}$
- ✓ 发现更加精细的自旋结构信息：
化学位移、自旋标量耦合、驰豫等
- ✓ 提出半经典演化方程：布洛赫方程
- ✓ 获得1952年诺贝尔奖物理学奖

$$\begin{cases} \frac{dM_X}{dt} = \gamma(M_Y B_0 + M_Z B_1 \sin \omega t) - \frac{M_X}{T_2} \\ \frac{dM_Y}{dt} = \gamma(-M_X B_0 + M_Z B_1 \cos \omega t) - \frac{M_Y}{T_2} \\ \frac{dM_Z}{dt} = \gamma(-M_X B_1 \sin \omega t - M_Y B_1 \cos \omega t) - \frac{M_Z - M_0}{T_1} \end{cases}$$

$$\begin{aligned} \frac{dM_X}{dt} &= \gamma(M_Y B_0 + M_Z B_1 \sin \omega t) - \frac{M_X}{T_2} \\ \frac{dM_Y}{dt} &= \gamma(-M_X B_0 + M_Z B_1 \cos \omega t) - \frac{M_Y}{T_2} \\ \frac{dM_Z}{dt} &= \gamma(-M_X B_1 \sin \omega t - M_Y B_1 \cos \omega t) - \frac{M_Z - M_0}{T_1} \end{aligned}$$

传统磁共振在20世纪取得了巨大成功



Otto Stern
1943, Physics

分子束方法
发现质子磁矩



Isidor Isaac Rabi
1944, Physics

用共振方法记录
原子核的磁特性



E. M. Purcell
1952, Physics

凝聚态样品核磁共振新方法



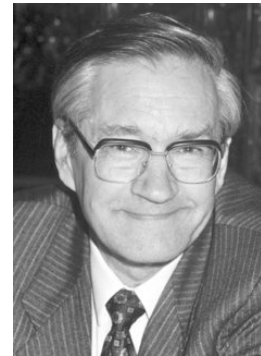
Felix Bloch
1952, Physics



医学磁共振成像

■ 基础科学突破

3次诺贝尔物理学奖



Richard R. Ernst
1991, Chemistry



Kurt Wüthrich
2002, Chemistry



Paul C. Lauterbur
2003, Medicine



Sir Peter Mansfield
2003, Medicine

高分辨率 蛋白质结构

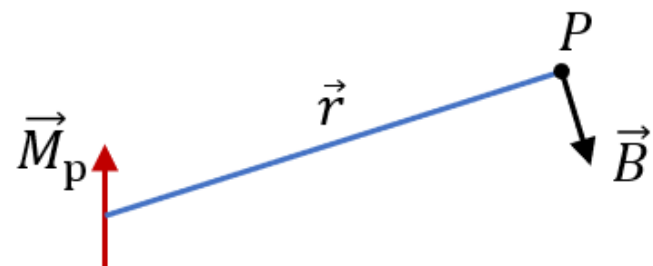
原子核自旋与磁矩

单个质子磁矩

$$\vec{M}_p = g_p \frac{e\hbar}{2m_p} \vec{I}$$

$$\vec{M}_p = 1.41060679736(60) \times 10^{-26} \text{ J} \cdot \text{T}^{-1} (\text{A} \cdot \text{m}^2)$$

在1cm处产生的磁场



$$\begin{aligned} \vec{B} &= -\frac{\mu_0}{4\pi} \frac{\vec{M}_p}{r^3} = -10^{-7} \times \frac{1.41060679736 \times 10^{-26}}{10^{-6}} \\ &= 1.41060679736 \times 10^{-27} \text{ T} \end{aligned}$$

原子核自旋与磁矩

宏观数量 (1mol) 质子产生的磁场

热平衡时，能级粒子布局数服从玻尔兹曼分布

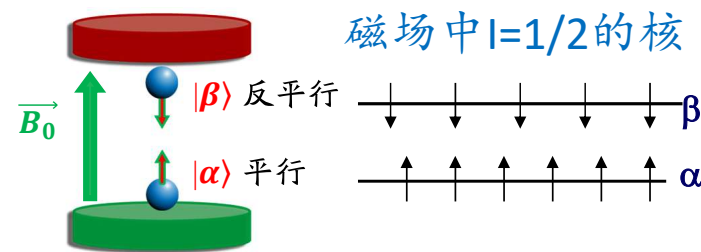
$$N = N_0 \exp\left(-\frac{E}{kT}\right)$$

室温和外磁场 ($\sim 10\text{T}$) 下，

热极化度 $p = \frac{N_+ - N_-}{N_+ + N_-} \sim 10^{-5}$

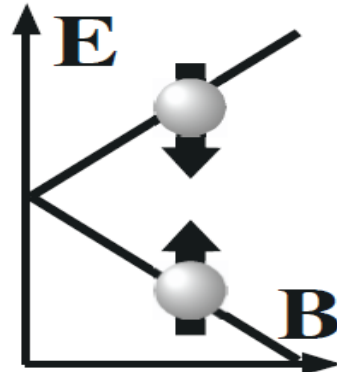
$$N_+ - N_- = 6.02 \times 10^{23} \times 10^{-5} = 6.02 \times 10^{18}$$

在1cm处产生的磁场 $\vec{B} = 8.4919 \times 10^{-9} \text{ T}$



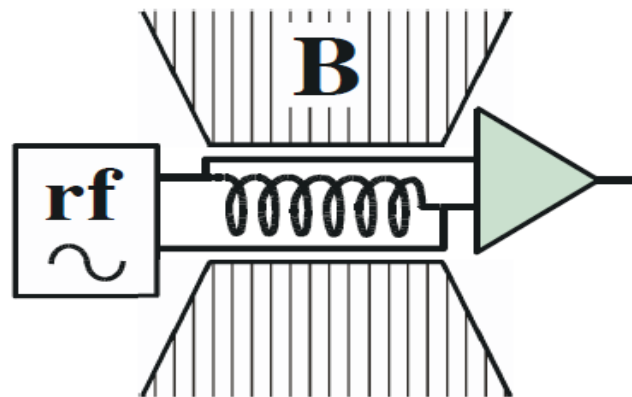
核磁共振实验

Zeeman分裂



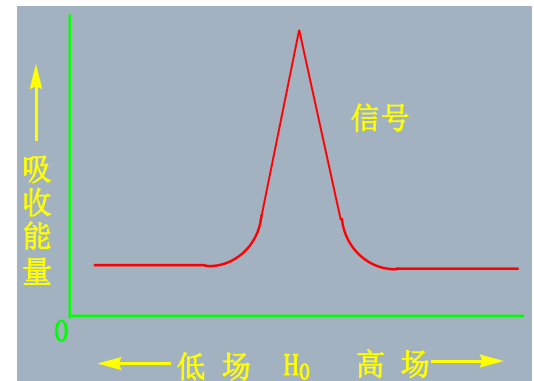
自旋感应磁场

NMR实验基本装置

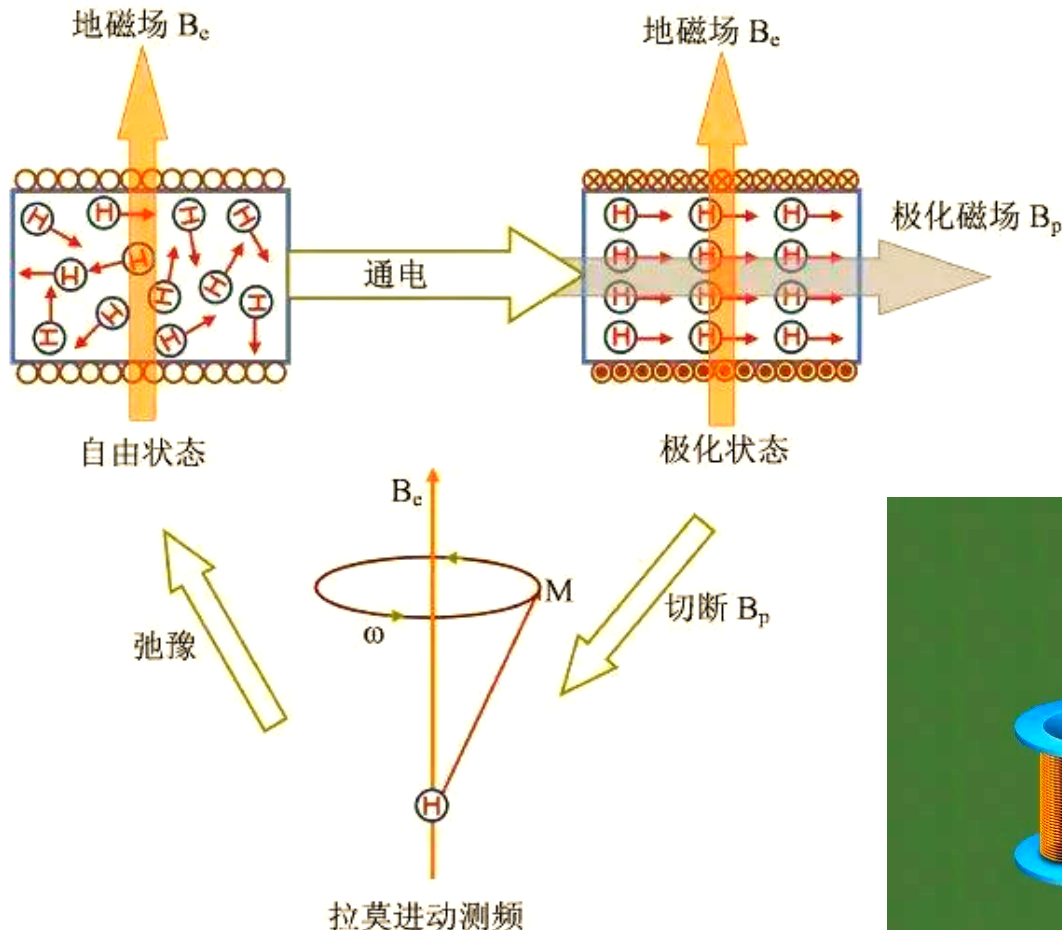


射频脉冲
激发核自
旋体系吸
收能量

探测
(电磁感应理论)



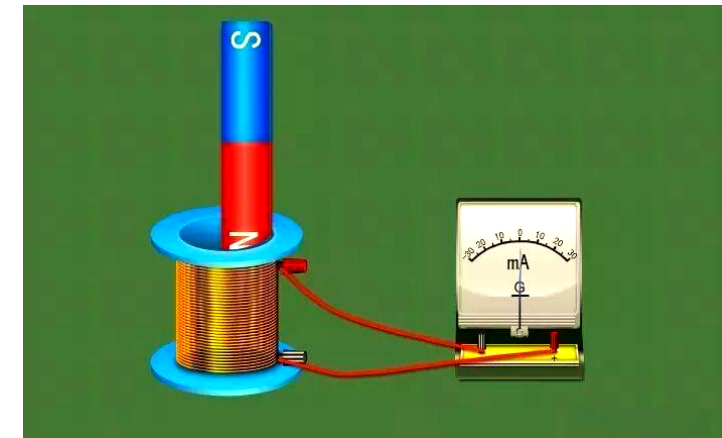
质子磁力计：利用氢核自旋的NMR效应



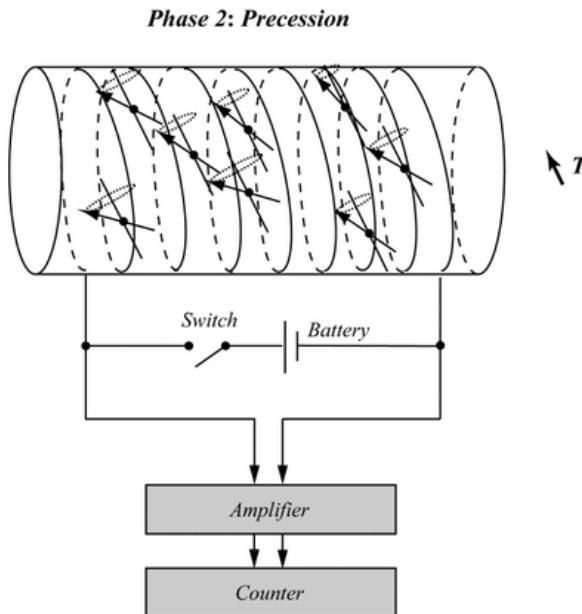
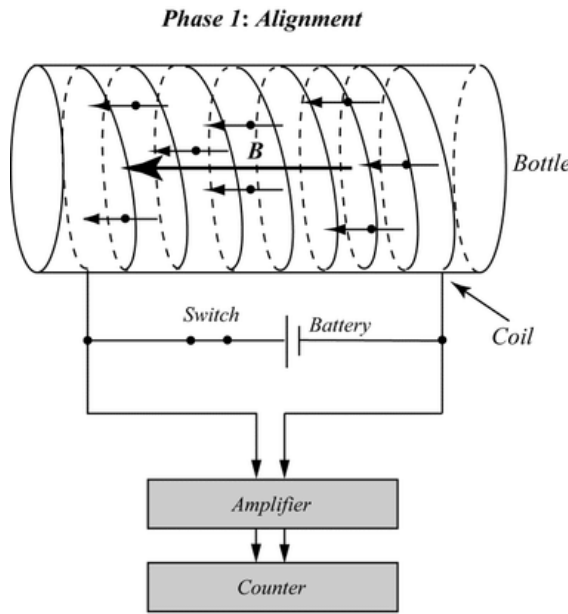
如何测量地磁场？

$$B \sim 50 \text{ uT}$$

$$\omega = \gamma B$$

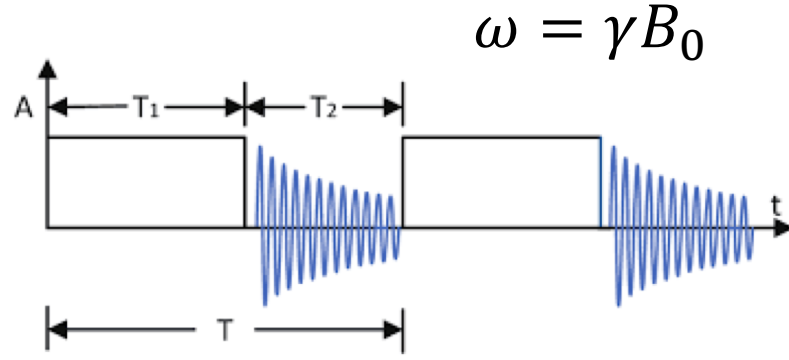


质子磁力计：利用氢核自旋的NMR效应



测量精度可
达0.5nT级别

功耗大，只能
进行间断测量，
灵敏度不高



1955年，美国成功研制出了第一台质子磁力仪

传统核磁共振谱仪

磁共振信号弱，检测灵敏度低

弱信号探测

$$\text{灵敏度} \propto B_0^{3/2}$$

传统核磁：向高磁场方向发展



1T



10T
~ 300万



15T
~ 800万



21T
>1000万

超导磁体：价格昂贵 、笨重、磁场不均匀

核磁共振实验谱仪



at the *National Gateway*
Ultrahigh Field NMR Center

如何提高NMR的灵敏度？

Cutting-Edge Technology

Bruker Ascend 1.2 GHz NMR

28.2 T \$17.8 million

**Only six 1.2GHz NMR
spectrometers in the world**

光磁共振法（双共振现象）

光抽运技术和射频或微波磁共振技术相结合的一种实验技术

- 1947年兰姆和雷瑟福用波谱学方法测定氢原子精细结构的兰姆位移
- 1949年美国的比特（F.Bitter）指出，可把射频波谱技术扩展到原子激发态的研究中。
- 卡斯特勒的想法“利用偏振光对恒定磁场中的气态原子或分子作用，有可能实现激发态塞曼子能级产生选择跃迁”
- 1950年布洛塞尔和比特按照卡斯特勒的思想做成了第一个光磁共振实验

光抽运改变了磁能级上的粒子数分布，同时采取光探测的方法，克服了磁共振信号弱的缺点，把探测灵敏度提高了七、八个数量级。

1966
年诺贝尔物理学奖

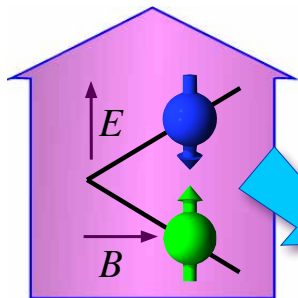


卡斯特勒
“激光之父”

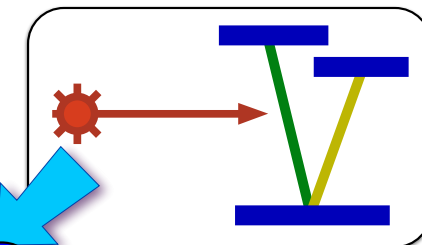


光磁共振法（双共振现象）

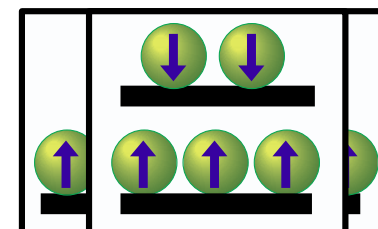
Magnetic resonance



Laser spectroscopy

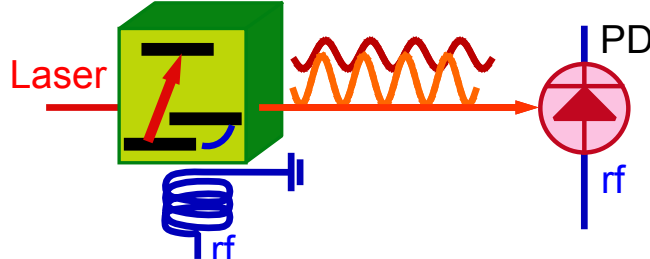


Polarization

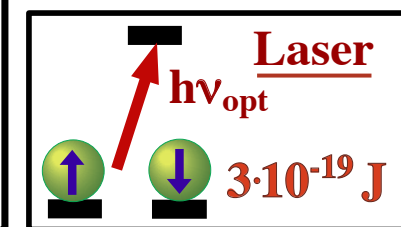
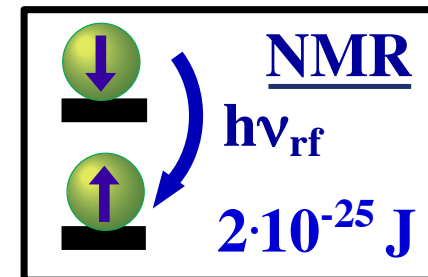


$$\text{NMR: } \frac{n_{\uparrow} - n_{\downarrow}}{n_{\uparrow} + n_{\downarrow}} \approx 10^{-5}$$

$$\text{Optically pumped: } \frac{n_{\uparrow} - n_{\downarrow}}{n_{\uparrow} + n_{\downarrow}} \Rightarrow 1$$



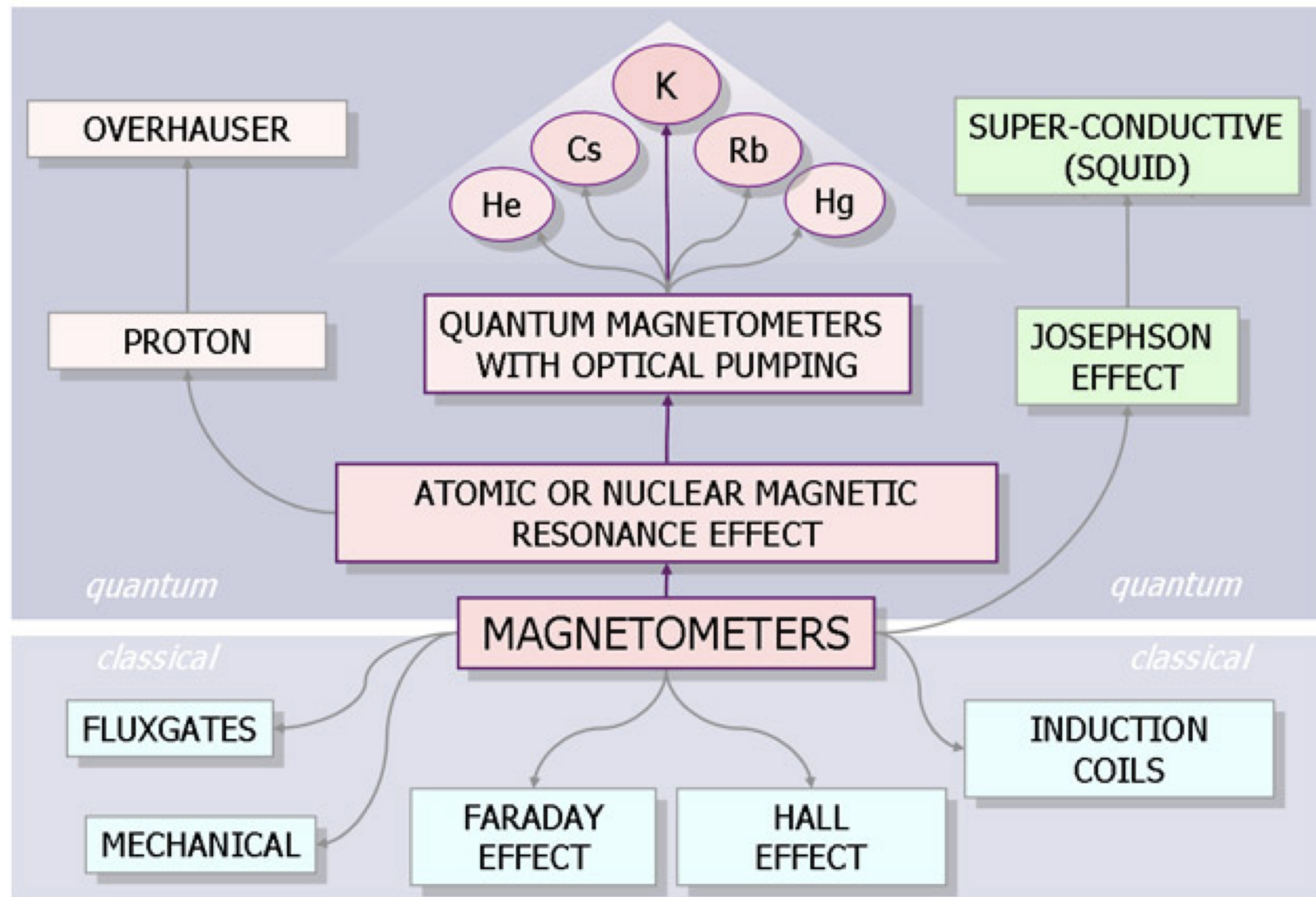
Signal Energy per Spin



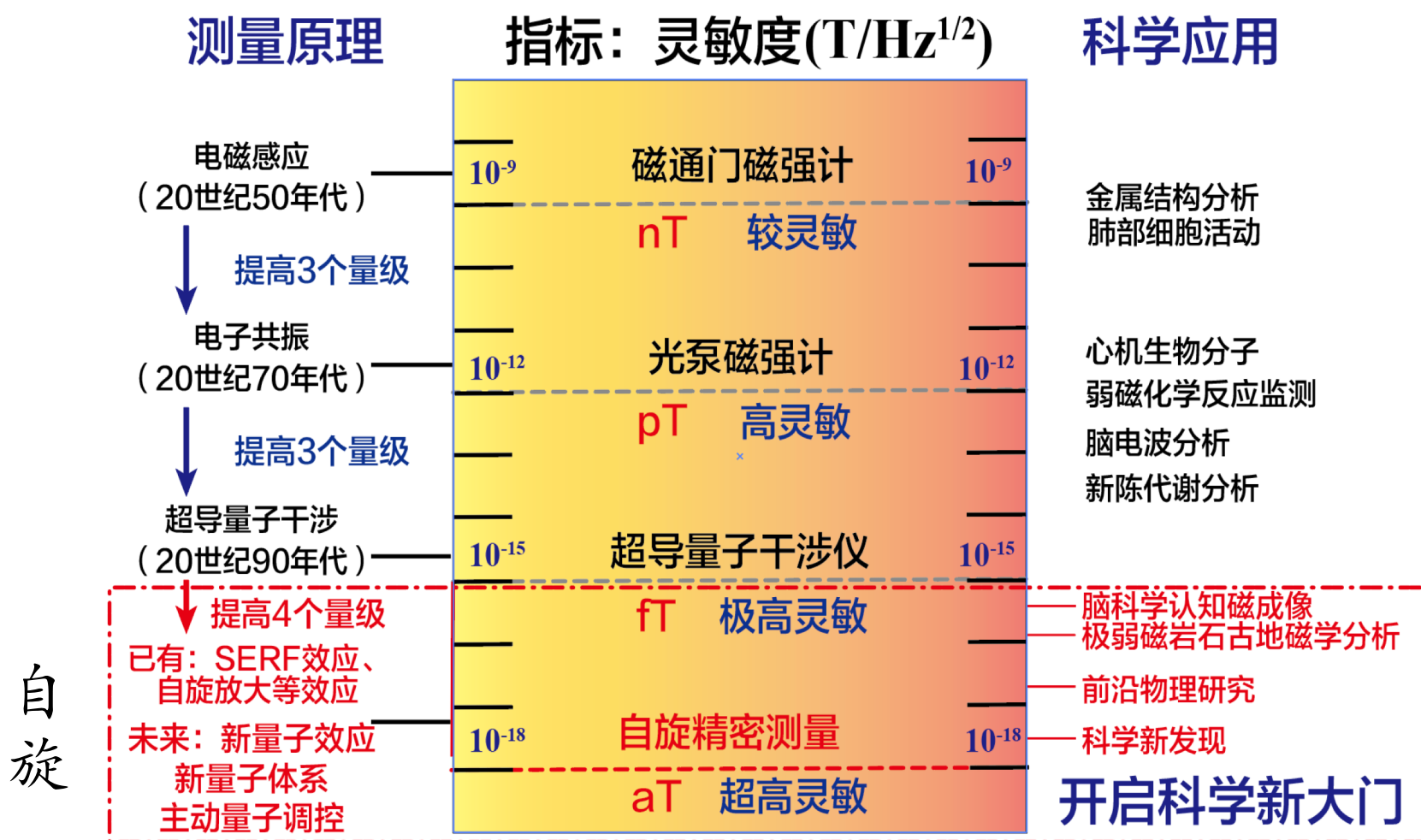
The role of the light

- polarize the spin system
- measure the spin polarization, serving as a detector
- influence the dynamics of the system.

Magnetometers

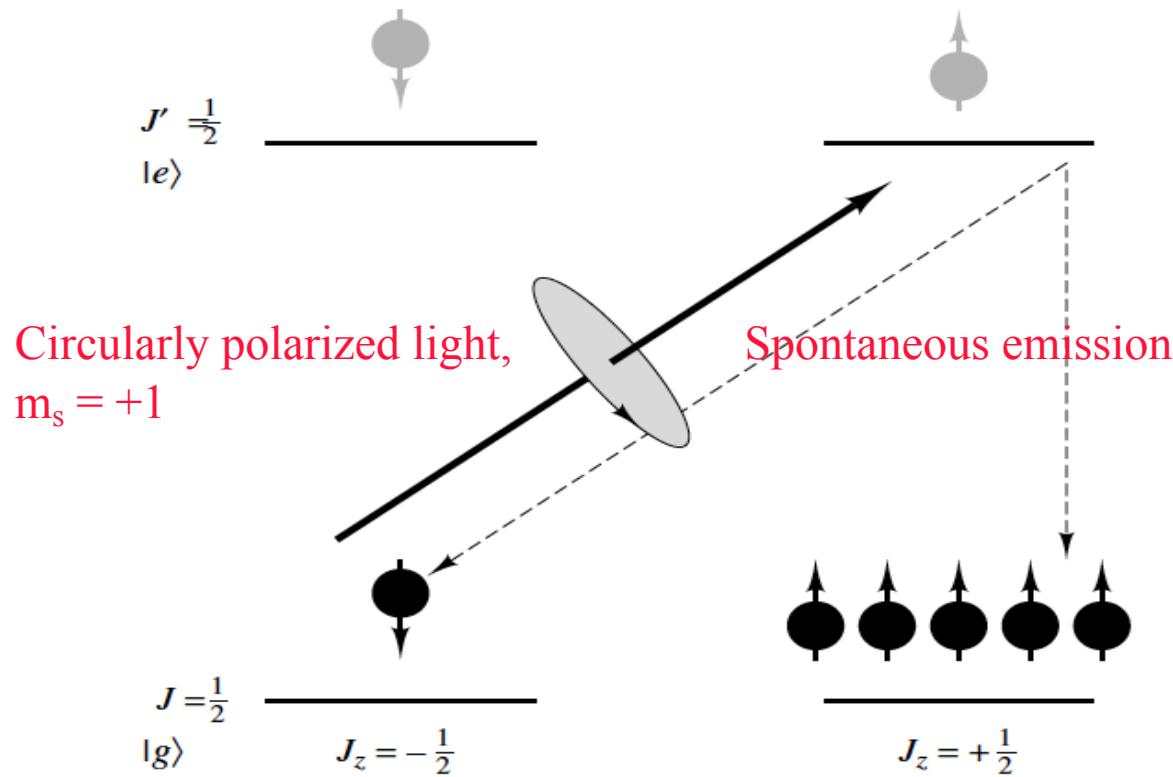


磁场精密测量：从经典到量子技术



Optical Pumping

- First suggested by Kastler [J. Phys. Radium, 1950, 11, 255. Science, 1967, 158, 214]

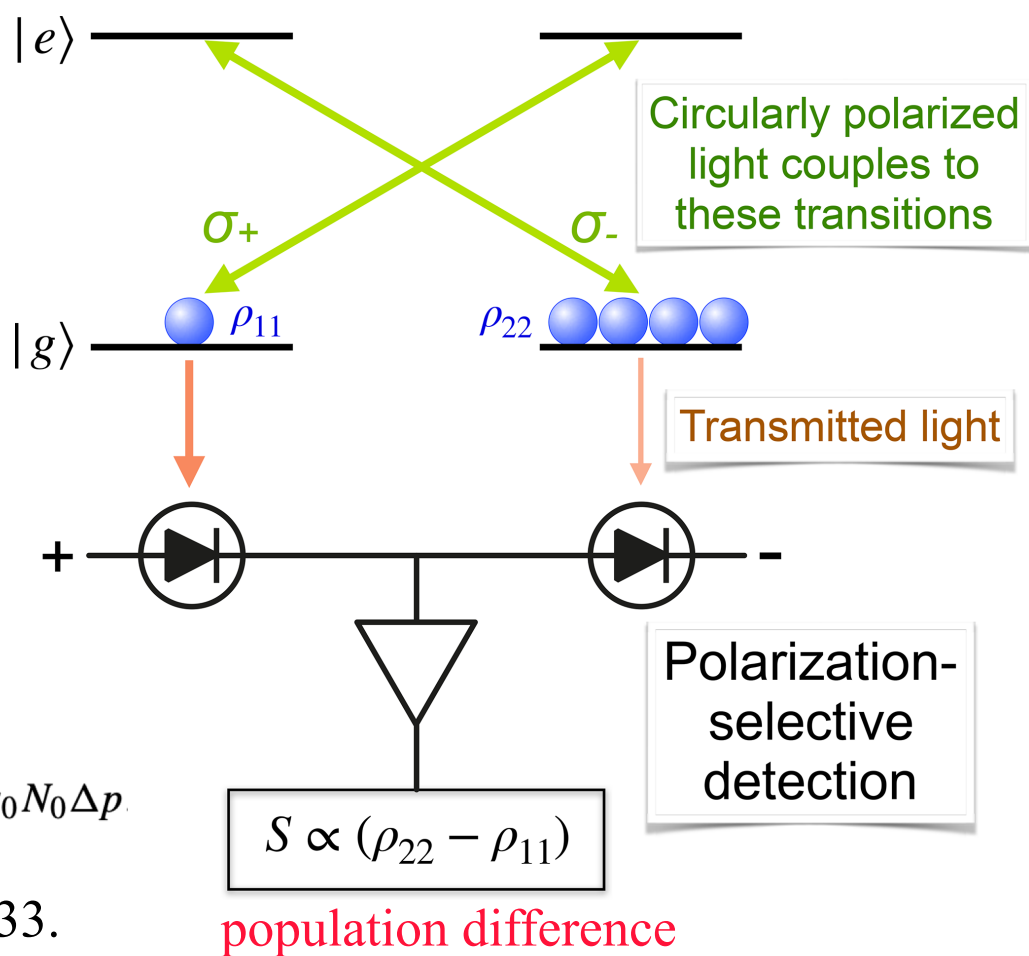


Optical detection: Circular Dichroism

The complement of optical pumping: it transfers spin angular momentum to the photons and polarization-selective detection measures the photon angular momentum.

$$\Delta n(\ell) = -2n_0\ell\alpha_0 N_0(p_+ - p_-) = -2n_0\ell\alpha_0 N_0\Delta p$$

F. Bitter, Phys. Rev., 1949, 76, 833.



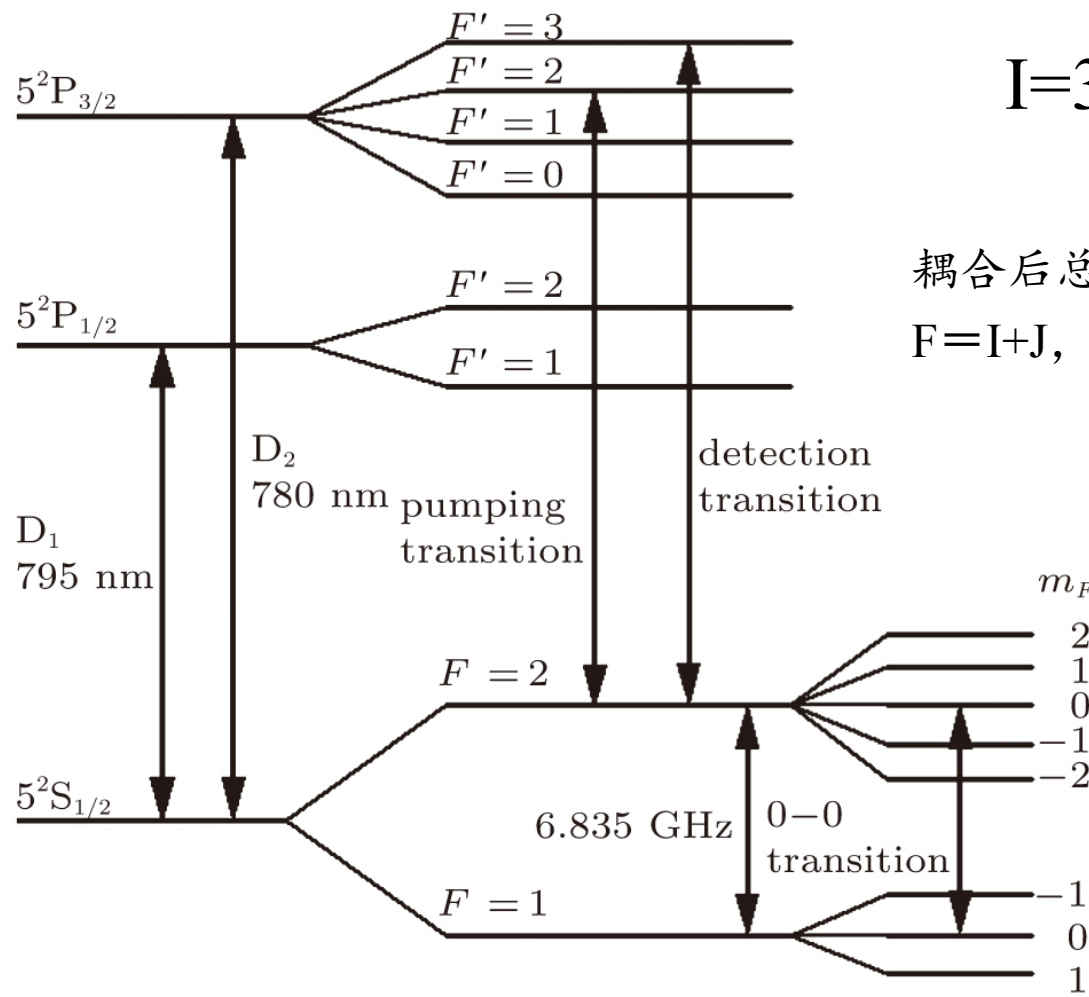
光泵磁共振的典型原子自旋

PERIODIC TABLE OF THE ELEMENTS

The Periodic Table of the Elements is shown with the following annotations:

- Element 26 (Iron):**
 - atomic number → 26
 - chemical symbol → Fe
 - name → Iron
 - atomic mass → 55.845
 - oxidation states (most common): +3, +2
 - STATE OF MATTER: SOLID, GAS, LIQUID
 - radioactive elements (indicated by a small symbol)
- Group 1 (Alkali Metals):** Elements 1 (H), 3 (Li), 13 (Na), 19 (K), 37 (Rb), and 55 (Cs) are highlighted with a red box.
- Group 2 (Alkaline Earth Metals):** Elements 2 (Be), 12 (Mg), 20 (Ca), 38 (Sr), and 56 (Ba) are highlighted with a red box.
- Transition Metals:** Elements 21 (Sc), 22 (Ti), 23 (V), 24 (Cr), 25 (Mn), 26 (Fe), 27 (Co), 28 (Ni), 29 (Cu), 30 (Zn), 31 (Ga), 32 (Ge), 33 (As), 34 (Se), 35 (Br), 36 (Kr), 40 (Zr), 41 (Nb), 42 (Mo), 43 (Tc), 44 (Ru), 45 (Rh), 46 (Pd), 47 (Ag), 48 (Cd), 49 (In), 50 (Sn), 51 (Sb), 52 (Te), 53 (I), 54 (Xe), 72 (Ta), 73 (W), 74 (Re), 75 (Os), 76 (Ir), 77 (Pt), 78 (Au), 79 (Hg), 80 (Tl), 81 (Pb), 82 (Bi), 83 (Po), 84 (At), 85 (Rn), 104 (Rf), 105 (Db), 106 (Sg), 107 (Bh), 108 (Hs), 109 (Mt), 110 (Ds), 111 (Rg), 112 (Cn), 113 (Nh), 114 (Fl), 115 (Mc), 116 (Lv), 117 (Ts), and 118 (Og) are highlighted with a yellow box.
- Lanthanoids:** Elements 57 (La), 58 (Ce), 59 (Pr), 60 (Nd), 61 (Pm), 62 (Sm), 63 (Eu), 64 (Gd), 65 (Tb), 66 (Dy), 67 (Ho), 68 (Er), 69 (Tm), 70 (Yb), and 71 (Lu) are highlighted with an orange box.
- Actinoids:** Elements 89 (Ac), 90 (Th), 91 (Pa), 92 (U), 93 (Np), 94 (Pu), 95 (Am), 96 (Cm), 97 (Bk), 98 (Cf), 99 (Es), 100 (Fm), 101 (Md), 102 (No), and 103 (Lr) are highlighted with a teal box.
- Nonmetals:** Elements 5 (B), 6 (C), 7 (N), 8 (O), 9 (F), 10 (Ne), 14 (Si), 15 (P), 16 (S), 17 (Cl), 18 (Ar), 33 (As), 34 (Se), 35 (Br), 52 (Te), 53 (I), 54 (Xe), 77 (I), 78 (Se), 79 (Br), 80 (Te), 81 (I), 82 (Po), 83 (At), 84 (Rn), 116 (Lv), 117 (Ts), and 118 (Og) are highlighted with a pink box.
- Alkaline Earth Metals:** Elements 3 (Li), 12 (Mg), 20 (Ca), 38 (Sr), and 56 (Ba) are highlighted with a purple box.
- Post-transition Metals:** Elements 13 (Al), 14 (Si), 15 (P), 16 (S), 17 (Cl), 18 (Ar), 32 (Ge), 33 (As), 34 (Se), 35 (Br), 52 (Te), 53 (I), 54 (Xe), 77 (I), 78 (Se), 79 (Br), 80 (Te), 81 (I), 82 (Po), 83 (At), 84 (Rn), 116 (Lv), 117 (Ts), and 118 (Og) are highlighted with a green box.
- Metalloids:** Elements 5 (B), 13 (Al), 14 (Si), 32 (Ge), 33 (As), 34 (Se), 52 (Te), 53 (I), 77 (I), 78 (Se), 79 (Br), 80 (Te), 81 (I), 82 (Po), 83 (At), 84 (Rn), 116 (Lv), 117 (Ts), and 118 (Og) are highlighted with a red box.
- Halogens:** Elements 7 (N), 8 (O), 9 (F), 10 (Ne), 14 (Si), 15 (P), 16 (S), 17 (Cl), 18 (Ar), 33 (As), 34 (Se), 35 (Br), 52 (Te), 53 (I), 54 (Xe), 77 (I), 78 (Se), 79 (Br), 80 (Te), 81 (I), 82 (Po), 83 (At), 84 (Rn), 116 (Lv), 117 (Ts), and 118 (Og) are highlighted with a cyan box.
- Noble Gases:** Elements 2 (He), 10 (Ne), 18 (Ar), 36 (Kr), 54 (Xe), 76 (Rn), and 86 (Og) are highlighted with a purple box.
- Lanthanoids:** Elements 57 (La), 58 (Ce), 59 (Pr), 60 (Nd), 61 (Pm), 62 (Sm), 63 (Eu), 64 (Gd), 65 (Tb), 66 (Dy), 67 (Ho), 68 (Er), 69 (Tm), 70 (Yb), and 71 (Lu) are highlighted with an orange box.
- Actinoids:** Elements 89 (Ac), 90 (Th), 91 (Pa), 92 (U), 93 (Np), 94 (Pu), 95 (Am), 96 (Cm), 97 (Bk), 98 (Cf), 99 (Es), 100 (Fm), 101 (Md), 102 (No), and 103 (Lr) are highlighted with a teal box.

碱金属元素：Na, K, Rb, Cs



I=3/2 (⁸⁷Rb)

耦合后总量子数

$$F = I + J, \dots, |I - J|$$

磁量子数

$$m_F = F, \ F-1, \ \dots, \ -F$$

光抽运效应

跃迁选择定则为

$$\Delta L = \pm 1,$$

$$\Delta F = 0, \pm 1,$$

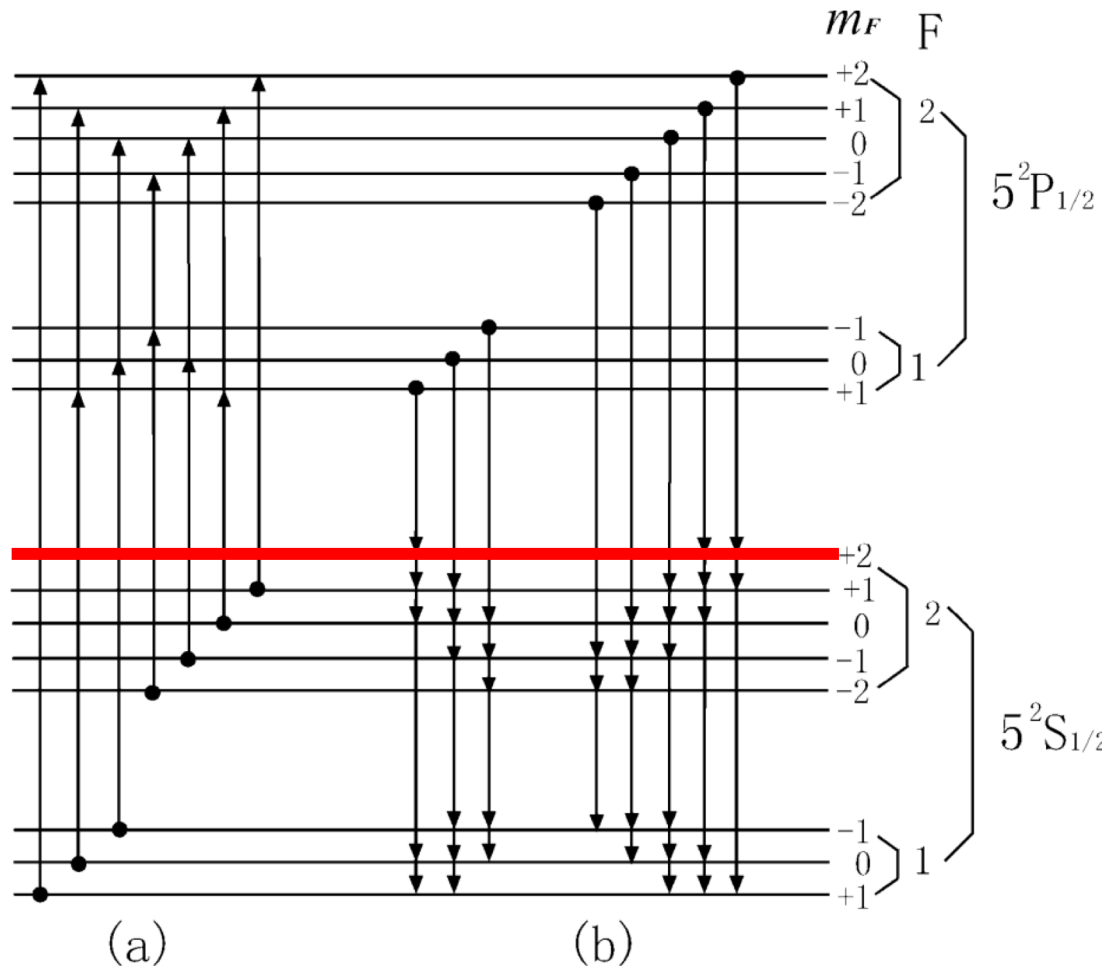
$$\Delta m_F = +1.$$

大量粒子被“抽运”到
 $m_F = +2$ 的子能级上

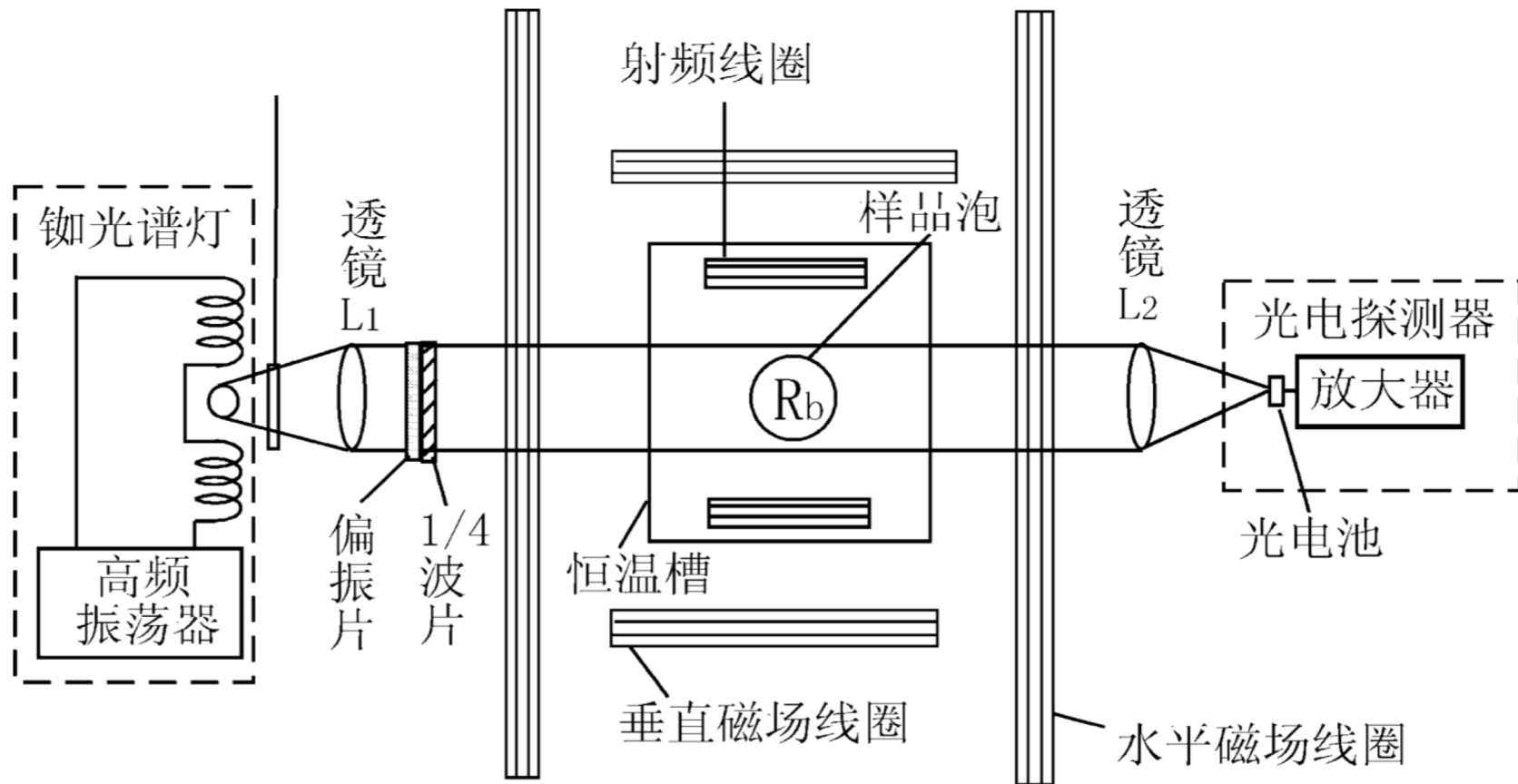
实现粒子分布的偏极化

(a) ^{87}Rb 基态粒子吸收 $D_1\sigma^+$
光子跃迁到激发态的过程

(b) ^{87}Rb 激发态粒子通过自发
辐射返回基态各子能级



光泵磁共振



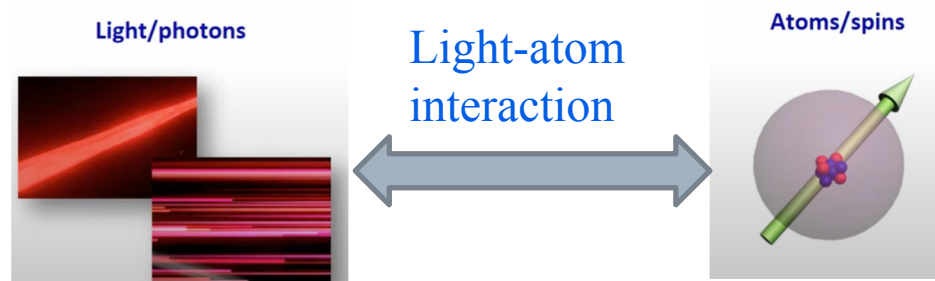
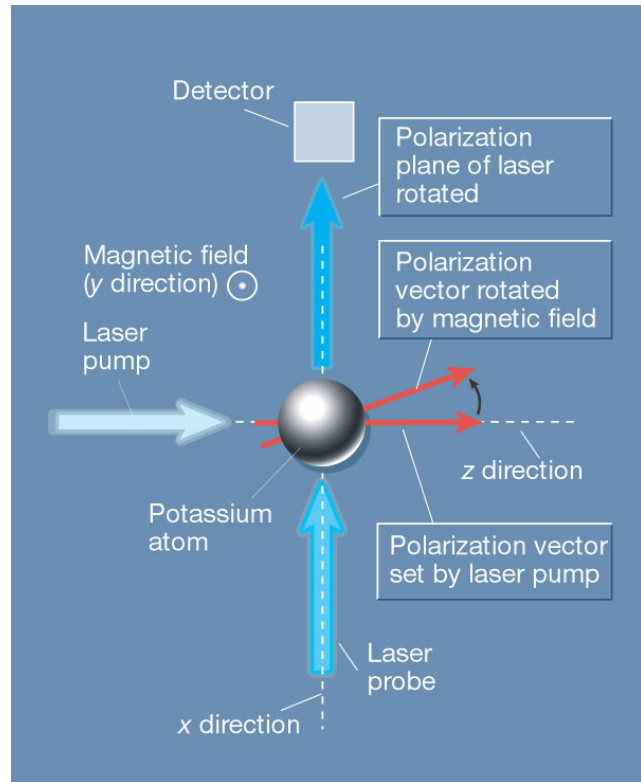
原子自旋磁力计

基本原理

Vapor cell: Alkali metal atoms

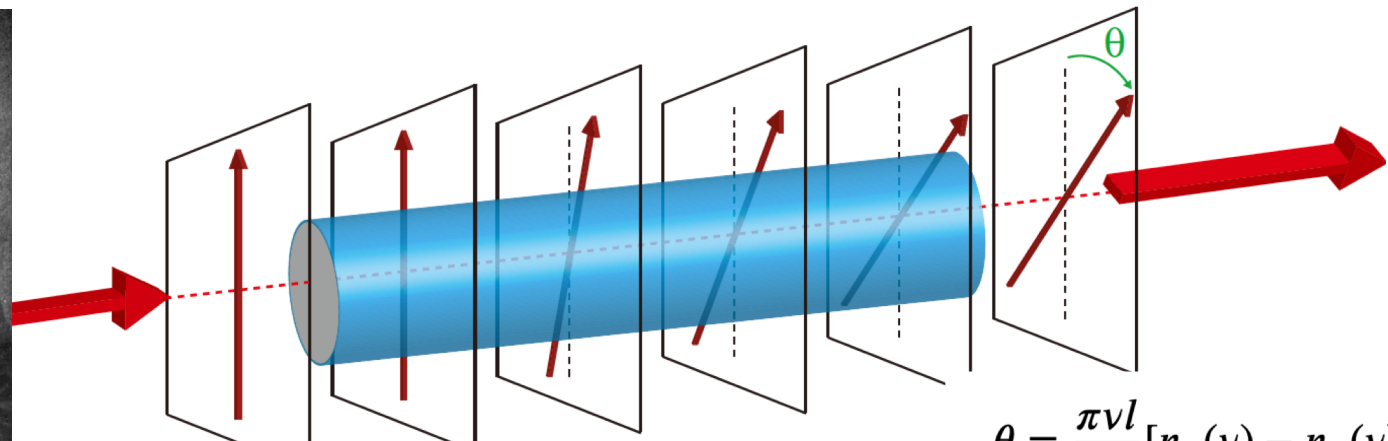
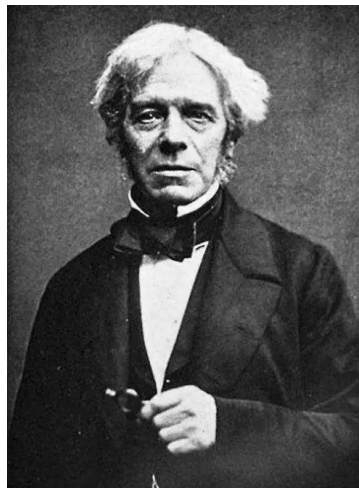
Figure from: D.Budker. : A new spin on magnetometry
Nature (News&Views) 422, 574 - 575 (2003)

- Optical pumping
- Spin precession
- Probe (light intensity/light polarization)



用光来测量原子角动量对磁场的响应

激光探测—法拉第 (Faraday) 效应



$$\theta = \frac{\pi v l}{c} [n_+(v) - n_-(v)],$$

$$\theta = \frac{\pi}{2} r_e c l n P \left[-f_{D1} \mathcal{D}(\nu - \nu_{D1}) + \frac{1}{2} f_{D2} \mathcal{D}(\nu - \nu_{D2}) \right]$$

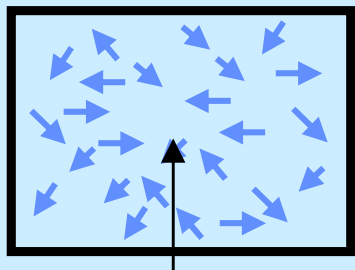
其中 $\mathcal{D}(\nu - \nu_0) = \frac{(\nu - \nu_0)/\pi}{(\nu - \nu_0)^2 + (\Gamma/2)^2}$. $f_{D2} \approx 2f_{D1}$

P 为沿着探测光传播方向的原子自旋极化分量

l 为光穿过原子气体室的有效长度 r_e 为经典电子半径

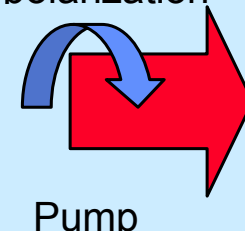
磁场测量基本过程

Alkali Vapor Cell

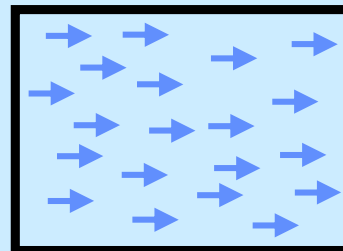


Randomly oriented
atomic spins

Circular
polarization

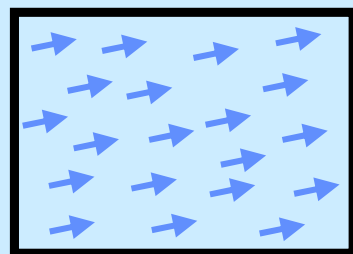
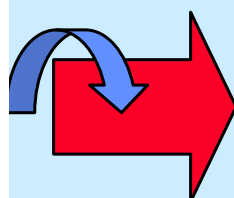


Optical pumping



Spins align with the
pump beam

Apply Small Magnetic Field

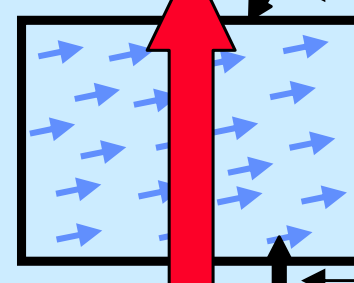
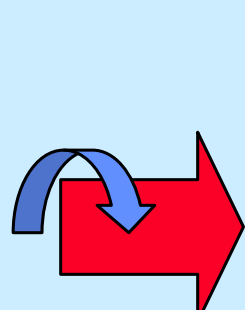


Spins precess in magnetic field

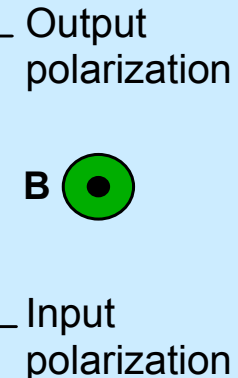


Out of
plane

Detect with probe beam



Probe beam



Out of
plane

Oriented spins rotate the polarization
(Faraday rotation)

弛豫过程

系统由非热平衡分布状态趋向于热平衡分布状态的过程称为弛豫过程。

- (1) Rb 原子与容器壁的碰撞。导致子能级之间的跃迁使原子恢复到热平衡分布，失去光抽运所造成的偏极化。
- (2) Rb 原子之间的碰撞。导致自旋—自旋交换弛豫，使粒子的磁矩发生改从而失去偏极化。
- (3) Rb 原子与缓冲气体之间的碰撞。将大大减少 Rb 原子与器壁碰撞的机会，从而保持了原子高度的偏极化。

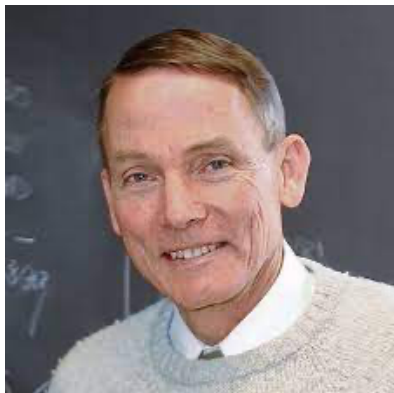
原子碰撞效应

$$R_{se} = n \sigma_{se} \bar{v}$$

K-K spin exchange

K- ^3He spin exchange

$$R_{se} = n \sigma_{se} \bar{v}$$



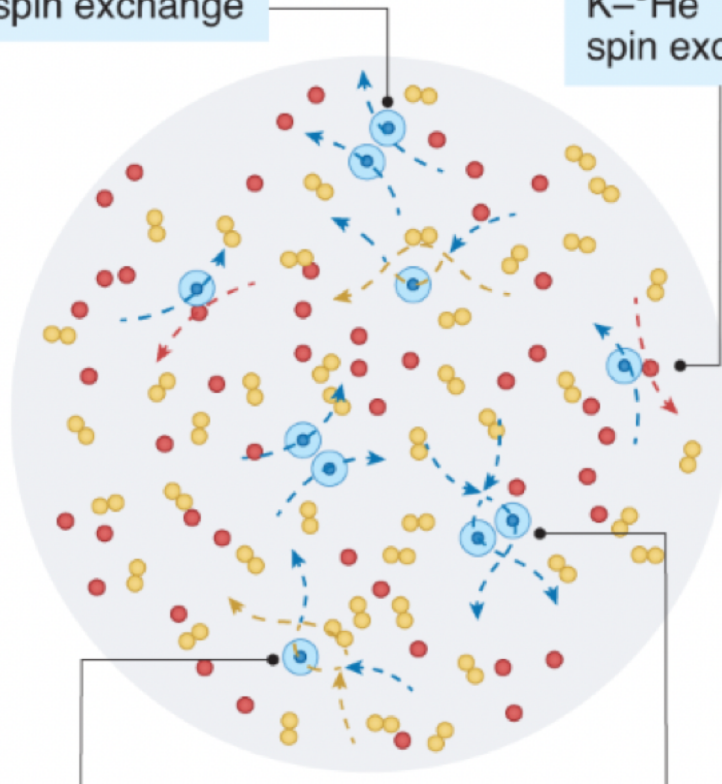
W. Happer

$$R_{sd} = n \sigma_{sd} \bar{v}$$

K-N₂ spin destruction

K-K spin destruction

$$R_{sd} = n \sigma_{sd} \bar{v}$$

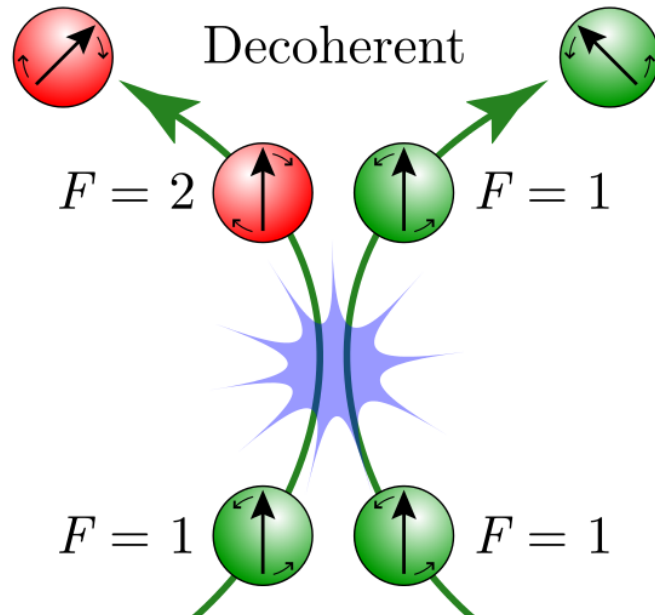


Wall collision:

$$R_{wall} = D \frac{P_0}{P_{\text{He}}(T)} \left(\frac{\pi}{r}\right)^2 q(P)$$

W. Happer and H. Tang, PRL **31**, 273 (1973); W. Happer and A. Tam, PRA **16**, 1877 (1977);

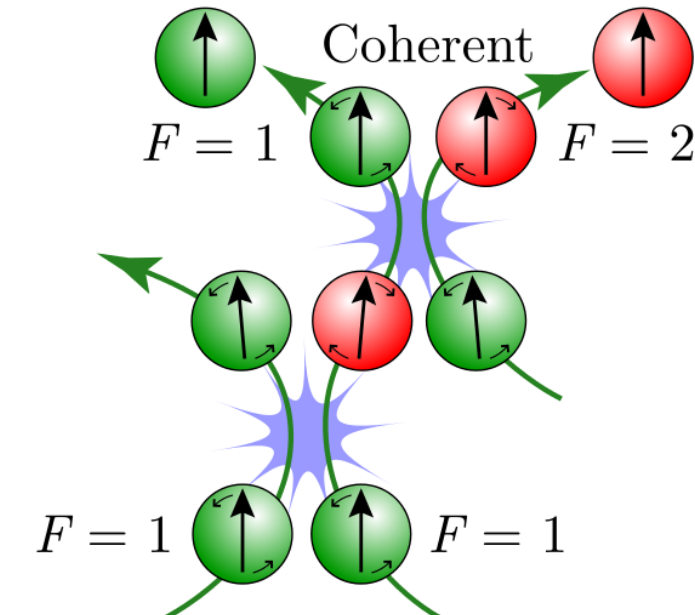
Spin exchange relaxation



$$R_{se} = \frac{1}{2\pi T_{se}} \left(\frac{2I(2I-1)}{3(2I+1)^2} \right)$$

preserves total angular momentum but changes the hyperfine state, causing the atoms to precess in opposite directions and decohere.

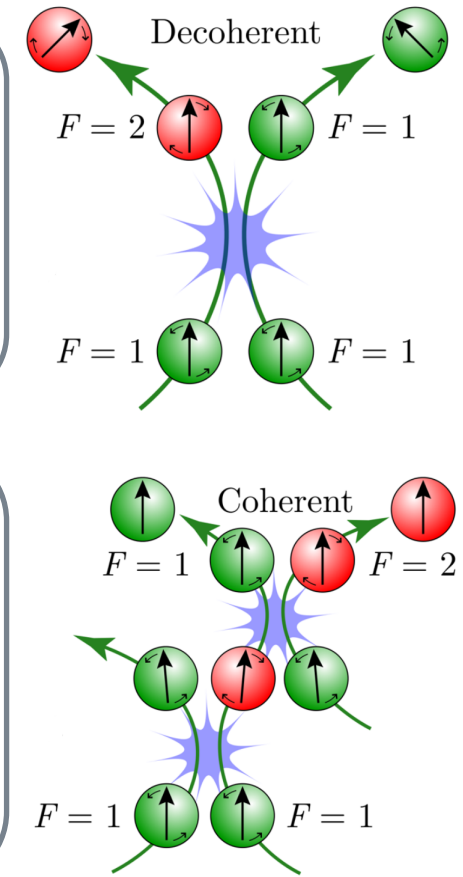
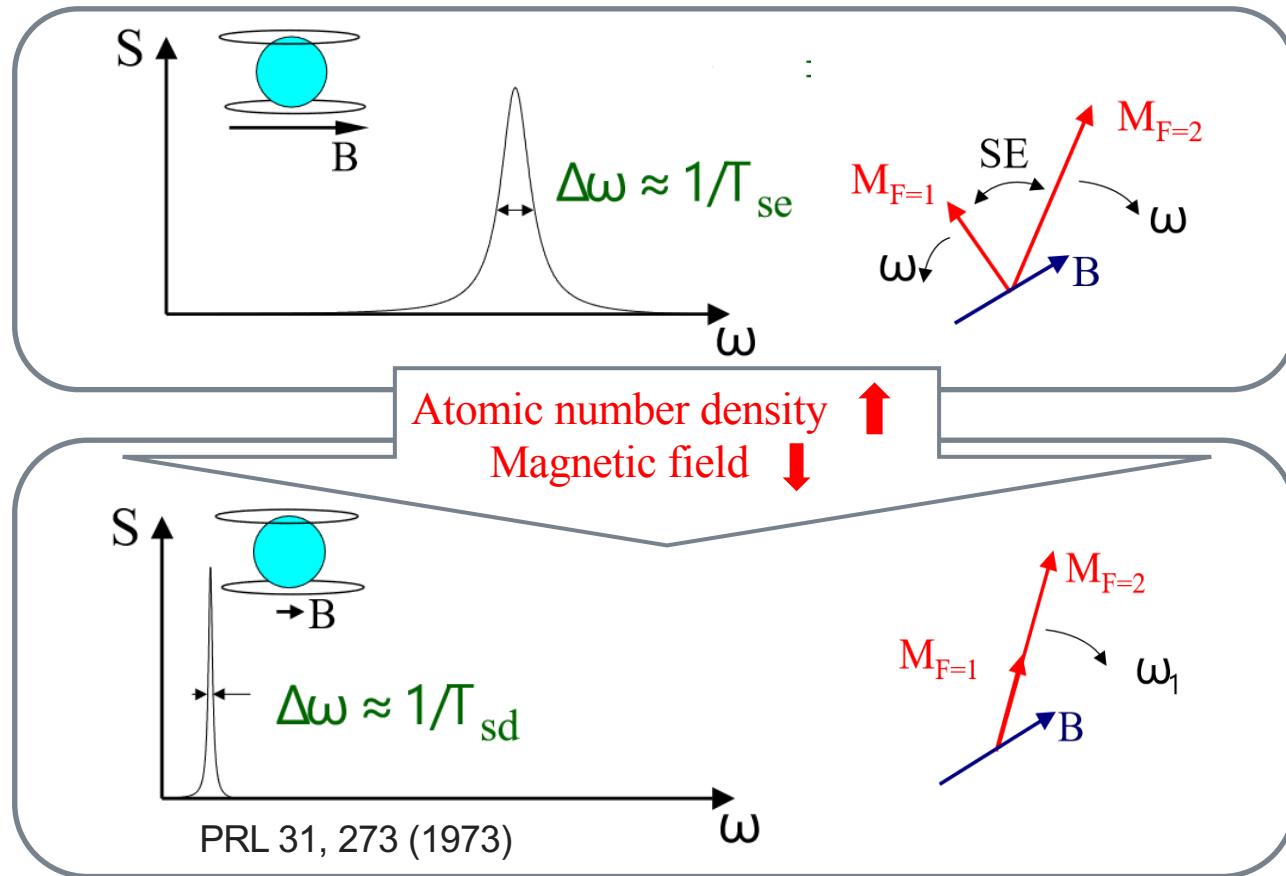
Q is the "slowing-down" constant



$$R_{se} = \frac{\gamma_e^2 B^2 T_{se}}{2\pi} \frac{1}{2} \left(1 - \frac{(2I+1)^2}{Q^2} \right)$$

experience two spin-exchange collisions in rapid succession, causing the atoms to precess in opposite directions only slightly before a second spin-exchange collision returns the atoms to the original hyperfine state.

无自旋交换弛豫效应 (SERF 效应)



1973 年, Happer 等发现, 1977 年推导出这一现象的理论解释

布洛赫 (Bloch) 方程

光与原子相互作用的精确描述需要用到密度矩阵，但是近似可以用一个简单的布洛赫(Bloch)方程来描述：

$$\frac{d\mathbf{P}}{dt} = \frac{1}{q} [\gamma_e \mathbf{B} \times \mathbf{P} + R_{\text{OP}}(\hat{z} - \mathbf{P}) - R_{\text{rel}} \mathbf{P}]$$

- ✓ \mathbf{P} 是电子极化度，第一项表示原子自旋受到外磁场所产生的力矩而做拉莫进动；
- ✓ 第二项表示泵浦光 \mathbf{R}_{op} 沿着 z 方向泵浦原子，同时也导致自旋弛豫；
- ✓ 第三项表示原子的自旋弛豫 \mathbf{R}_{rel} ，包括原子与气壁碰撞、自旋之间碰撞、激光与原子相互作用导致的弛豫等
- ✓ q ：由于原子存在核自旋导致的缓慢因子 $\approx 2I+1$ ， ^{87}Rb 约等于 4

Bloch方程的稳态解

当外磁场变化很缓慢时，可以求出布洛赫方程的准静态解

$$\gamma_e \mathbf{B} \times \mathbf{P} - (R_{\text{rel}} + R_{\text{OP}}) \mathbf{p} + R_{\text{OP}} \hat{\mathbf{z}} = 0.$$

其中 $\beta = \gamma_e \mathbf{B} / (R_{\text{OP}} + R_{\text{rel}})$, $P_0 = R_{\text{OP}} / (R_{\text{OP}} + R_{\text{rel}})$ B=0 时平衡
自旋极化

$$P_z = P_0 \frac{1 + \beta_z^2}{1 + |\beta|^2},$$

$$P_y = P_0 \frac{\beta_x + \beta_z \beta_y}{1 + |\beta|^2},$$

$$P_x = P_0 \frac{\beta_y + \beta_z \beta_x}{1 + |\beta|^2}.$$



磁场测量原理

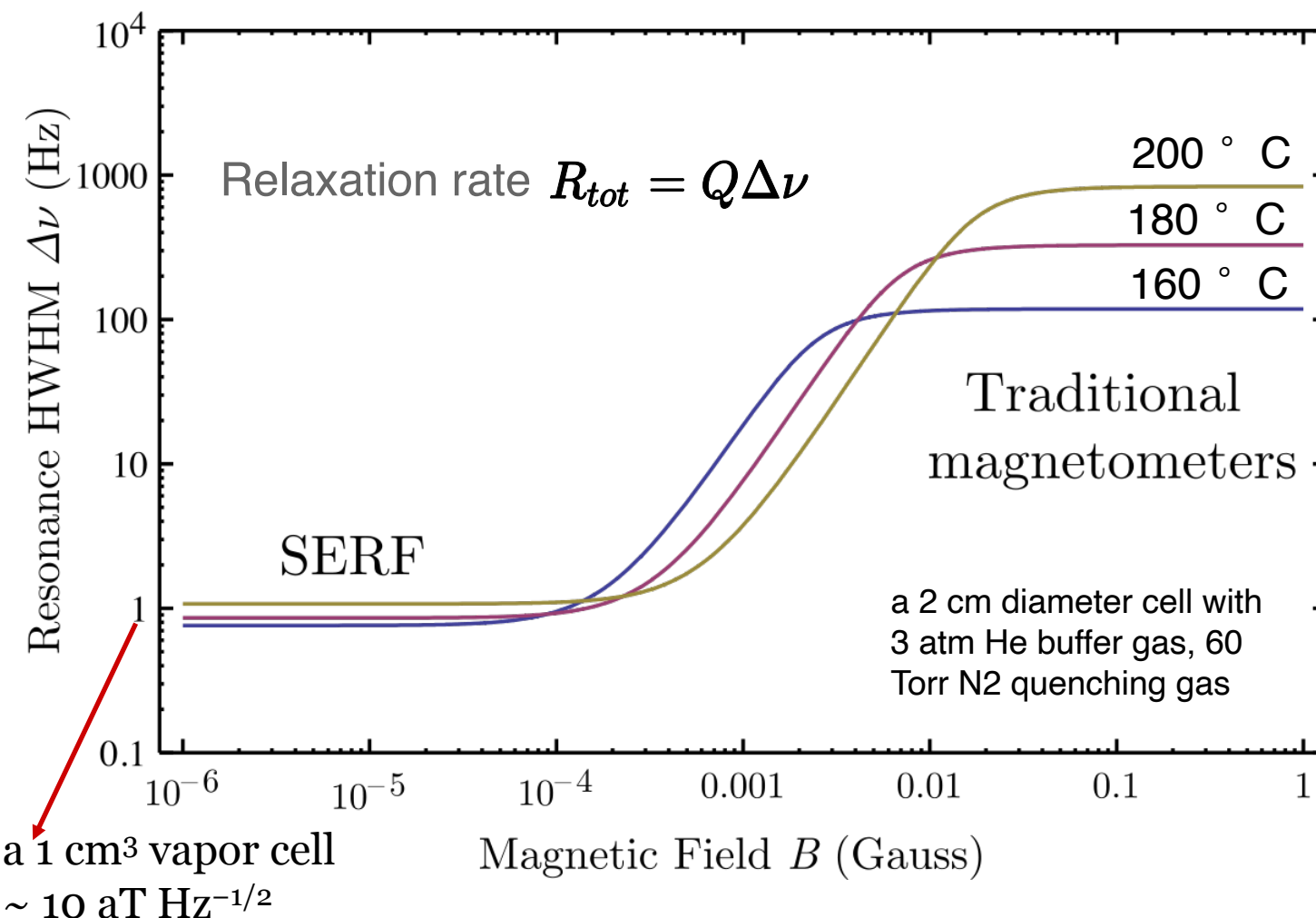
当待测磁场非常微弱 $|\beta| \ll 1$ $\gamma_e B_x, \gamma_e B_y \ll R_{op} + R_{rel}$


$$P_x \approx P_0 \frac{(R_{op} + R_{rel})\gamma_e B_y}{(\gamma_e B_z)^2 + (R_{op} + R_{rel})^2}.$$

$$\theta = \frac{\pi}{2} r_e \text{cln} P \left[-f_{D1} \mathcal{D}(\nu - \nu_{D1}) + \frac{1}{2} f_{D2} \mathcal{D}(\nu - \nu_{D2}) \right]$$

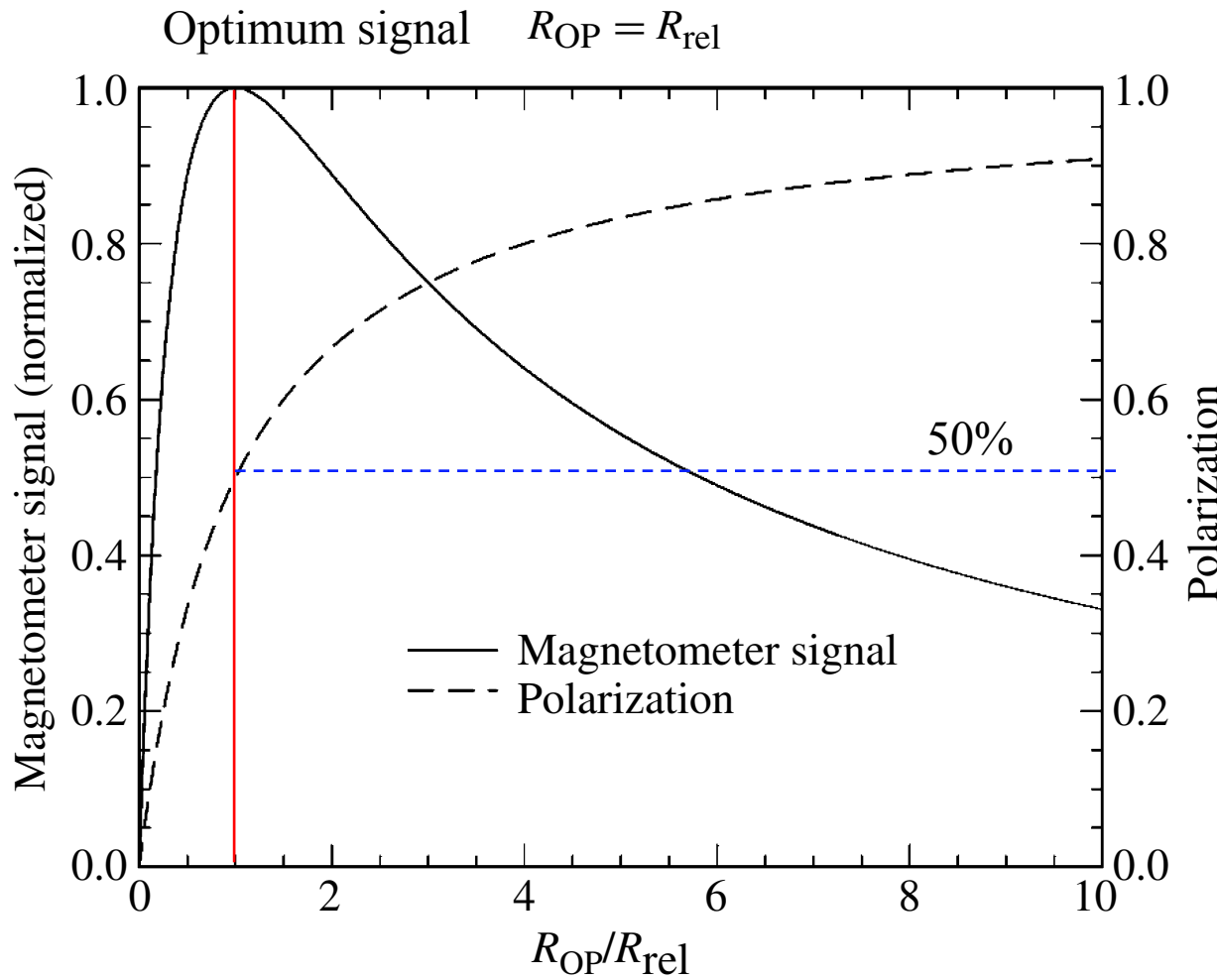
最灵敏的方向：与pump和probe方向正交

Spin exchange relaxation-free (SERF) magnetometer

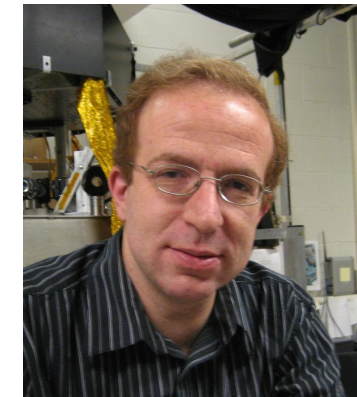
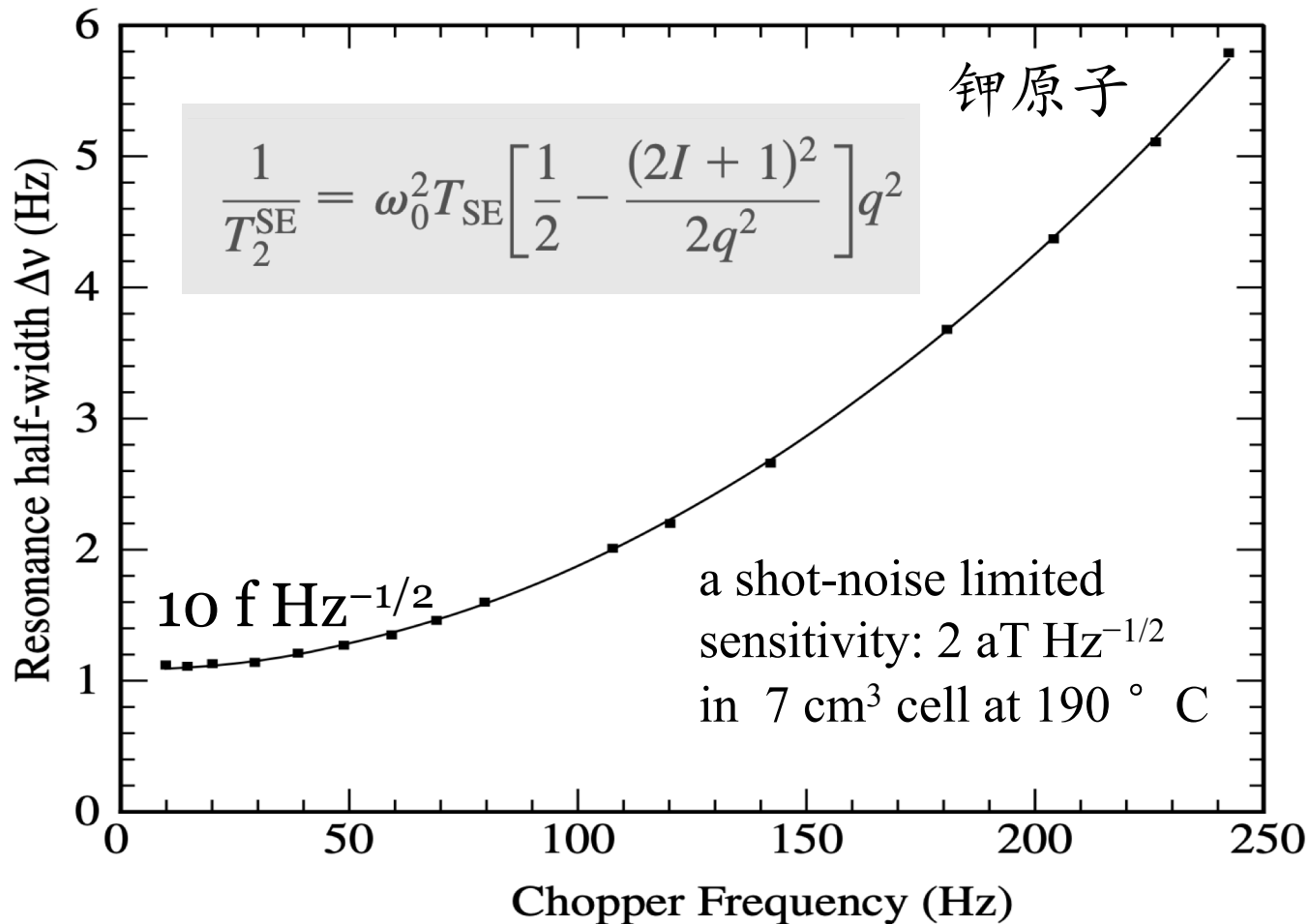


SERF magnetometer signal

$$S_x = S_0 \frac{\beta(\beta B_x B_z + B_y)}{1 + \beta^2(B_x^2 + B_y^2 + B_z^2)}$$



无自旋交换弛豫效应 (SERF 效应)



M. Romalis
普林斯顿大学
首次实现
SERF态

SERF原子磁强计

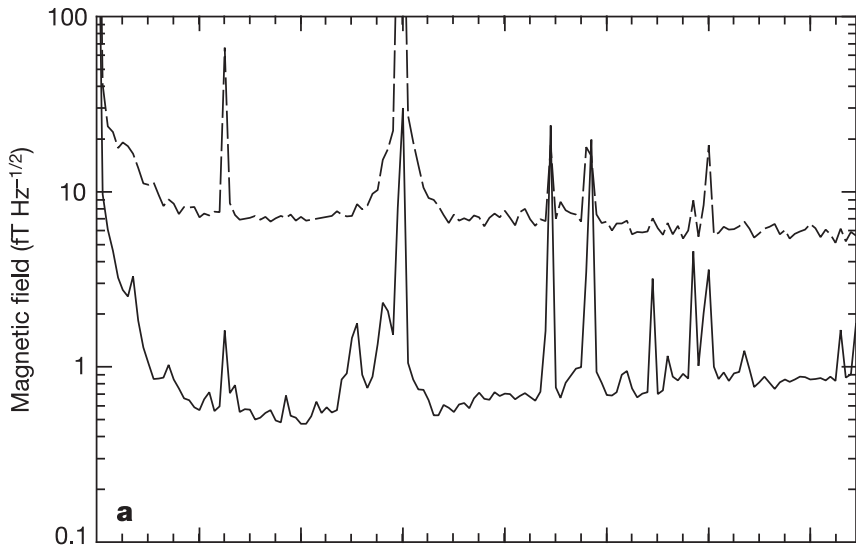
A subfemtotesla multichannel atomic magnetometer

I. K. Kominis^{*,†}, T. W. Kornack^{*}, J. C. Allred[‡] & M. V. Romalis^{*}

^{*} Department of Physics, Princeton University, Princeton, New Jersey 08544, USA

[‡] Department of Physics, University of Washington, Seattle, Washington 98195, USA

The magnetic field is one of the most fundamental and ubiquitous physical observables, carrying information about all electromagnetic phenomena. For the past 30 years, superconducting quantum interference devices (SQUIDs) operating at 4 K have been unchallenged as ultrahigh-sensitivity magnetic field detectors¹, with a sensitivity reaching down to $1 \text{ fT Hz}^{-1/2}$ ($1 \text{ fT} = 10^{-15} \text{ T}$). They have enabled, for example, mapping of



钾原子

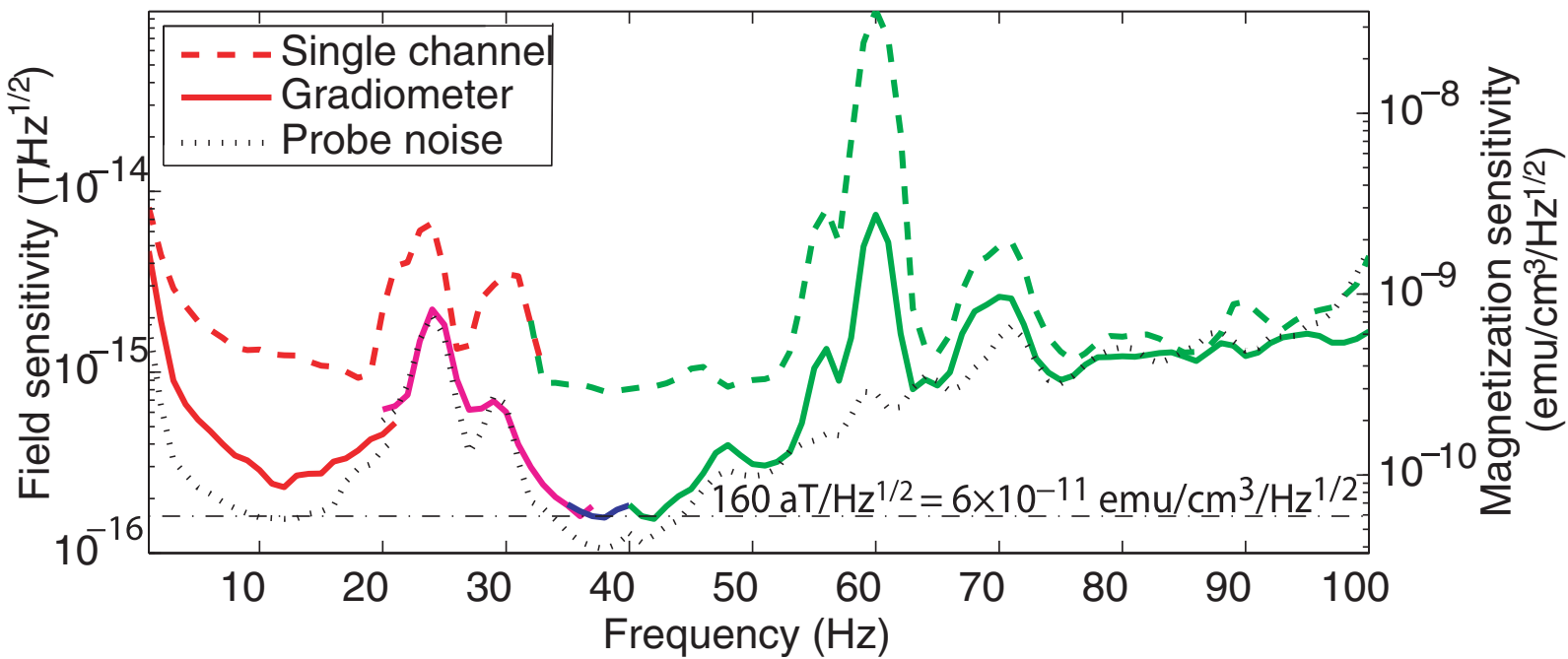
$0.54 \text{ fT Hz}^{-1/2}$ in 0.3 cm^3

180 ° C

SERF原子磁强计：世界上最灵敏的磁力计

钾原子

$0.16 \text{ fT Hz}^{-1/2}$ in 0.45 cm^3 , 200° C



SERF 原子磁强计

碱金属气室是超高灵敏磁场和惯性测量的灵敏核心，原子源种类决定了测量灵敏度的极限。

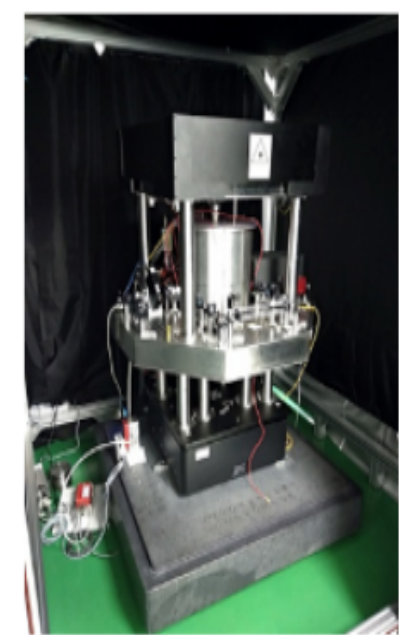
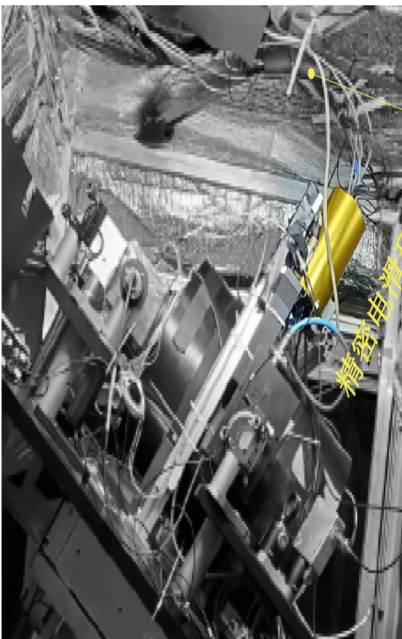
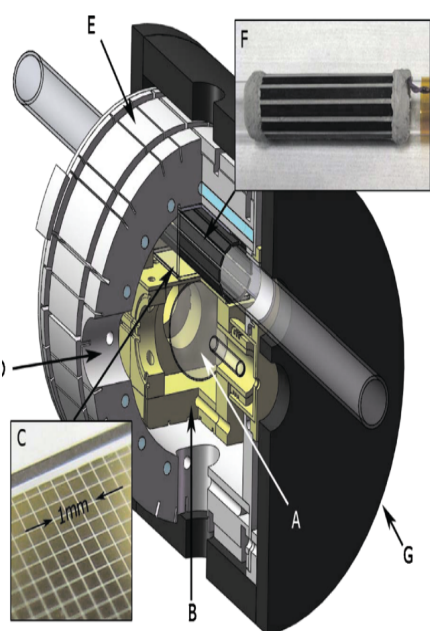
碱金属原子	加热温度/ °C	实测灵敏度/(fT·Hz ^{-1/2})	年份
钾	180	0.54	2003
钾	200	0.16	2010
铷	200	5	2010
铷	180	4	2014
铷	150	15	2018
铯	103	40	2008
铯	85	55	2015
铯	120	10	2017
钾-铷	195	5	2014
钾-铷	180	15	2018
钾-铷	190	0.68	2019

不同碱金属原子的加热温度及其实测灵敏度

SERF 磁强计的灵敏度尚未达到极限，小型化 SERF 原子磁强计的灵敏度仍有提升空间，其次，SERF 原子磁强计的成本还有降低空间，基于 MEMS 的气室研究将进一步降低其气室成本。解决其在地磁环境下的应用也很重要，这将使其扩展更广泛的应用领域，如磁异常探测、军事反潜等。

SERF磁力计：国内外研究组

无自旋交换弛豫 (SERF) 原子磁力计是当前灵敏度最高的磁力计 ($0.16\text{fT/Hz}^{1/2}$)，且具有无需低温、可小型化、结构简单等优势，已成为 SQUID 的有力替代方案。



普林斯顿大学组

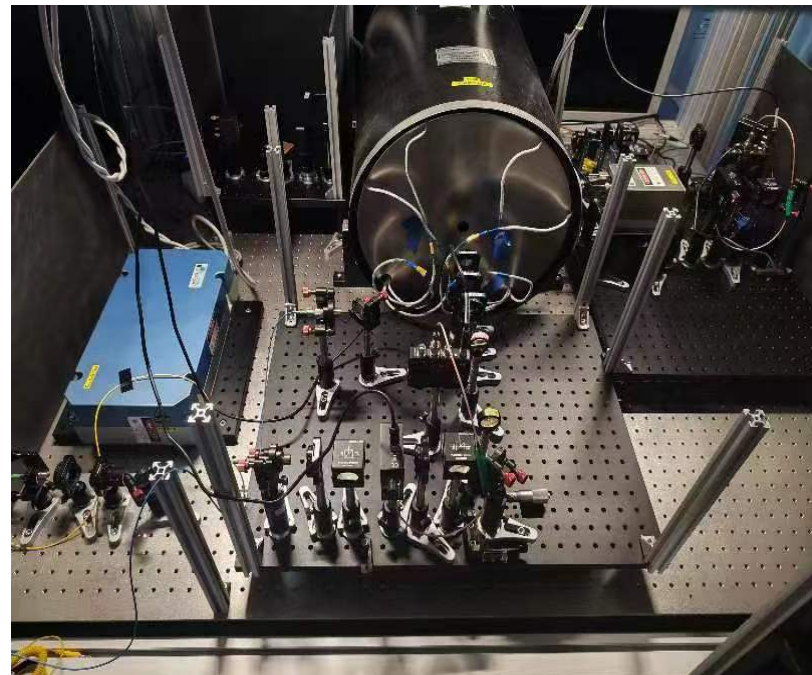
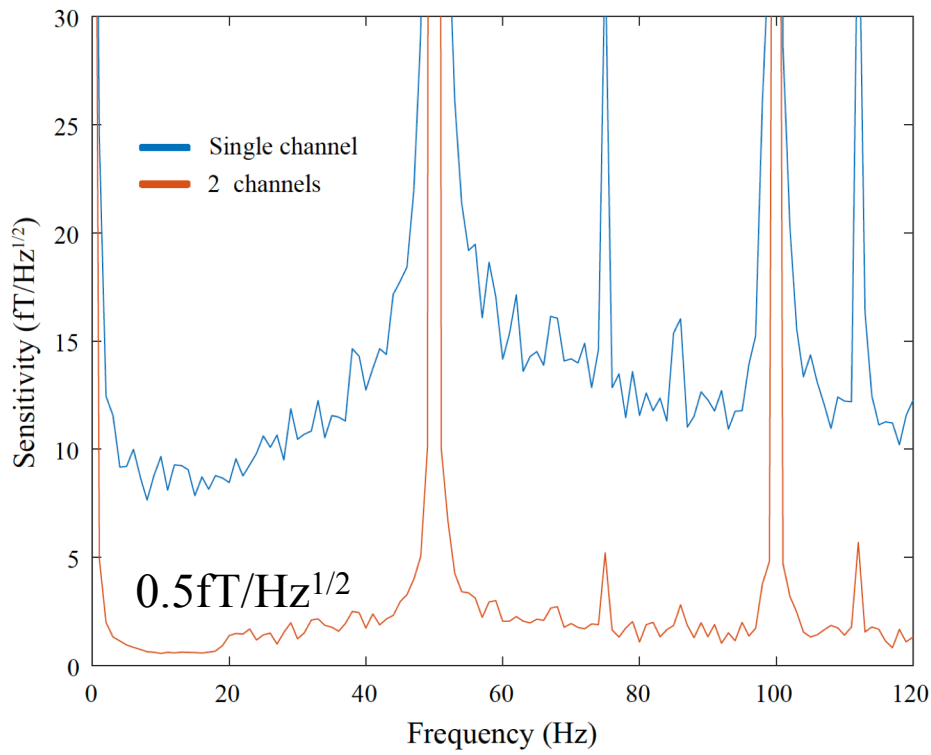
中科大卢征天、盛东组

中科大彭新华、江敏组

北航房建成组

我们组的研究进展：SERF磁力计

实现 $0.5\text{fT}/\text{Hz}^{1/2}$ 磁场探测灵敏度（地磁场的1000亿分之一）

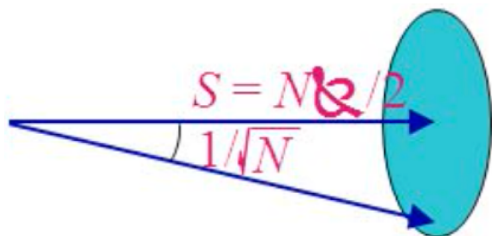


中国科大实验平台

基于自旋的磁场测量量子极限：海森堡测不准关系

海森堡测不准关系

$$[F_x, F_y] = iF_z, \quad \delta F_x \delta F_y \geq \frac{|F_z|}{2}$$



标准量子极限
(自旋投影噪声)

$$\delta B = \frac{1}{\gamma P \sqrt{n V T_2 t}}$$

理论极限： $\sim 1 \text{ aT}$



如何进一步提高
弱磁探测灵敏度？

- ✓ 自旋极化度 P
- ✓ 测量时间 t
- ✓ 自旋数目 $N = nV$
- ✓ 自旋弛豫时间 T_2

Fundamental sensitivity limits

Spin-projection- noise-limited (or *atomic shot-noise-limited*) sensitivity δB_{SNL}

$$\delta B_{\text{SNL}} \approx \frac{1}{\gamma} \sqrt{\frac{\Gamma_{\text{rel}}}{N\tau}}.$$

$$\tau \gg \Gamma_{\text{rel}}^{-1}$$

N : the total number of atoms
 Γ_{rel} : the spin-relaxation rate
 τ : measurement time

Photon-shot-noise-limited sensitivity

$$\delta\varphi \approx \frac{1}{2} \sqrt{\frac{1}{\Phi\tau}} \quad \text{in rad/}\sqrt{\text{Hz}}$$

φ : the probed photon flux (photons/s) detected after the atomic sample

For an atomic-vapor-based optical magnetometer the dominant spin-relaxation mechanism becomes either spin-exchange or spin-destruction collisions $\Gamma_{\text{rel}} = \xi n$

$$N = nV \quad \delta B_{\text{opt}} \approx \frac{1}{\gamma} \sqrt{\frac{\xi}{V\tau}} \quad \begin{array}{l} \text{The relaxation constant } \xi : \\ 10^{-9} \text{ cm}^3/\text{s and } \sim 10^{-13} \text{ cm}^3/\text{s} \end{array}$$

$V = 1 \text{ cm}^3$ magnetic sensor ranges between 10^{-11} and $10^{-13} \text{ G}/\sqrt{\text{Hz}}$ (1 to 0.01 ft/ $\sqrt{\text{Hz}}$)

光泵磁共振的典型原子自旋

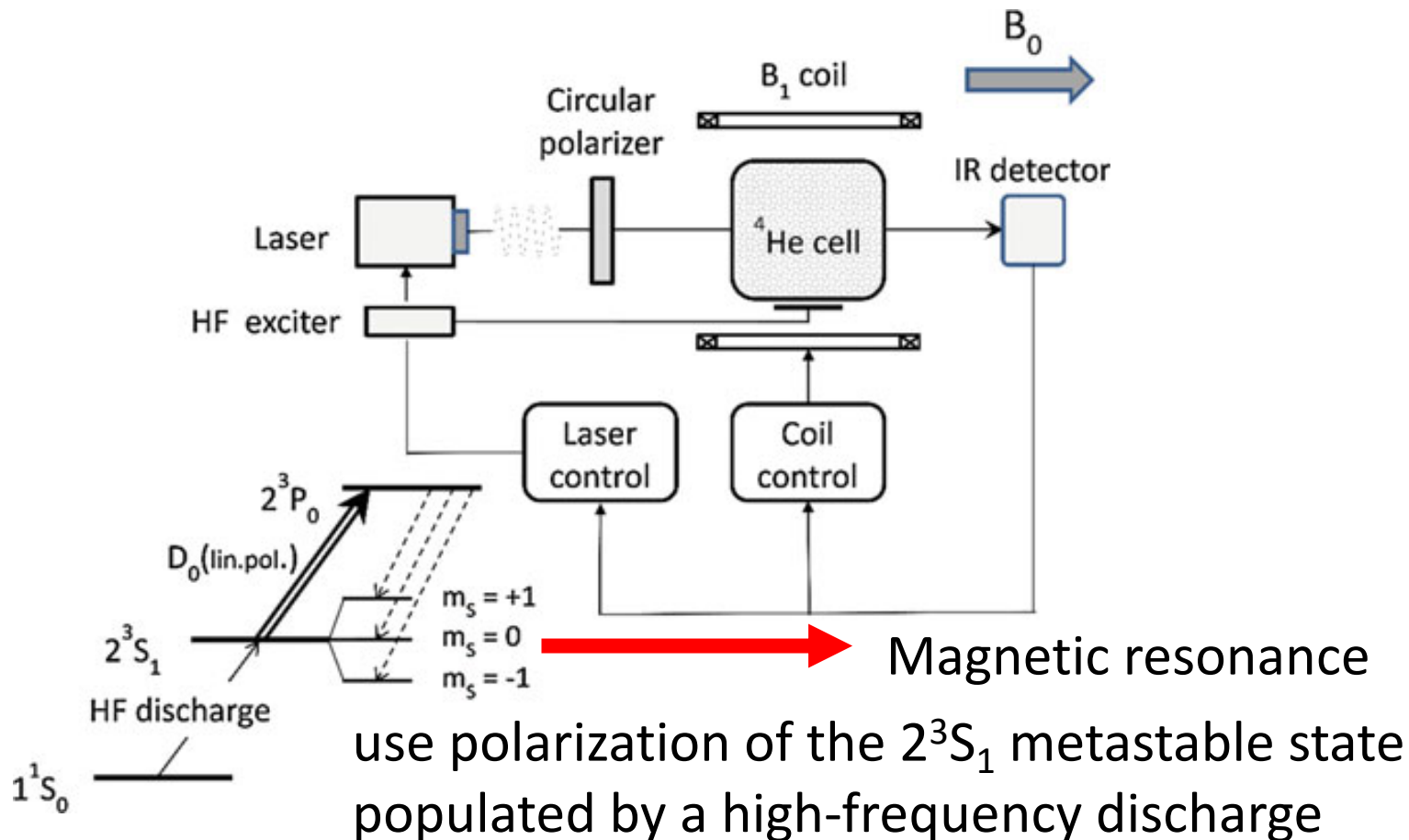
PERIODIC TABLE OF THE ELEMENTS

The Periodic Table of the Elements is shown with the following annotations:

- Central Element:** Iron (Fe, atomic number 26) is highlighted with a yellow box. Labels around it include:
 - atomic number → 26
 - chemical symbol → Fe
 - name → Iron
 - atomic mass → 55.845
 - oxidation states (most common): +3, +2
 - STATE OF MATTER: SOLID, GASS, LIQUID
 - radioactive elements (indicated by a small bomb icon)
- Groups 1 and 2:** The first two groups (Alkali metals and Alkaline earth metals) are highlighted with a red box.
- Group 18:** The noble gases (He, Ne, Ar, Kr, Xe) are highlighted with a red box.
- Lanthanoids:** A bracket on the left indicates the lanthanoid series (lanthanum to lutetium, atomic numbers 57-71).
- Actinoids:** A bracket on the left indicates the actinoid series (rutherfordium to lawrencium, atomic numbers 99-103).
- Color-Coding:** Elements are color-coded into groups:
 - Nonmetals (pink)
 - Alkali metals (purple)
 - Alkaline earth metals (light blue)
 - Transition metals (yellow)
 - Metalloids (red)
 - Post-transition metals (light green)
 - Halogens (light blue)
 - Noble gases (light purple)
 - Lanthanoids (orange)
 - Actinoids (teal)

Helium (He) magnetometers

Optically Pumped He-4 Magnetometers



混合原子气室

核心思想

取长补短

碱金属

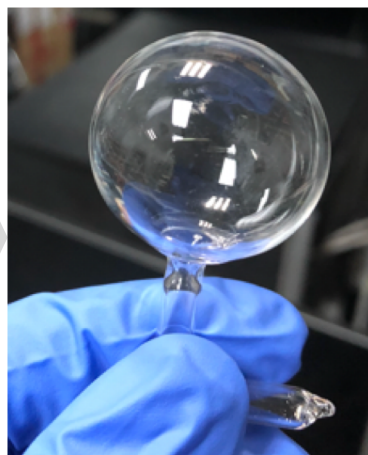
电子自旋
磁矩大

自旋寿命短
(ms级别)

数密度小
(10^{14}cm^{-3})

11 Na
19 K
37 Rb
55 Cs

混合原子气室



2 He
10 Ne
54 Xe

惰性气体

核自旋
磁矩小 (小 10^3 倍)

自旋寿命长
(100s级别)

数密度大
(10^{19}cm^{-3})

基本灵敏度

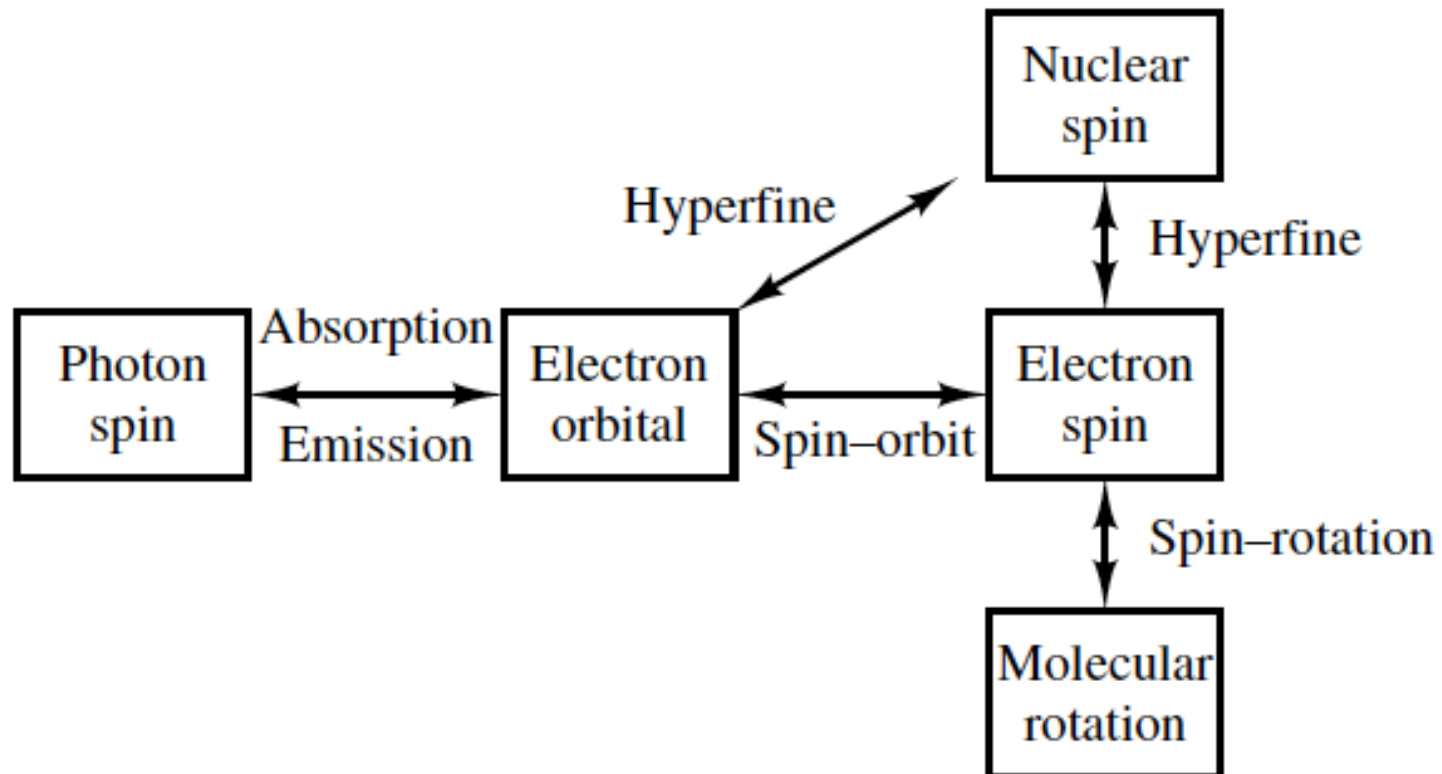
$$\delta B = \frac{1}{\gamma P \sqrt{n V T_2 t}}$$

相互补充?
新的效应?

提升灵敏度?

Angular Momentum Reservoirs

No direct transfer to nuclear spins from photon. However, the coupling between electronic and nuclear angular momentum is usually strong enough to provide an efficient transfer mechanism.

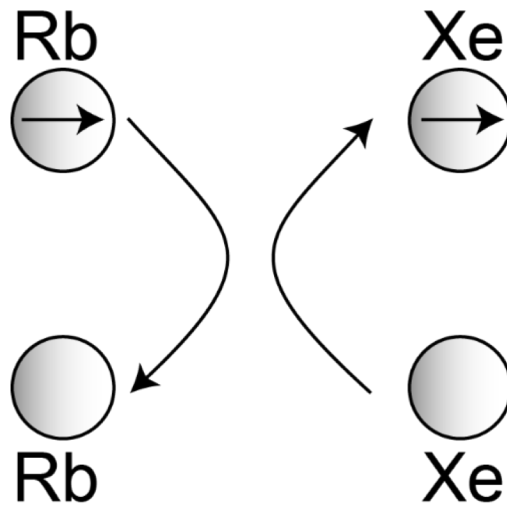


惰性气体核自旋超极化

NUCLEAR POLARIZATION IN He^3 GAS INDUCED BY OPTICAL PUMPING AND DIPOLAR EXCHANGE*

M. A. Bouchiat,[†] T. R. Carver,[‡] and C. M. Varnum

Palmer Physical Laboratory, Princeton University, Princeton, New Jersey
(Received September 26, 1960)



- 电子自旋容易被极化
- 可以通过自旋交换碰撞将电子自旋传递给核自旋



$$H_{se} = \boxed{\frac{8\pi}{3} g_s \mu_B \frac{\mu_I}{|I|} \kappa |\psi(R)|^2 \mathbf{I} \cdot \mathbf{S}} + \frac{\mu_I}{|I|} \mathbf{I} \cdot \frac{3\mathbf{r}\mathbf{r} - r^2 \mathbf{1}}{r^5} \cdot \mathbf{S},$$

核自旋平衡极化度

平衡态下，惰性气体核自旋的极化率 P^n 由自旋交换速率 R_{se} 与核自旋的纵向弛豫寿命 T_1 以及碱金属原子自旋极化率 P^e 有关

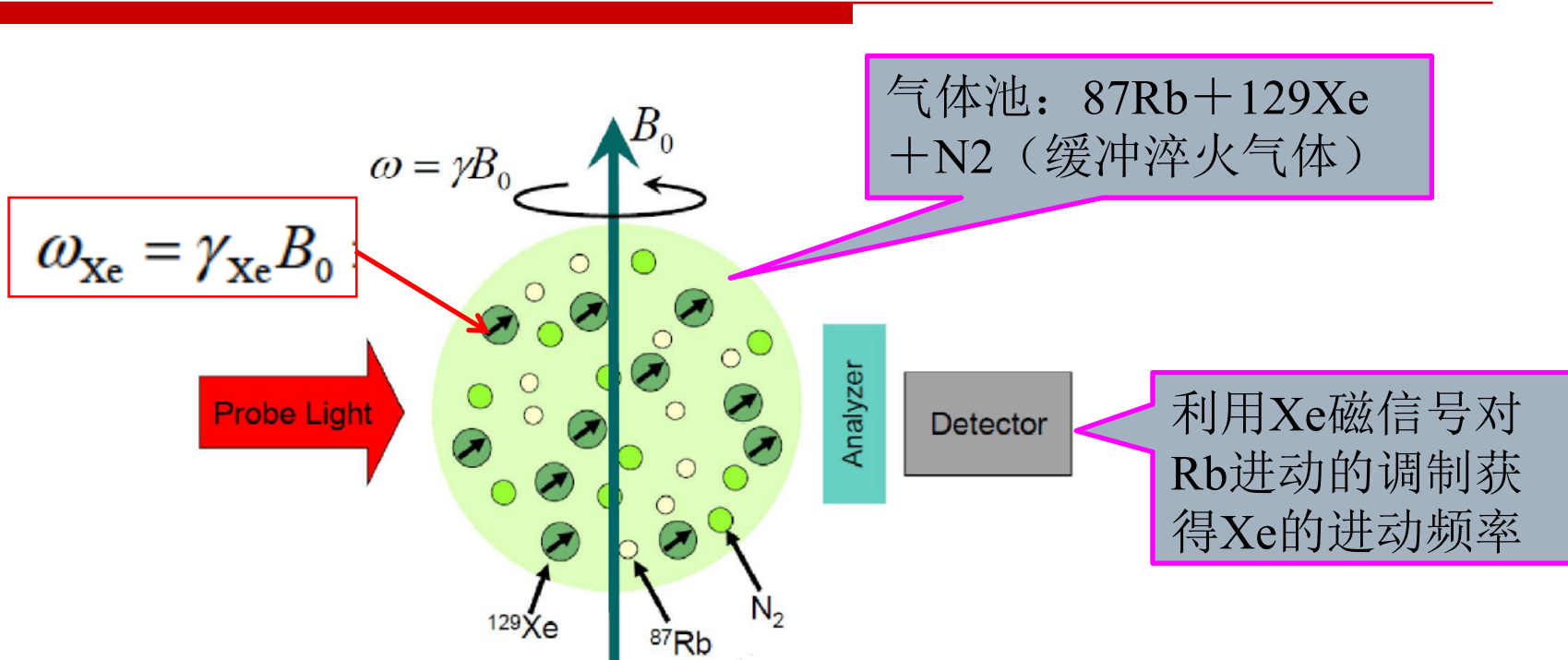
$$p^n = p^e \frac{R_{se}}{R_{se} + 1/T_1^n}.$$

碱金属
(K, Rb, Cs)
极化度

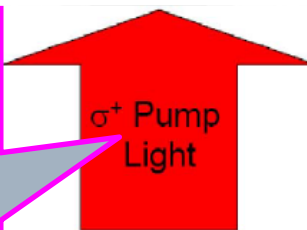
碱金属-惰性气体
自旋交换速率

惰性气体
纵向退相干时间

碱金属-惰性气体混合气室

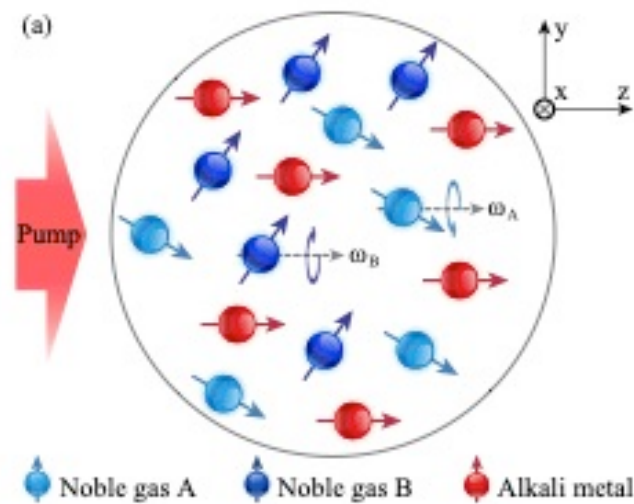


激光抽运使Rb原子极化，
自旋交换作用将 129Xe 的
核自旋极化（ 129Xe 核自
旋的弛豫时间长）



Clock-comparison comagnetometer

^{129}Xe : spin-1/2



^{131}Xe : spin-3/2

$$|\Omega_{129}| = |\gamma_{129}|B + \Omega_{\text{rot}}$$

$$|\Omega_{131}| = |\gamma_{131}|B - \Omega_{\text{rot}}$$

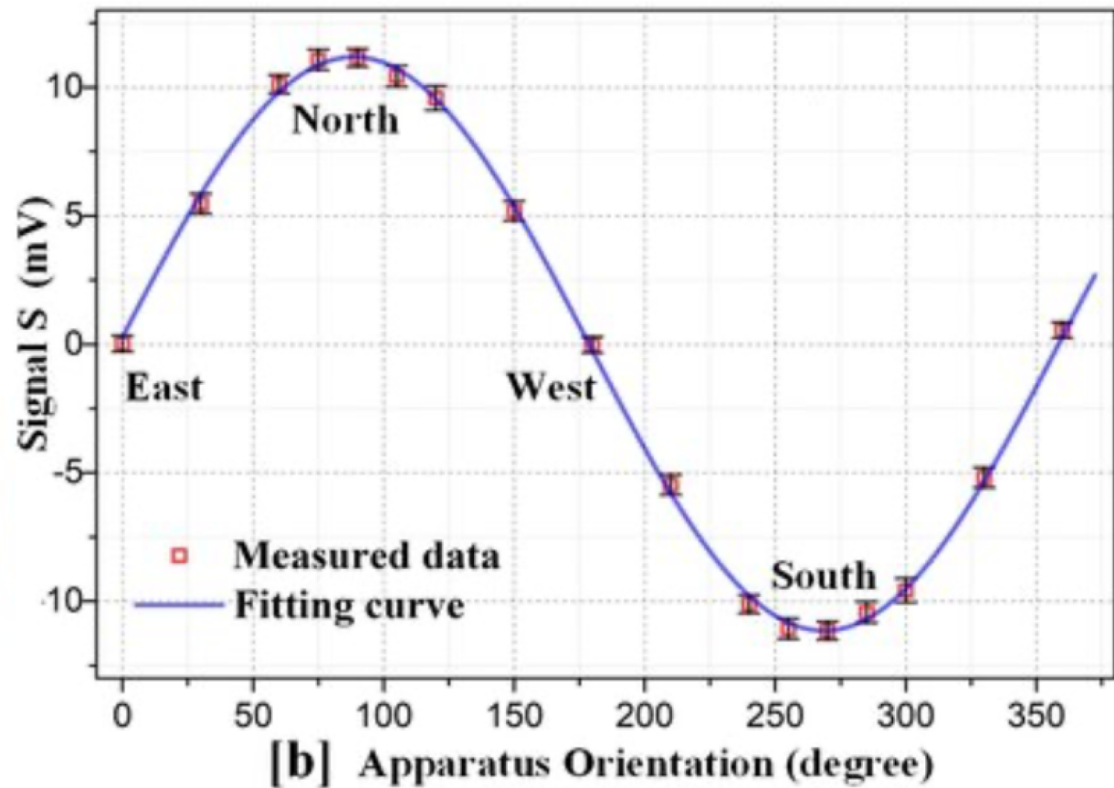
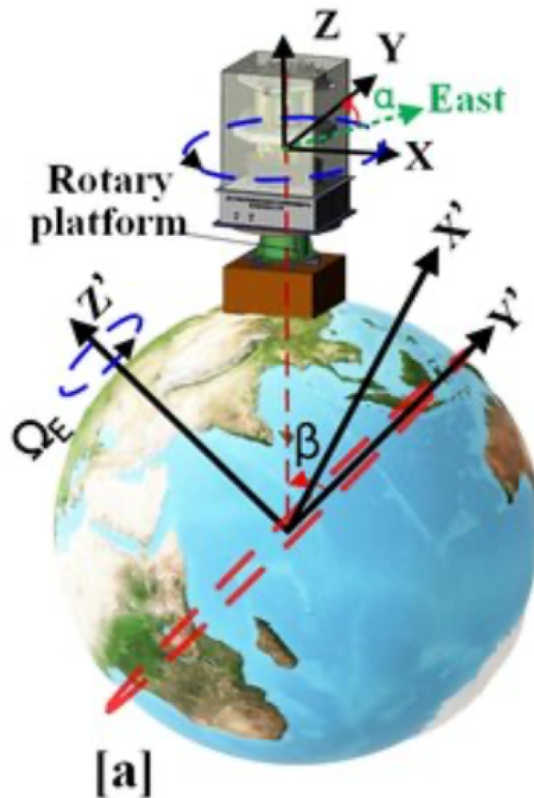
$$\gamma_{129} = -2\pi \times 11.86 \text{ mHz/nT}$$

$$\gamma_{131} = 2\pi \times 3.516 \text{ mHz/nT}$$

$$\Omega_{\text{rot}} = \frac{|\gamma_{129}| \Omega_{131} - |\gamma_{131}| \Omega_{129}}{|\gamma_{129}| + |\gamma_{131}|}$$

Magnetic fluctuations (e.g., due to current noise) can be eliminated.

共磁力仪:测量地球转动



地球转动：在核自旋产生等效的磁场 ($\sim \text{pT}$)

磁场自补偿效应：对低频磁场噪声不敏感

PRL 95, 230801 (2005)

PHYSICAL REVIEW LETTERS

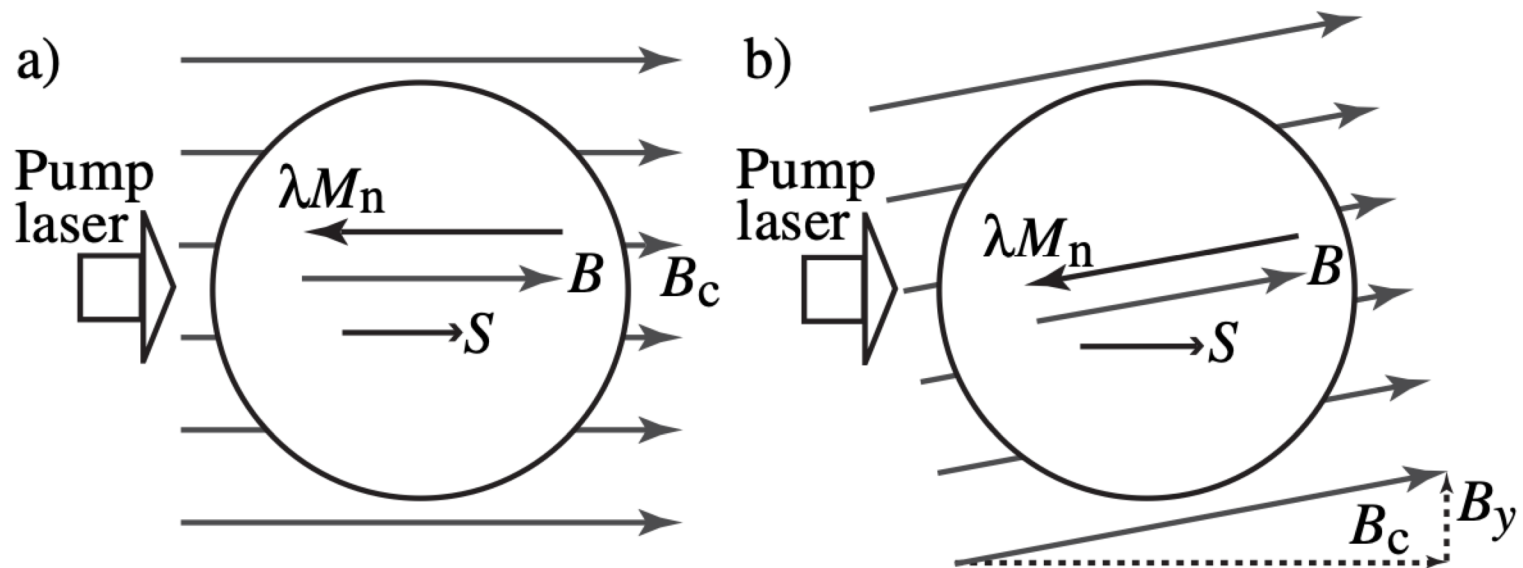
week ending
2 DECEMBER 2005

Nuclear Spin Gyroscope Based on an Atomic Comagnetometer

T. W. Kornack, R. K. Ghosh, and M. V. Romalis

Department of Physics, Princeton University, Princeton, New Jersey 08550 USA

(Received 6 May 2005; published 29 November 2005)



两种自旋的耦合布洛赫方程

惰性气体-碱金属自旋演化的布洛赫方程

电子自旋
$$\frac{\partial \mathbf{P}^e}{\partial t} = \frac{\gamma_e}{Q} (B_z^0 \hat{z} + \underline{\beta M_0^n \mathbf{P}^n}) \times \mathbf{P}^e + \frac{P_0^e \hat{z} - \mathbf{P}^e}{T_e Q},$$

静磁场 等效磁场 $\beta M_0^e \mathbf{P}^e \ll \beta M_0^n \mathbf{P}^n$

核自旋
$$\frac{\partial \mathbf{P}^n}{\partial t} = \gamma_n (B_z^0 \hat{z} + B_{ac} \hat{y} + \underline{\beta M_0^n \mathbf{P}^e}) \times \mathbf{P}^n + \frac{P_0^n \hat{z} - \mathbf{P}^n}{\{T_{2n}, T_{2n}, T_{1n}\}},$$

待测交流磁场

Spin Dynamics

The transverse polarization components

$$P_x^n = \frac{1}{2} P_0^n \gamma_n B_{\text{ac}}^y \frac{T_{2n} \cos(2\pi\nu t) + 2\pi(\nu - \nu_0) T_{2n}^2 \sin(2\pi\nu t)}{1 + (\gamma_n B_{\text{ac}}^y / 2)^2 T_{1n} T_{2n} + [2\pi(\nu - \nu_0)]^2 T_{2n}^2} + C e^{-t/T_{2n}} \cos(2\pi\nu_0 t),$$

$$P_y^n = \frac{1}{2} P_0^n \gamma_n B_{\text{ac}}^y \frac{T_{2n} \sin(2\pi\nu t) - 2\pi(\nu - \nu_0) T_{2n}^2 \cos(2\pi\nu t)}{1 + (\gamma_n B_{\text{ac}}^y / 2)^2 T_{1n} T_{2n} + [2\pi(\nu - \nu_0)]^2 T_{2n}^2} + C e^{-t/T_{2n}} \sin(2\pi\nu_0 t),$$

The effective field experienced by ^{87}Rb atoms $\mathbf{B}_{\text{eff}} = \lambda M^n \mathbf{P}^n$

Steady-state response

$$\mathbf{B}_{\text{eff}}^n = \underbrace{\frac{1}{2} \lambda M^n P_0^n \gamma_n B_{\text{ac}}^y \frac{T_{2n} \cos(2\pi\nu t) + 2\pi(\nu - \nu_0) T_{2n}^2 \sin(2\pi\nu t)}{1 + (\gamma_n B_{\text{ac}}^y / 2)^2 T_{1n} T_{2n} + [2\pi(\nu - \nu_0)]^2 T_{2n}^2} \mathbf{x}}_{\text{effective field generated by } ^{129}\text{Xe } x \text{ magnetization}} \\ + \underbrace{\frac{1}{2} \lambda M^n P_0^n \gamma_n B_{\text{ac}}^y \frac{T_{2n} \sin(2\pi\nu t) - 2\pi(\nu - \nu_0) T_{2n}^2 \cos(2\pi\nu t)}{1 + (\gamma_n B_{\text{ac}}^y / 2)^2 T_{1n} T_{2n} + [2\pi(\nu - \nu_0)]^2 T_{2n}^2} \mathbf{y}}_{\text{effective field generated by } ^{129}\text{Xe } y \text{ magnetization}}$$

自旋的磁场放大效应

ARTICLES

<https://doi.org/10.1038/s41567-021-01392-z>

nature
physics

 Check for updates

Search for axion-like dark matter with spin-based amplifiers

Min Jiang^{1,2,3,7}, Haowen Su^{1,2,3,7}, Antoine Garcon^{4,5}, Xinhua Peng^{1,2,3}  and Dmitry Budker^{4,5,6}

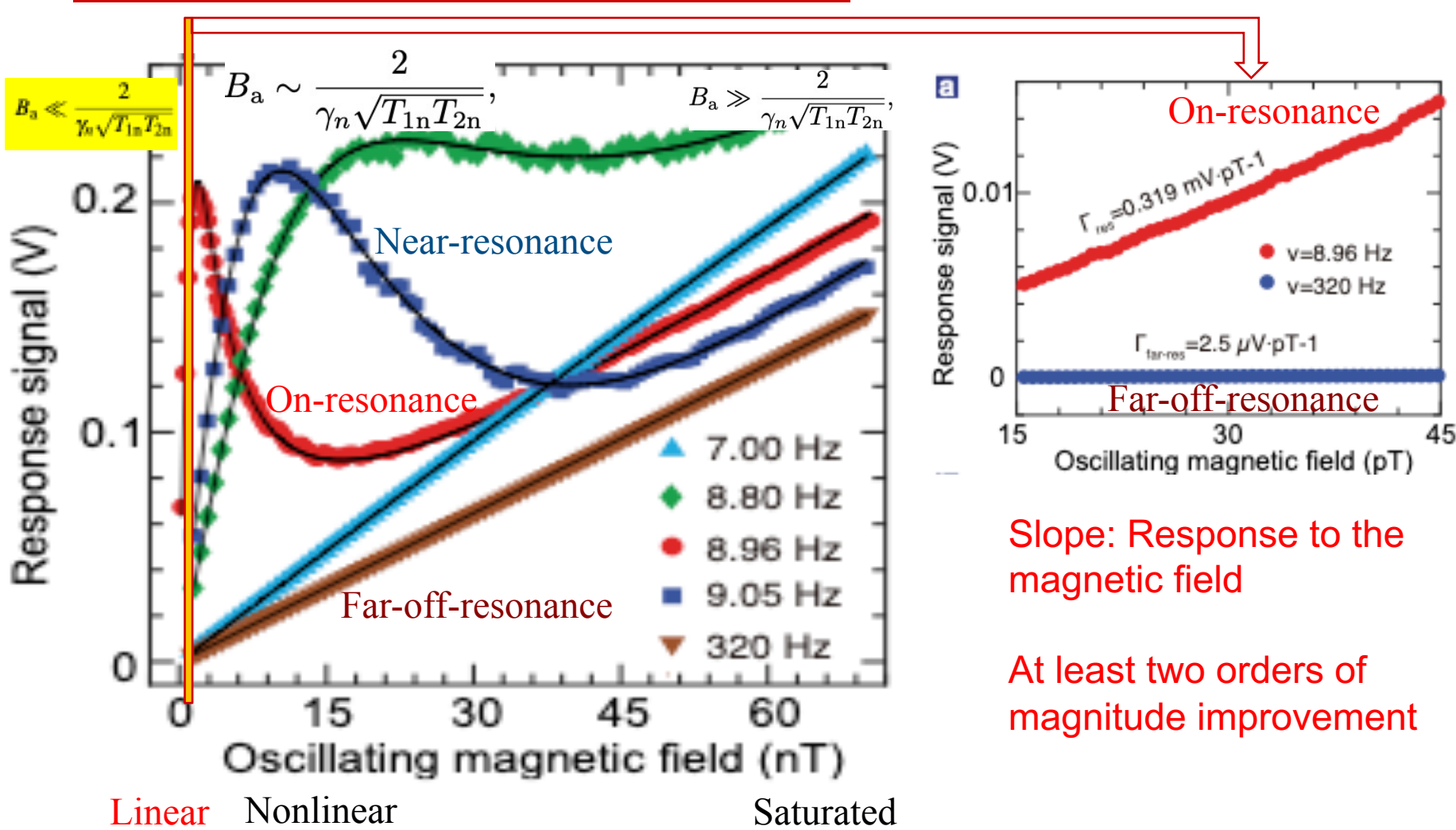
$$\mathbf{B}_{\text{eff}} = \frac{1}{2} \lambda M^n P_0^n \gamma_n T_{2n} B_{\text{ac}} \frac{\cos(2\pi\nu t) + 2\pi(\nu - \nu_0) T_{2n} \sin(2\pi\nu t)}{1 + (\gamma_n B_{\text{ac}}^y / 2)^2 T_{1n} T_{2n} + [2\pi(\nu - \nu_0)]^2 T_{2n}^2} \mathbf{x} \\ + \frac{1}{2} \lambda M^n P_0^n \gamma_n T_{2n} B_{\text{ac}} \frac{\sin(2\pi\nu t) - 2\pi(\nu - \nu_0) T_{2n} \cos(2\pi\nu t)}{1 + (\gamma_n B_{\text{ac}}^y / 2)^2 T_{1n} T_{2n} + [2\pi(\nu - \nu_0)]^2 T_{2n}^2} \mathbf{y}$$

磁场放大因子 功率饱和效应 共振响应

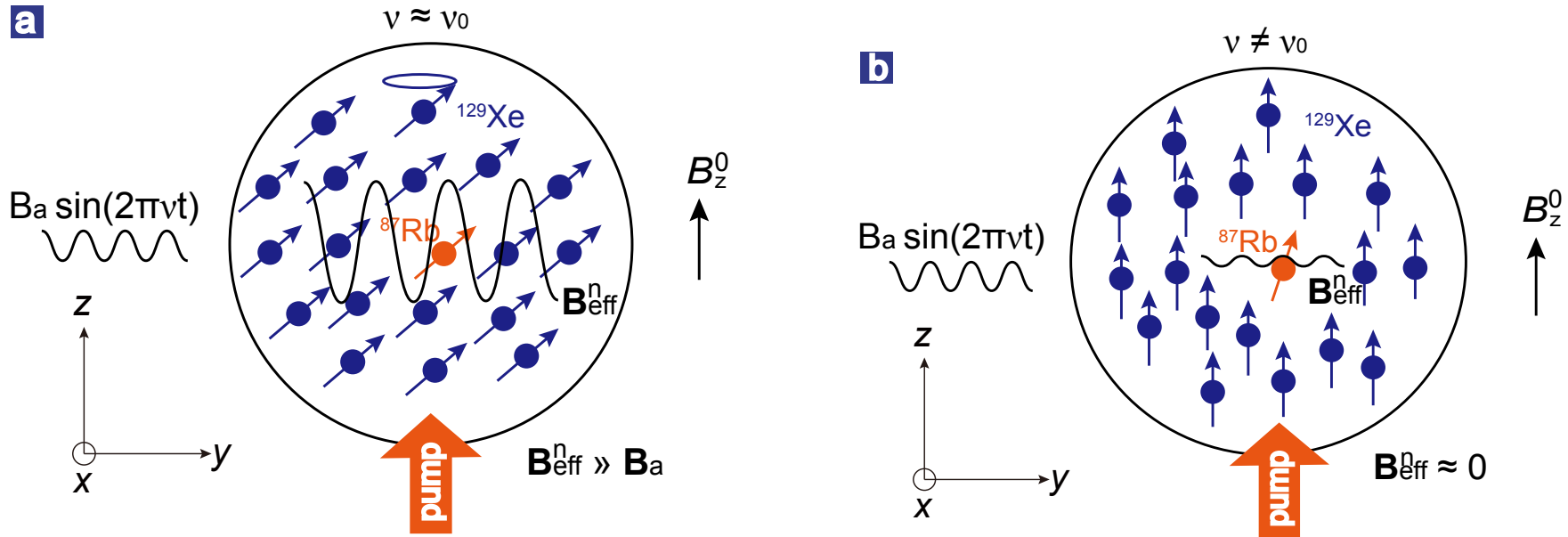
磁场放大倍数：

$$\eta = \frac{1}{2} \lambda M^n P_0^n \gamma_n T_{2n}$$

Intrinsic time-independent spin systems



Resonant amplification of magnetic field



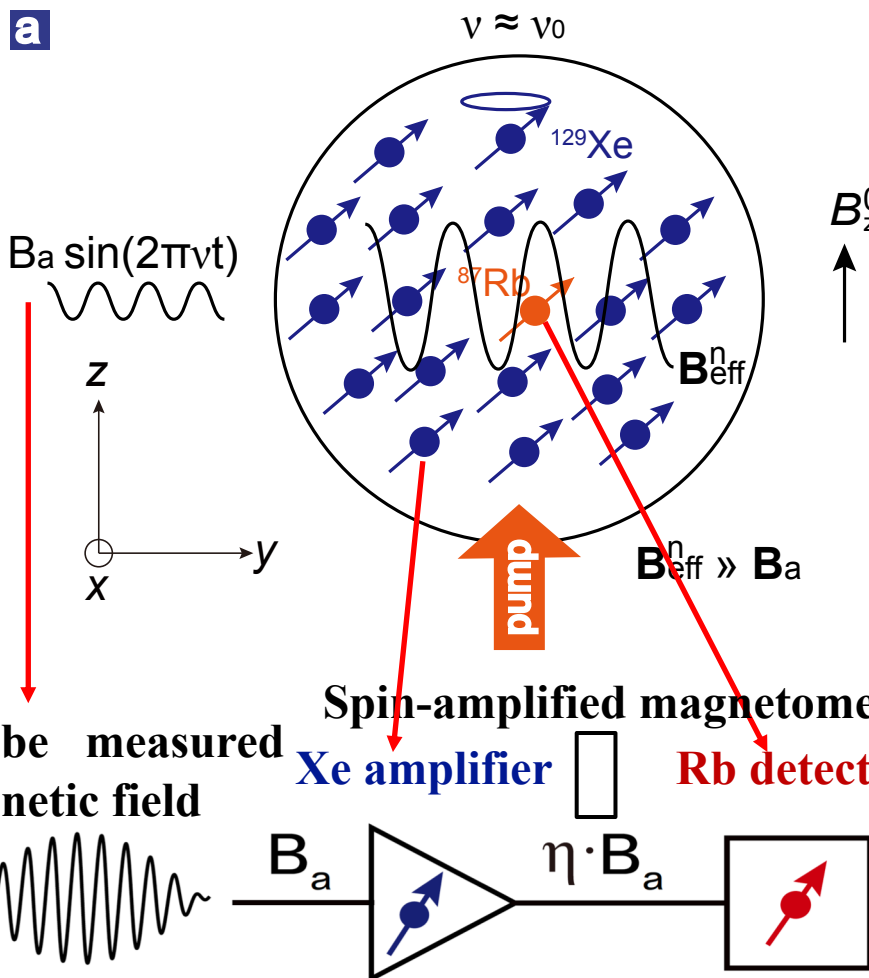
Amplification $\eta = |\mathbf{B}_{\text{eff}}^n / \mathbf{B}_a|$:
factor:

$$\eta = \frac{1}{2} \beta M_0^n P_0^n \gamma_n T_{2n} \gg 1$$

$$\eta \approx 0$$

Magnetometer with spin-based amplifier

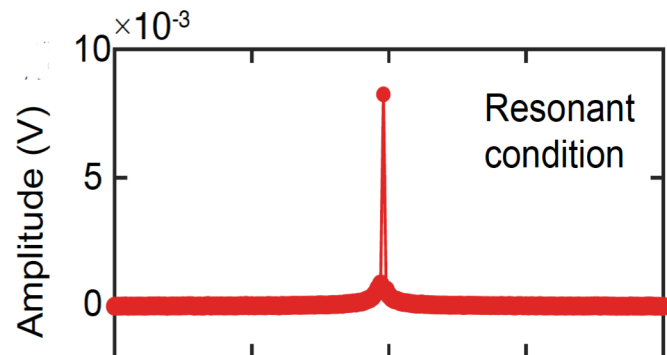
a



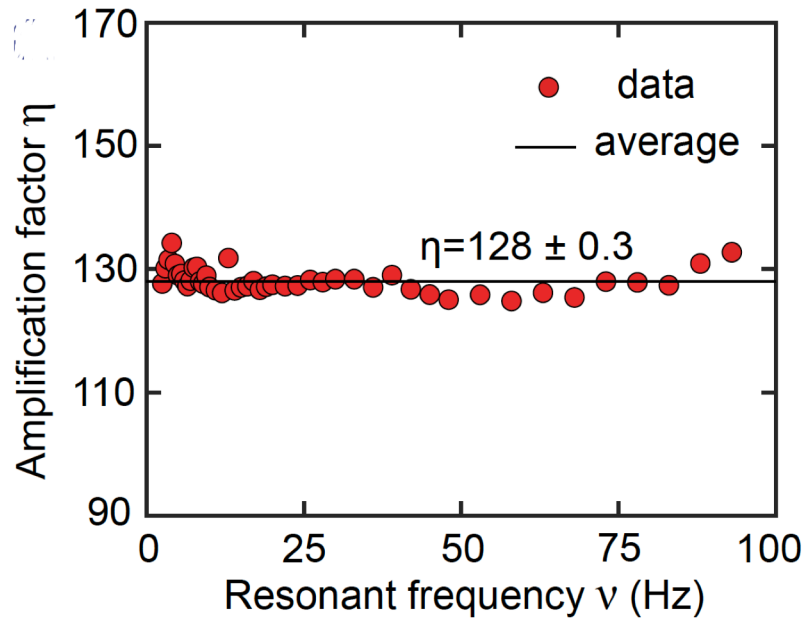
Amplification factor:

$$\eta = \frac{1}{2} \beta M_0^n P_0^n \gamma_n T_{2n} \gg 1$$

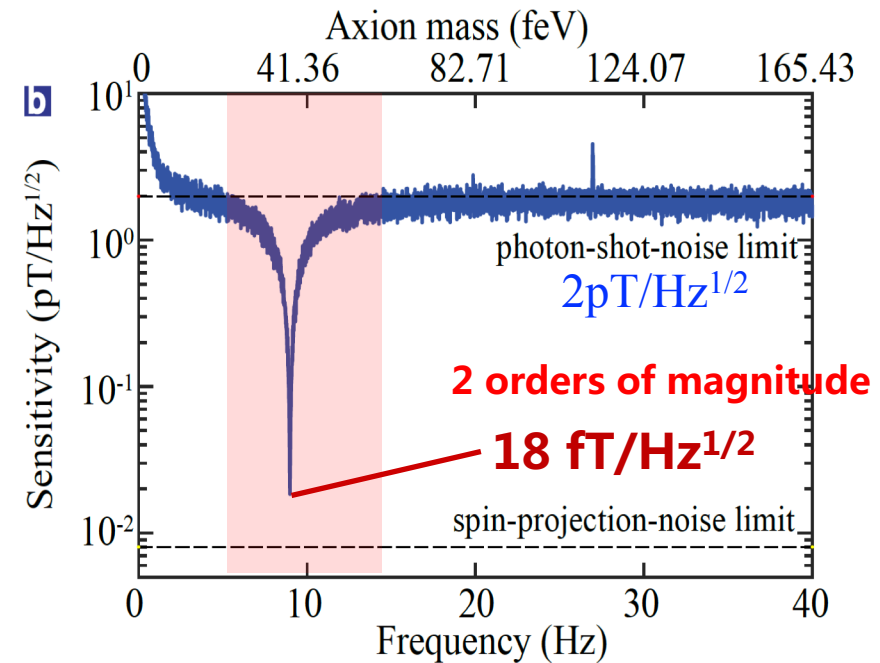
$$\delta B = \frac{1}{\eta P \gamma \sqrt{N T_2 t}}$$



Ultrasensitive magnetic field sensing



Magnetic field is
amplified by a factor
of more than 100!



Femtotesla-level
sensitivity!

$$1\text{fT} = 10^{-15}\text{T}$$

磁场测量新方法：自旋放大效应

核心思想

取长补短

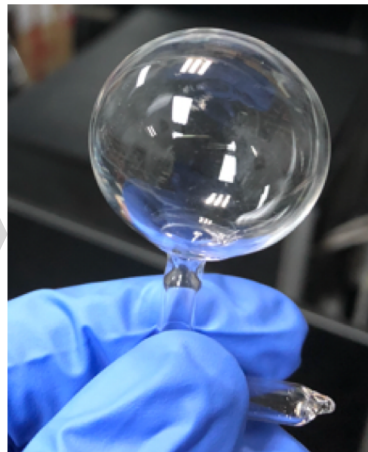
碱金属

电子自旋
磁矩大
自旋寿命短
(ms级别)
密度小
(10^{14}cm^{-3})

极化、读出

11 Na
19 K
37 Rb
55 Cs

混合原子气室



惰性气体

核自旋
磁矩小 (小 10^3 倍)
自旋寿命长
(100s级别)
密度大
(10^{19}cm^{-3})

量子放大介质

$1 \text{fT} = 10^{-15} \text{T}$ 相当于地磁场的1000亿分之一 !

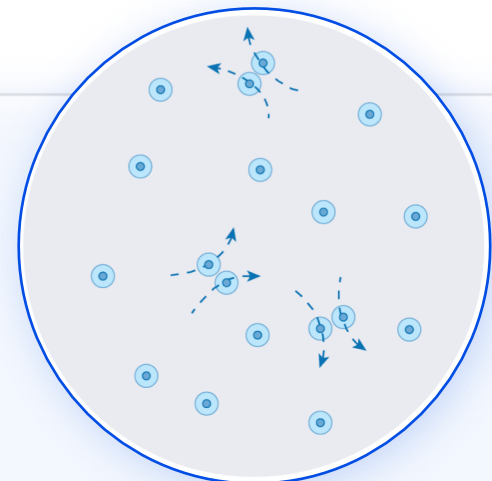
基本灵敏度

$$\delta B = \frac{1}{\gamma P \sqrt{nV T_2 t}}$$



$$\delta B = \frac{1}{\eta P \gamma \sqrt{nV T_2 t}}$$
$$\eta = \frac{1}{2} \beta M_0^n P_0^n \gamma_n T_{2n} \gg 1$$

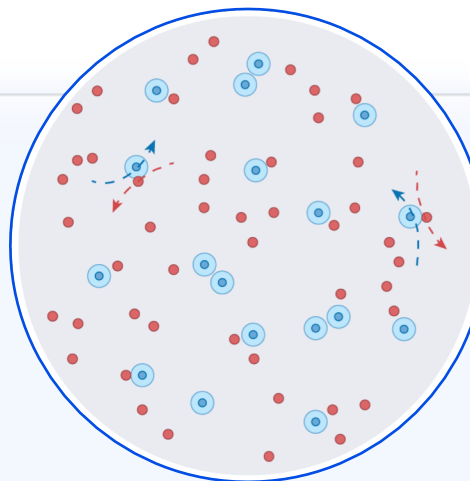
磁场测量新方法：自旋放大效应



近独立的碱金属气体

无自旋交换碰撞效应等
目前最高指标 $0.16\text{fT/Hz}^{1/2}$

引入惰性
气体原子



关联的混合气态原子

量子关联放大等
有望超越国际最高指标

$$\eta = \frac{1}{2} \beta M_0^n P_0^n \gamma_n T_{2n}$$

突破亚fT探测灵敏度

混合体系的优化

^{87}Rb - ^{129}Xe

自旋破坏碰撞截影响大

Xe原子相干时间短($\sim 10\text{s}$)

放大倍数(~ 100)

^{39}K - ^3He

自旋破坏碰撞小5个量级

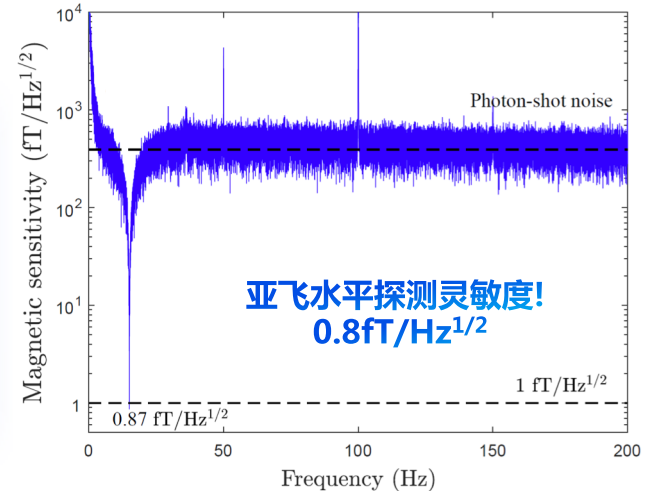
He原子相干时间长(1000s)

更大的放大倍数 (> 1000)

关键技术的突破

- 长相干时间低漏率的优质K-3He混合原子气室
- 坡莫合金与铁氧体的低磁噪声屏蔽系统
- 超低噪声的高稳定性无磁控温系统

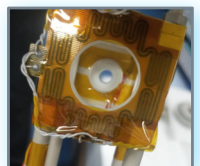
成为国际第三家自旋磁测量灵敏度突破fT的研究组



低漏率
K-3He
气室



低噪声铁
氧体屏蔽



无磁超
稳控温

Hybrid spin systems

Significant amplification using dark spins

PNAS

RESEARCH ARTICLE

PHYSICS

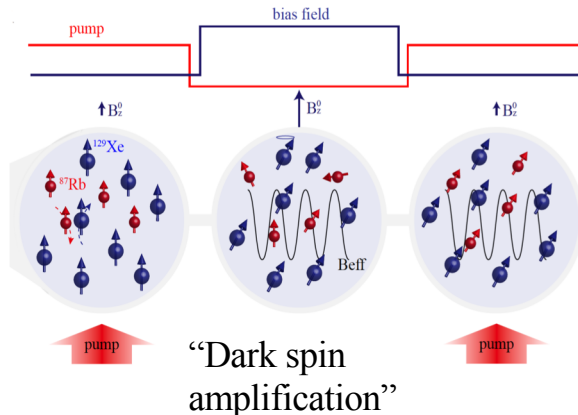


Observation of magnetic amplification using dark spins

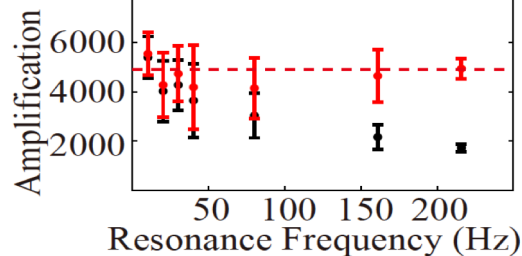
Min Jiang^{a,b,c,1} , Ying Huang^{a,b,c,1}, Chang Guo^{a,b,c}, Haowen Su^{a,b,c}, Yuanhong Wang^{a,b,c}, Xinhua Peng^{a,b,c,2}, and Dmitry Budker^{d,e,f}

Edited by Joshua Combes, University of Colorado, Boulder, CO; received September 9, 2023; accepted February 10, 2024, by Editorial Board Member Bernard F. Schutz

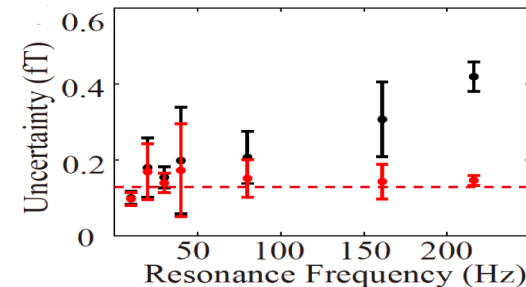
$$\text{Amp. Factor: } \Sigma = \lambda \gamma M P T_2$$



Dark noble-gas nuclear spins
without pump light



$T_2 \sim 6$ minutes



两种自旋的耦合布洛赫方程

惰性气体-碱金属自旋演化的布洛赫方程

$$\text{电子自旋} \quad \frac{\partial \mathbf{P}^e}{\partial t} = \frac{\gamma_e}{Q} (B_z^0 \hat{z} + \beta M_0^n \mathbf{P}^n) \times \mathbf{P}^e + \frac{P_0^e \hat{z} - \mathbf{P}^e}{T_e Q},$$

静磁场 等效磁场 $\beta M_0^e \mathbf{P}^e \ll \beta M_0^n \mathbf{P}^n$

$$\text{核自旋} \quad \frac{\partial \mathbf{P}^n}{\partial t} = \gamma_n (B_z^0 \hat{z} + B_{ac} \hat{y} + \beta M_0^n \mathbf{P}^e) \times \mathbf{P}^n + \frac{P_0^n \hat{z} - \mathbf{P}^n}{\{T_{2n}, T_{2n}, T_{1n}\}},$$

待测交流磁场

Keep this term

How about bidirectional coupling?

Amplification mechanism with interacting atomic gases

$$\frac{\partial \mathbf{M}^e}{\partial t} = \frac{\gamma_e}{Q} (\mathbf{B} + \lambda \mathbf{M}^n) \times \mathbf{M}^e + \frac{M_0^e \mathbf{z} - \mathbf{M}^e}{\{T_{2e}, T_{2e}, T_{1e}\} Q},$$

$$\frac{\partial \mathbf{M}^n}{\partial t} = \gamma_n (\mathbf{B} + \lambda \mathbf{M}^e) \times \mathbf{M}^n + \frac{M_0^n \mathbf{z} - \mathbf{M}^n}{\{T_{2n}, T_{2n}, T_{1n}\}}.$$

Holstein-Primakoff
transformation



$$\hat{a} = \frac{M_+^a}{\sqrt{2\gamma_a M_z^a}}, \hat{b} = \frac{M_+^b}{\sqrt{2\gamma_b M_z^b}}$$

$$\partial_t \begin{pmatrix} \hat{a} \\ \hat{b} \end{pmatrix} = i \begin{pmatrix} \omega_a + i\Gamma_a & -J \\ -J & \omega_b + i\Gamma_b \end{pmatrix} \begin{pmatrix} \hat{a} \\ \hat{b} \end{pmatrix} + \begin{pmatrix} h_a \\ h_b \end{pmatrix}$$

Larmor frequency

$$\begin{aligned} \omega_a &= \gamma_a (B_z + \lambda M_z^b) \\ \omega_b &= \gamma_b (B_z + \lambda M_z^a) \end{aligned}$$

Bidirectional interaction

Decoherence rates
(noninteracting)

$$\Gamma_{a,b}$$

$$J = \lambda \sqrt{\gamma_a \gamma_b M_z^a M_z^b}$$

Amplification mechanism with interacting atomic gases

Eigenvalues of the coefficient matrix:

$$\tilde{\omega}_{a,b} + i\tilde{\Gamma}_{a,b} = \omega_0 + i\chi \pm \sqrt{J^2 + \Gamma^2}$$

Dressed decoherence rates

$$\tilde{\Gamma}_b = \chi - \text{Im} \sqrt{J^2 + (\delta + i\beta)^2}$$

$$\begin{aligned}\omega_0 &= (\omega_a + \omega_b)/2, \\ \chi &= (\Gamma_a + \Gamma_b)/2, \\ \Gamma &= \delta + i\beta, \\ \delta &= (\omega_a - \omega_b)/2, \\ \beta &= (\Gamma_a - \Gamma_b)/2.\end{aligned}$$

Steady-state response (Fano profile)

$$F(\varepsilon) = \mathcal{A}(\varepsilon) \frac{(q + \varepsilon)^2}{1 + \varepsilon^2} + \mathcal{B}(\varepsilon)$$

noninterference

interference

alkali \longleftrightarrow noble

$$\varepsilon = \frac{\omega - \tilde{\omega}_b}{\tilde{\Gamma}_b}, \quad \text{Fano parameter} \quad q = \frac{\tilde{\omega}_b - \omega_{ab}}{\tilde{\Gamma}_b} \quad \omega_{ab} = \omega_b + \gamma_b \lambda M_z^b$$

Amplification mechanism with interacting atomic gases

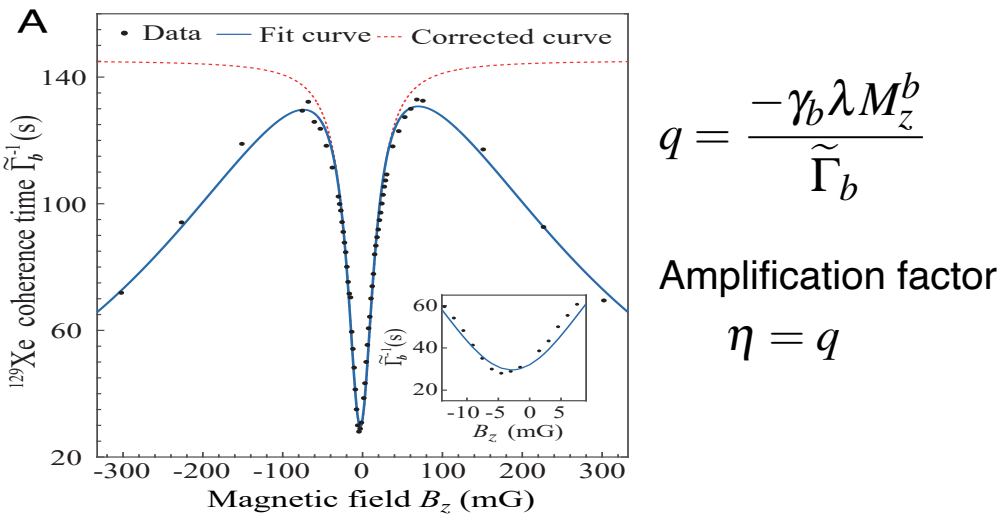
Weak coupling regime

^{87}Rb and ^{129}Xe is $\Gamma_a \approx 30 \text{ kHz}$ and $\Gamma_b \approx 7 \text{ mHz}$

$$J \approx 30 \text{ Hz} \quad J/\beta \approx 6 \times 10^{-3} \ll 1$$

$$\tilde{\omega}_b \approx \omega_b \text{ and } \tilde{\omega}_a \approx \omega_a$$

$$\tilde{\Gamma}_b = \chi - \text{Im} \sqrt{J^2 + (\delta + i\beta)^2}$$



Strong coupling regime

$$J > \beta$$

$$\tilde{\Gamma}_b = \chi \approx \Gamma_a/2$$

Measurement bandwidth to be half that of alkali-metal spins

$$|q| = \frac{\gamma_b \lambda M_z^b + \sqrt{J^2 - \beta^2}}{\tilde{\Gamma}_b}$$

additional amplification

e.g., K-³He system

$$J/\beta \sim 100 \quad (\text{Prediction})$$

Advantage: much broader amplification bandwidths with a suitable amplification factor

Amplification mechanism with interacting atomic gases

Interference destructive

Quantum Suppression

$$\epsilon = -q$$

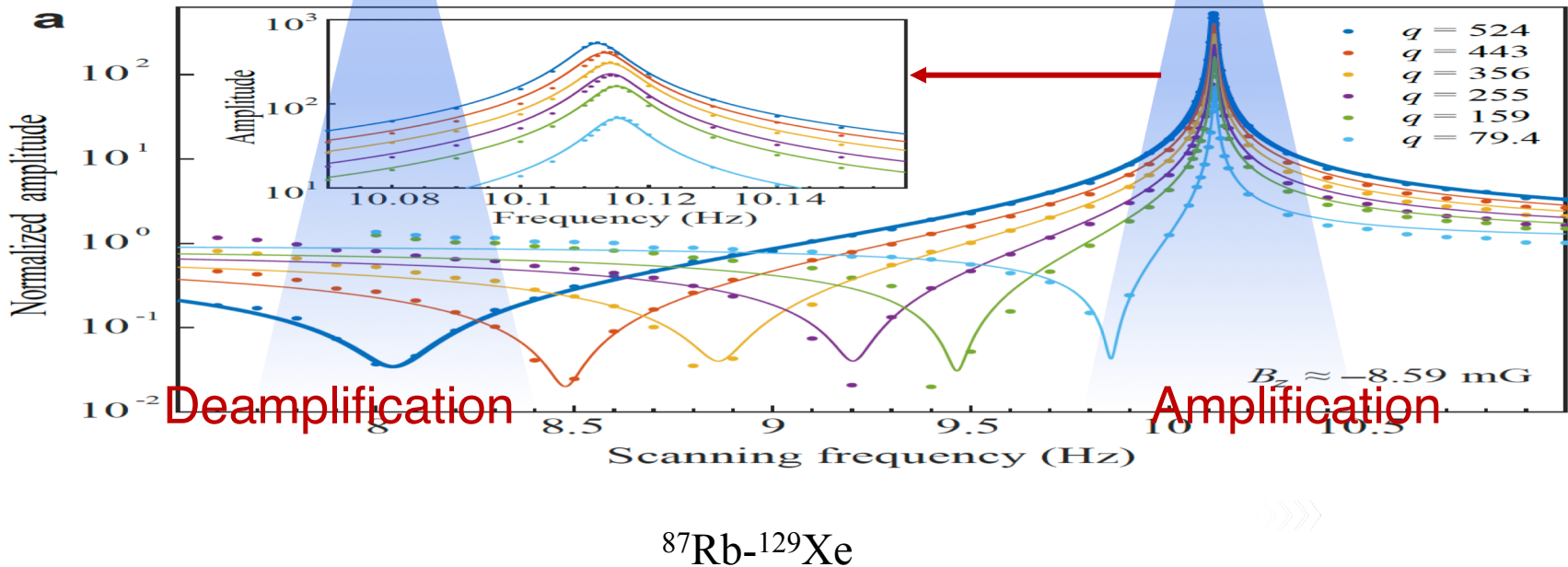
$$F(\epsilon) = \mathcal{A}(\epsilon) \frac{(q + \epsilon)^2}{1 + \epsilon^2} + \mathcal{B}(\epsilon)$$

Fano profile

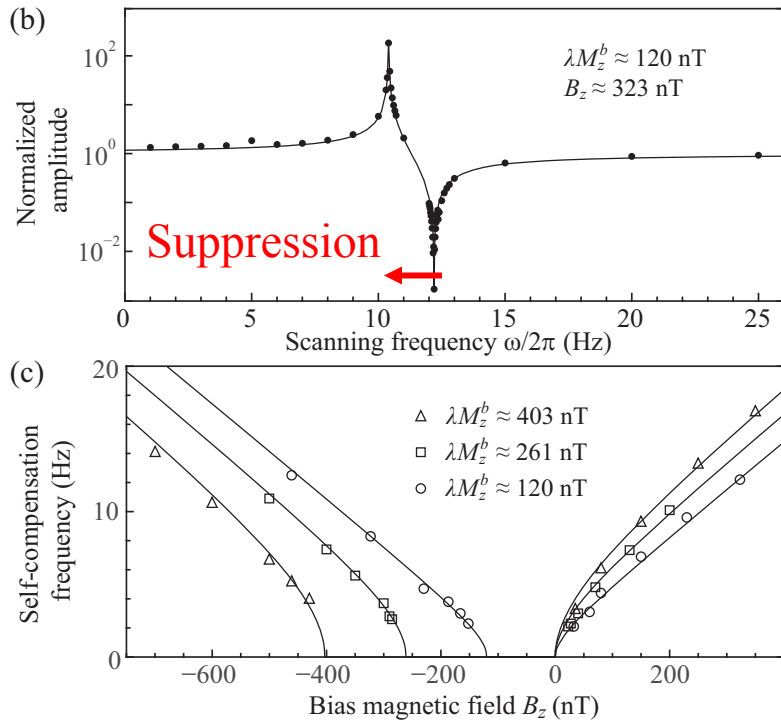
Interference enhancement

Quantum amplification

$$\epsilon = 0$$



Magnetic noise self-compensation effects



◆ K : a
◆ ^3He : b

$$A(\omega) \approx A_0(\omega) \left[\frac{(q + \varepsilon)^2}{1 + \varepsilon^2} \right]^{1/2}$$

Deamplification frequency

$$\omega_F \approx \gamma_b [(B_z + \lambda M_z^a + \lambda M_z^b)(B_z + \lambda M_z^a)]^{1/2}$$

can be adjusted by the bias field B_z

Previous comagnetometer (a special case)
(Phys. Rev. Lett. 89, 253002, 2002)

$$B_z + \lambda M_z^a + \lambda M_z^b = 0$$

$$\omega_F \approx \gamma_b [(B_z + \lambda M_z^a + \lambda M_z^b)(B_z + \lambda M_z^a)]^{1/2} = 0$$

Self-compensation at near-DC (< 1Hz)

Interaction strengths of existing experiments with hybrid atomic gases

$$J = \lambda \sqrt{\gamma_a \gamma_b M_z^a M_z^b}$$

K-³He system: more readily to achieve strong-coupling regime

Spin System	Operation Types	λM_z^a	λM_z^b	$J/2\pi$	$\beta/2\pi$	J/β
K- ³ He (5)	Comagnetometer	24 nT	1094 nT	78 Hz	3.65 Hz	21
K- ³ He (6)	Comagnetometer	14 nT	500 nT	38 Hz	60 Hz	0.64
K- ³ He (3)	Comagnetometer	2 nT	100 nT	6.7 Hz	4 Hz	1.6
K- ³ He (7)	Comagnetometer	1.4 nT ^a	100 nT	5.6 Hz	1.6 Hz	3.5
Rb- ²¹ Ne (8)	Comagnetometer	110.6 nT	579.4 nT	40 Hz	74 Hz	0.54
Rb- ²¹ Ne (9)	Comagnetometer	104 nT ^b	250 nT	25 Hz	80 Hz	0.31
Rb- ¹²⁹ Xe (10)	Comagnetometer	0.33 nT	53 nT	1.2 Hz	37 Hz	3×10^{-2}
Rb- ¹²⁹ Xe (2)	Spin Amplifier	20 nT	200 nT	18 Hz	10 kHz	1.8×10^{-3}
Cs- ¹²⁹ Xe (11)	Comagnetometer	4 nT	340 nT ^c	11 Hz	680 Hz	1.6×10^{-2}
Cs- ¹²⁹ Xe (12)	NMR Gyroscope	18 nT ^d	100 nT	12 Hz	300 Hz	4.0×10^{-2}
Rb- ¹²⁹ Xe	This work	1 nT	300 nT	4.8 Hz	1.6 kHz	6×10^{-3}

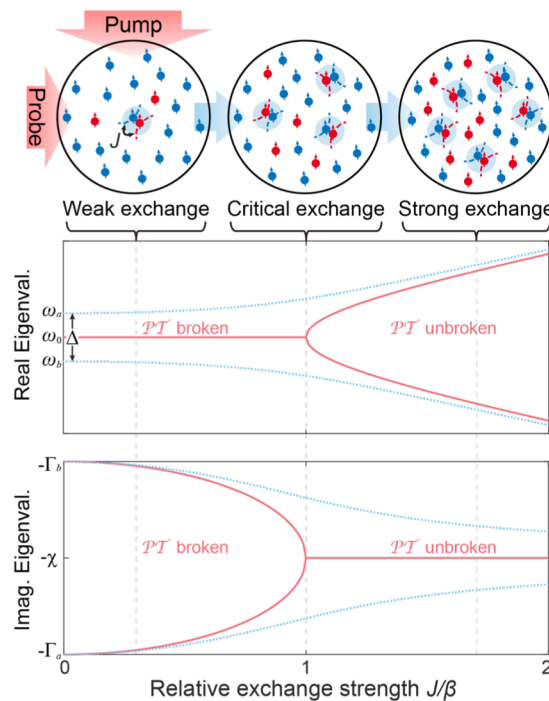
Ongoing experiments for strong coupling regime

Coupling-induced
PT phase transition

K-³He system:

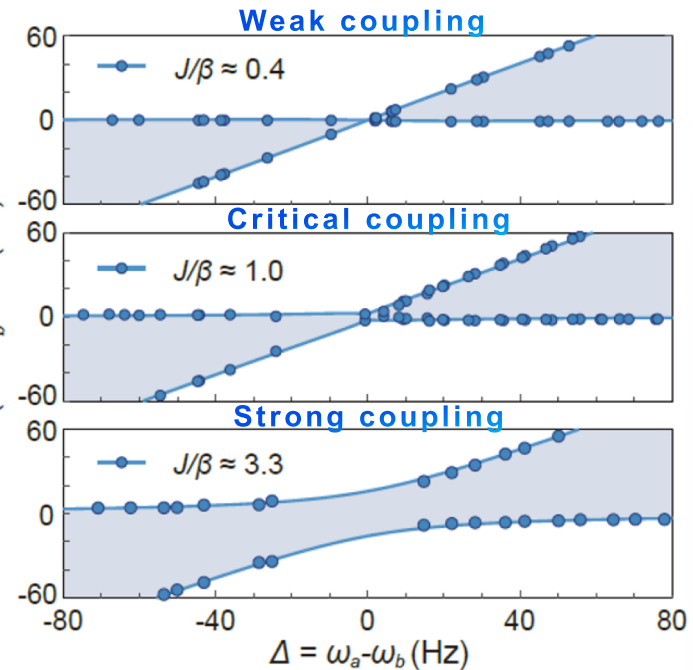
$$\Gamma_a \approx 2\pi \times 10 \sim 40 \text{ Hz},$$

$$\Gamma_b \approx 2\pi \times 0.1 \text{ Hz}$$



Strong coupling : $J > \beta = \frac{\Gamma_a - \Gamma_b}{2}$

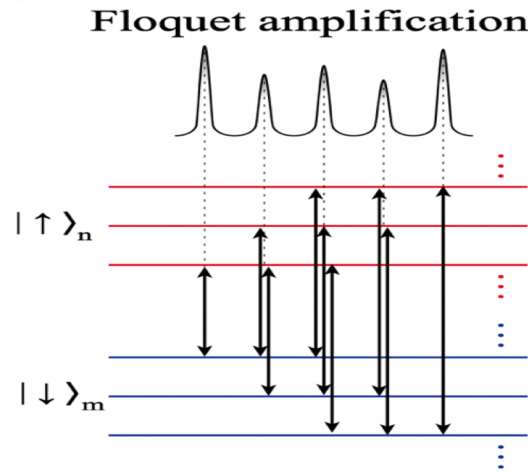
System eigenfrequencies



(submitted)

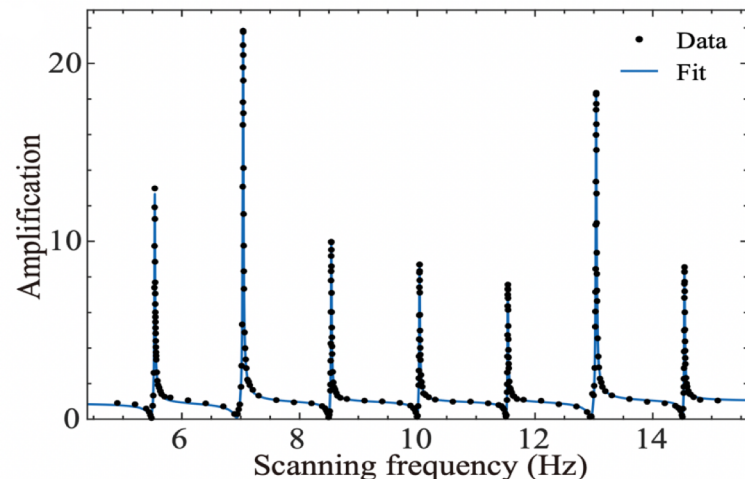
提出自旋放大频梳技术，实现多频段探测

挑战：放大频率带宽有限，仅在共振频率附近才能实现放大



提出 Floquet spin amplification概念，给出理论放大增益

$$\eta_{k,0}(u) = \frac{4\pi}{3} \kappa_0 M^n P_0^n \gamma_n T_{2n} J_k^2(u)$$

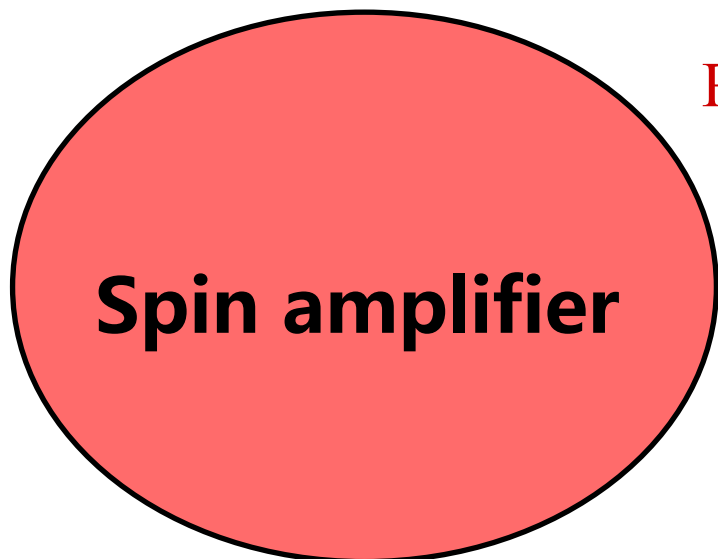


提高放大带宽 ~ 10 倍，均达到 $\text{fT}/\text{Hz}^{1/2}$ 灵敏度

PRL: Editors' suggestion

Noble-gas Masing Effect

Spin amplification combines with a feedback



A feedback mechanism

Radiation Damping

$$T_d/T_{2n} \ll 1$$



Spin Maser

**Coherent spin
oscillations
“Atomic clocks”**

Measurement-feedback spin amplification

Nobel Prize: Maser and atomic clock



C. Townes



G. Basov



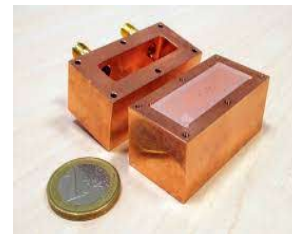
M. Prokhorov



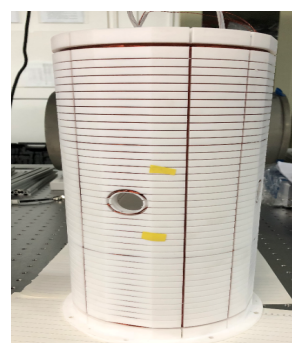
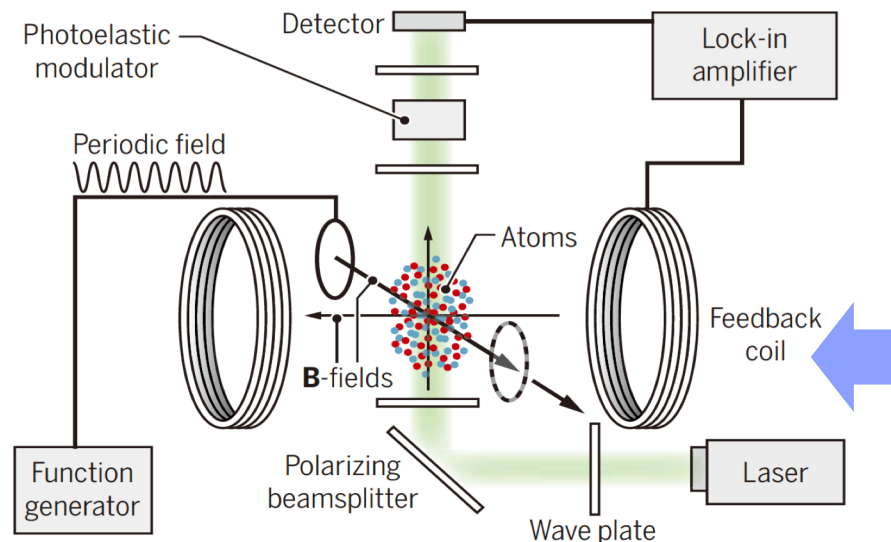
N. F. Ramsey



Optical frequency
(Optical cavity)



Microwave frequency
(Cavity)



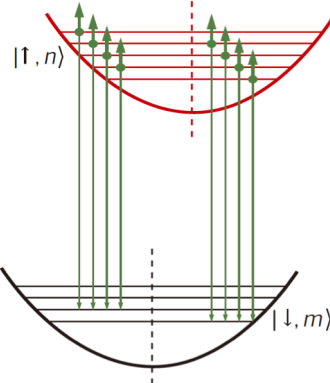
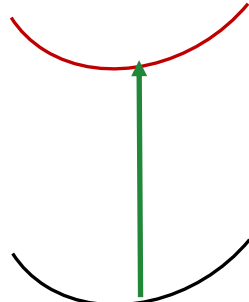
Radio frequency
(feedback Coils)

“Floquet maser”：周期性系统

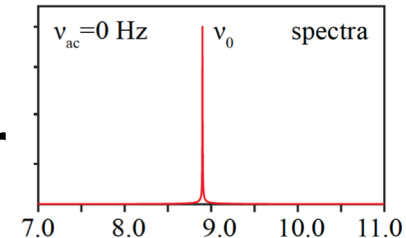


C. Floquet

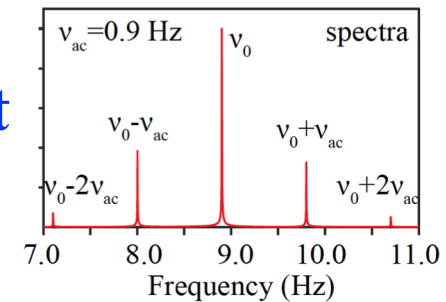
周期性系统可以用
一系列的Floquet
能级表示



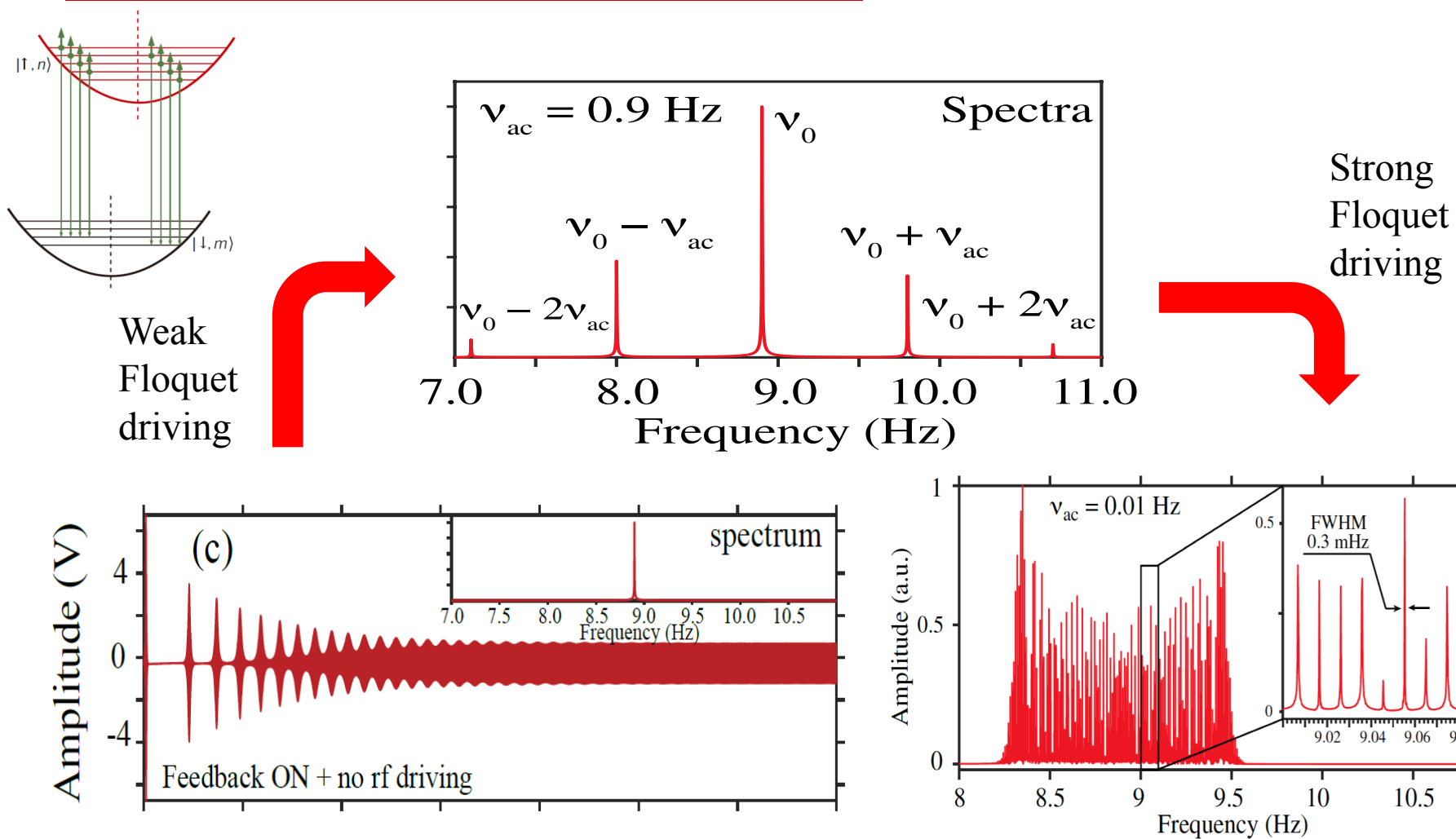
传统
maser



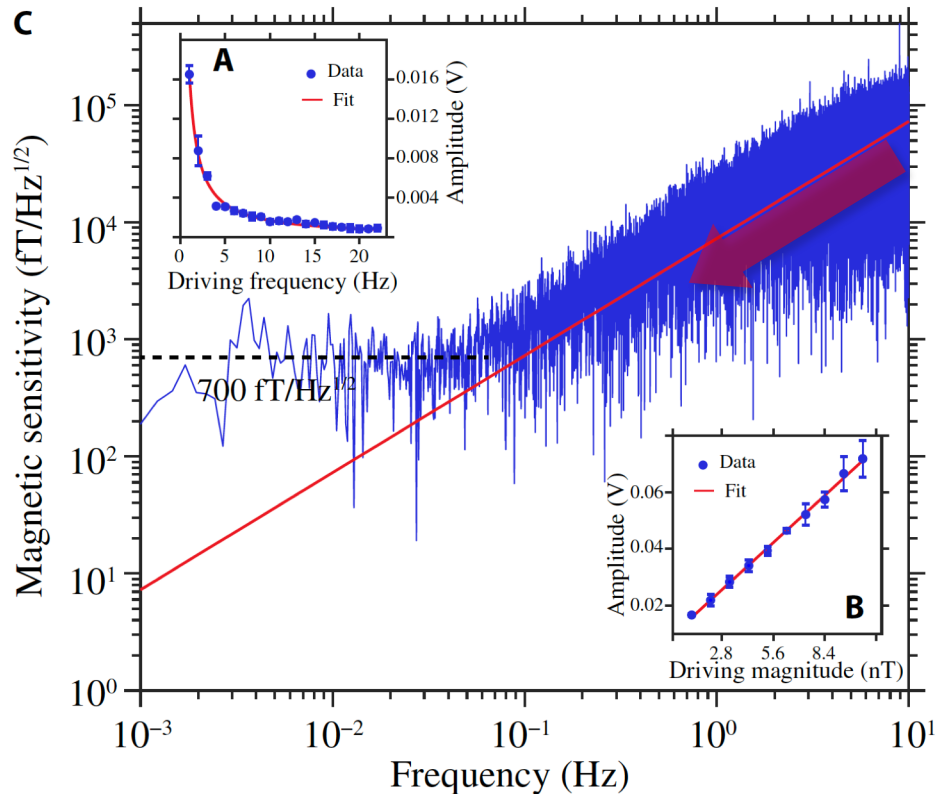
Floquet
maser



Floquet maser : 首次使用Floquet介质作为增益介质

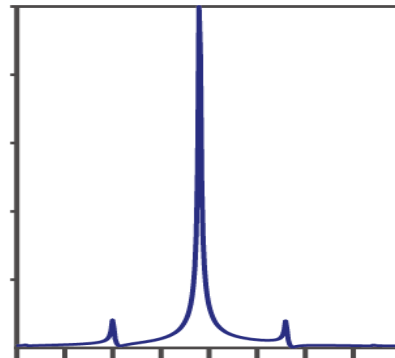


磁场精密测量 (via 量子振荡器) : 超低频率段



世界上最佳的超低频灵敏度 !

$$S_1 \propto J_1\left(\frac{\gamma B_{ac}}{\nu_{ac}}\right) \approx \frac{\gamma}{2\nu_{ac}} B_{ac}$$



边带测磁灵敏度 :

$$\delta B \propto \nu_{ac}$$

突破低频噪声极限和磁
屏蔽约束 !

SHARE



Floquet maser



PHYSICS

Science

A masing ladder

A maser that amplifies emission of periodically modulated quantum states has uses in metrology

By Ren-Bao Liu^{1,2}

《Science》 Perspectives reports:
“... demonstrate a new type of maser... Conceivable applications of this work include precision clocks and detection of ultralight dark matter particles such as axions”

PHYS ORG

Extending maser techniques to Floquet systems

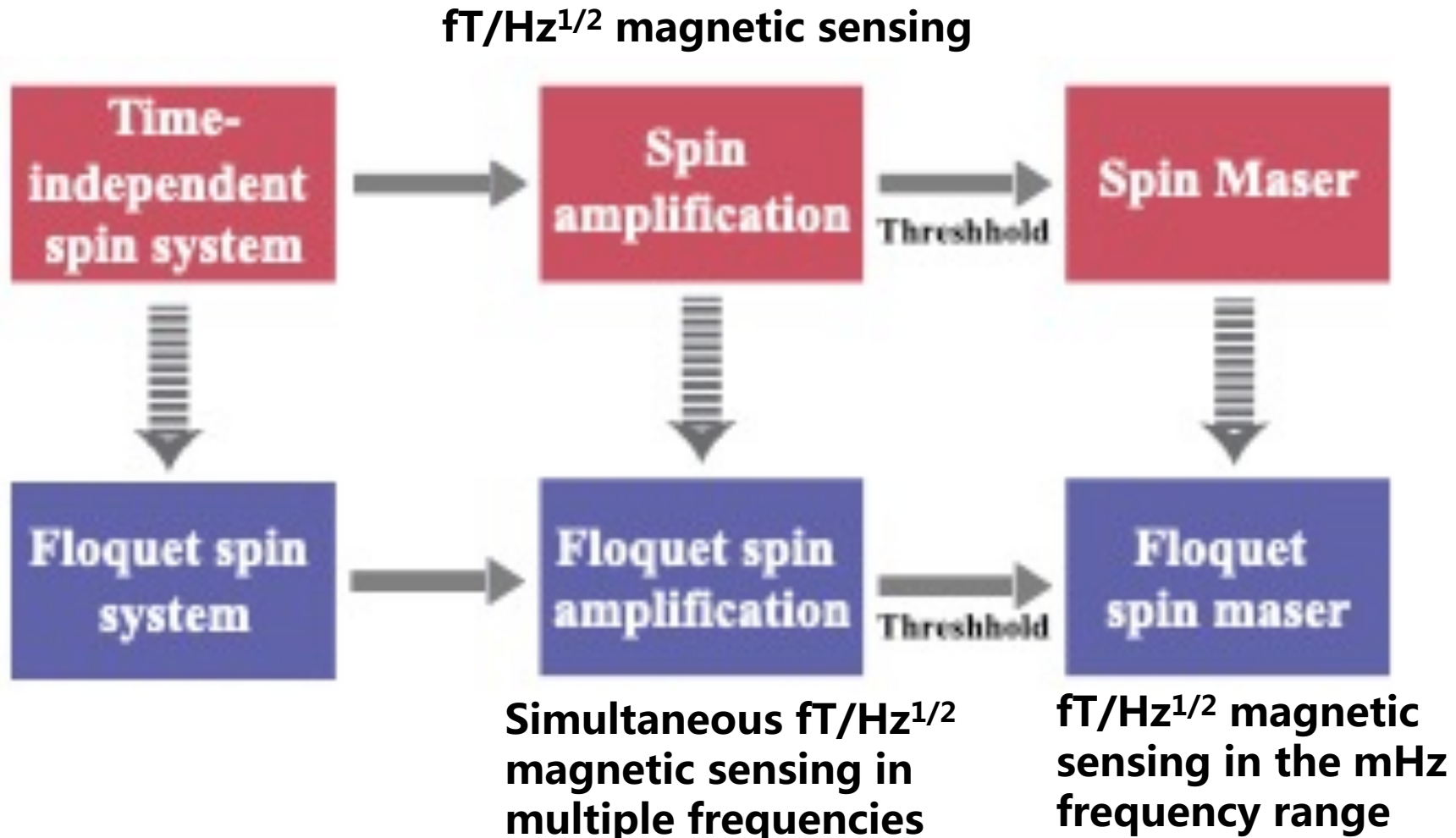
techniques to Floquet systems. In their paper published in the journal *Science Advances*, the group describes their approach to creating a new type of maser by amplifying radio frequencies in Floquet systems. Ren-Bao Liu, with the Chinese

physicsworld

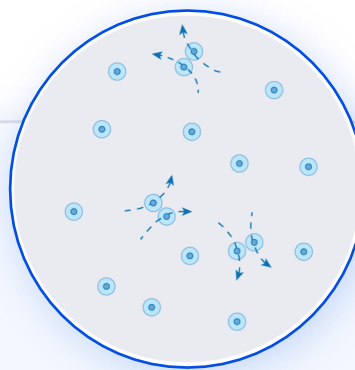
SEARCH UPDATE

New Floquet maser is very good at detecting low frequency magnetic fields

Spin-based amplification



Opportunity: Interaction, Correlation, and Entanglement

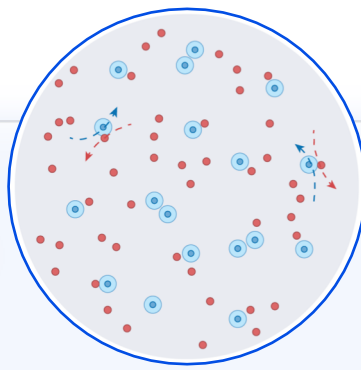


Alkali-metal spin gas

NMOR effect
SERF effect

$$\text{SQL: } 1/\sqrt{N}$$

Noble gas

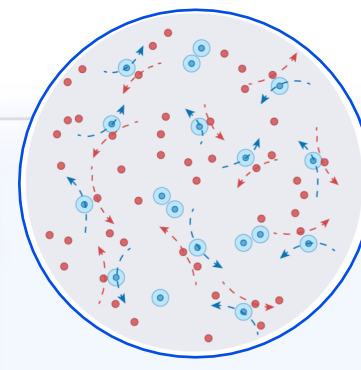


Correlated alkali-noble gas

Nuclear spin amplification
Fano resonance effect

$$\text{SQL: } 1/\sum\sqrt{N}$$

Entanglement



Entangled spin gases

Nuclear spin squeezing
Memory-based sensing

$$\text{Heisenberg Limit: } 1/N$$

测量极限

给定一个物理装置, 对于一个物理可观察量能够得到的测量精度是什么?

测量是一个物理过程, 测量的精度是由物理规律所限定.

标准量子极限 (standard quantum limit): 通过经典的重复测量方法不可突破的极限 $1/\sqrt{N}$

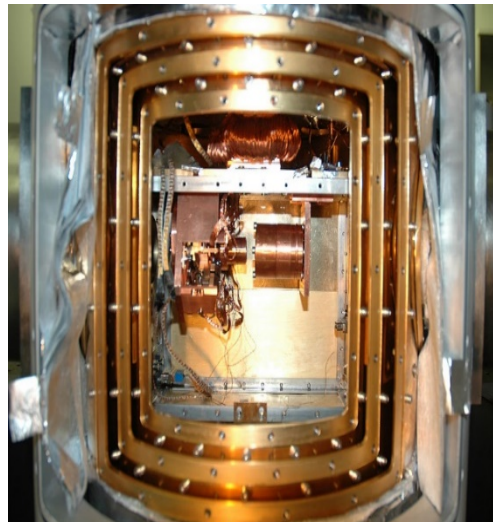
海森堡极限 (Heisenberg limit): 量子力学的基本性质 — 海森堡不确定原理为量子精密测量理论设置了下限 $1/N$, 是量子测量理论中可能实现的最高精度。

超海森堡极限 (Super-Heisenberg Limit): 非线性量子精密测量 (粒子之间的相互作用) 最佳精度能够突破海森堡极限 $1/N$ 。

N 是重复测量的次数

量子精密测量：利用量子力学基本原理

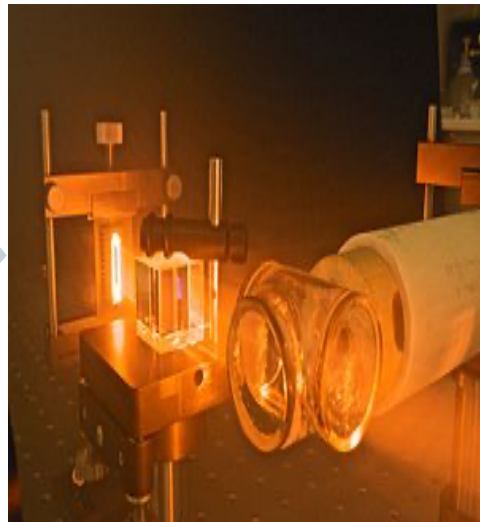
量子体系分立能级



单电子晶体管
光力传感器等

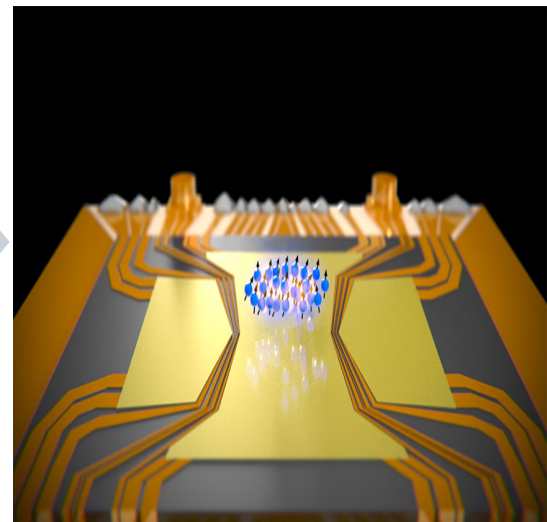
测量精度受限于标准量子极限 $1/\sqrt{N}$

量子相干叠加



原子磁力仪、
金刚石缺陷等

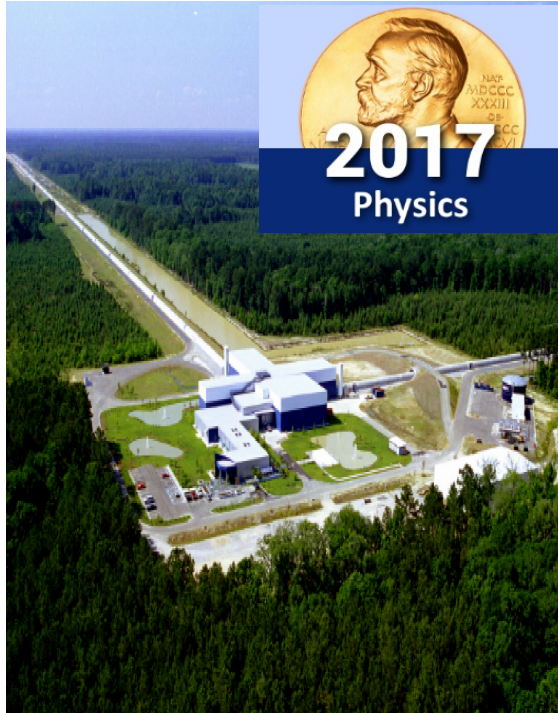
量子纠缠（关联）特性



压缩态、NOON态

有望突破经典物理极限 $1/N$

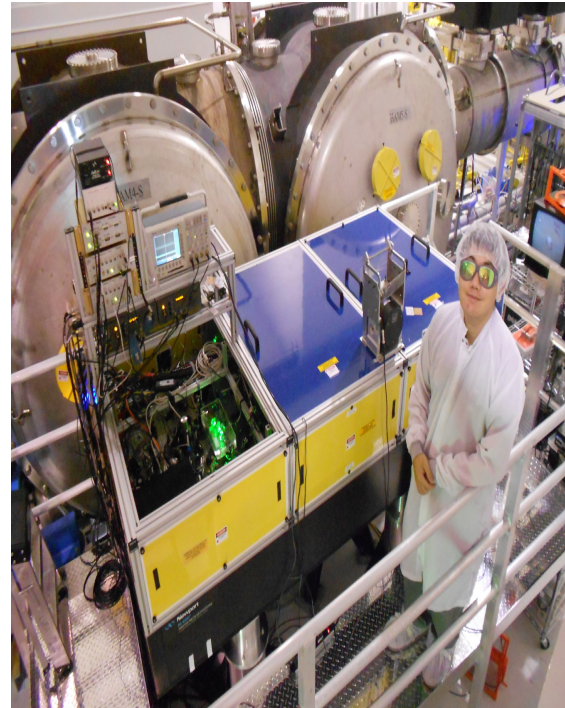
著名案例：引力波探测



2015年4月
LIGO首次直接探测
到引力波

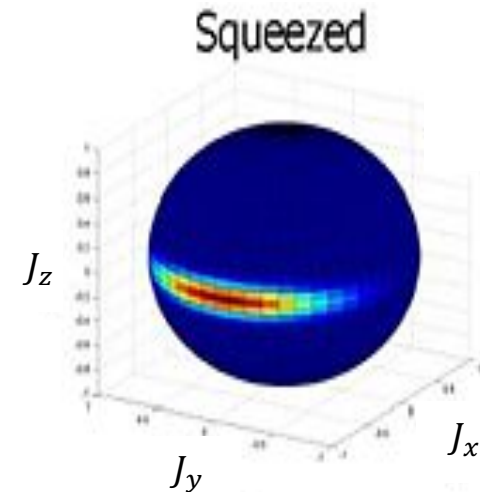
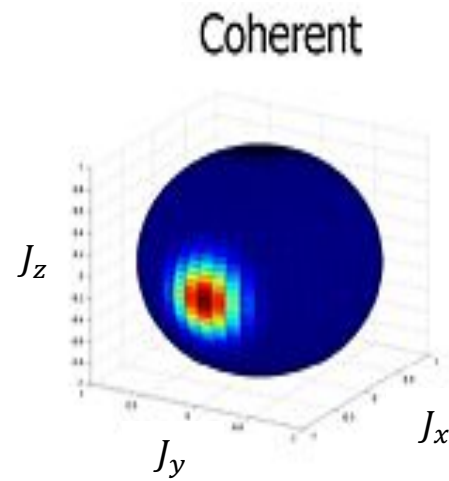


2017年8月
LIGO与VIRGO共同探
测到引力波



2019年4月
利用压缩光降低量子噪声，
引力波探测数增加20%至50%

量子压缩自旋噪声



标准量子极限

海森堡极限

利用光与原子的相互作用，
实现了原子自旋散粒噪声压缩

$$\frac{1}{\sqrt{N_{at}}}$$

$$\frac{1}{N_{at}}$$

利用量子压缩技术有望实现aT级别的灵敏度

基于系统探测的商用自旋磁共振谱仪



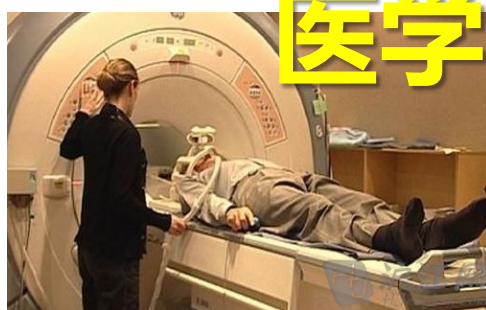
核磁共振谱仪

自旋数
 $10^{17}-10^{10}$

电子顺磁共振谱仪

$10^{12}-10^{10}$

商用磁共振谱仪面向**自旋系统样品**，通过探测自旋系统(大于百亿个自旋)的**空间及时间平均信号**，获取**统计平均**下的物质组成和结构的信息。这一技术已被广泛应用于前沿科学和经济生活的诸多领域，对人类社会产生了意义深远的影响



医学



化学

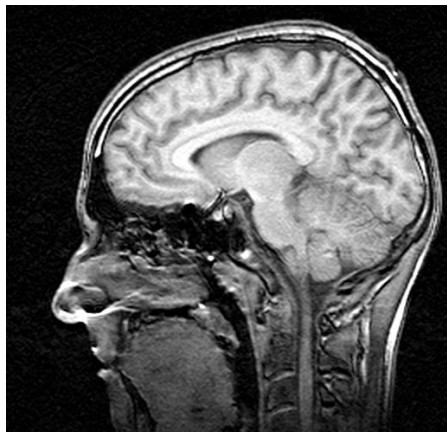


生物



能源

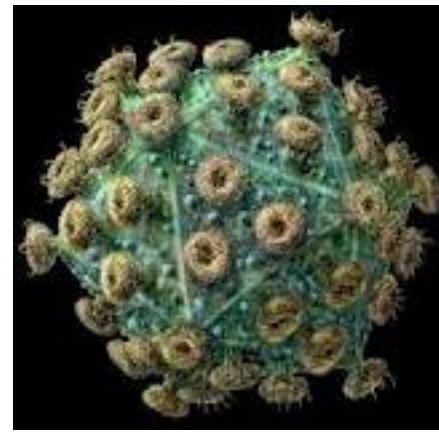
微观尺度磁共振探测



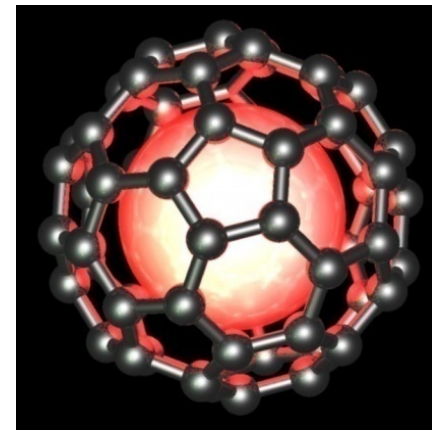
大脑组织轮廓



单个红细胞



单个艾滋病毒



单个富勒烯分子

10毫米

10微米

10纳米

1纳米

看得清

看不清

看不见

手段

传统磁共振 ✓

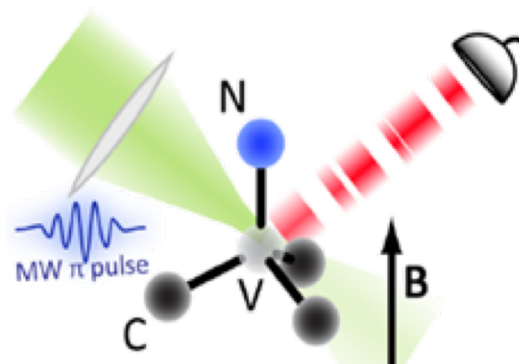
力探测磁共振 ✓

单核自旋探测

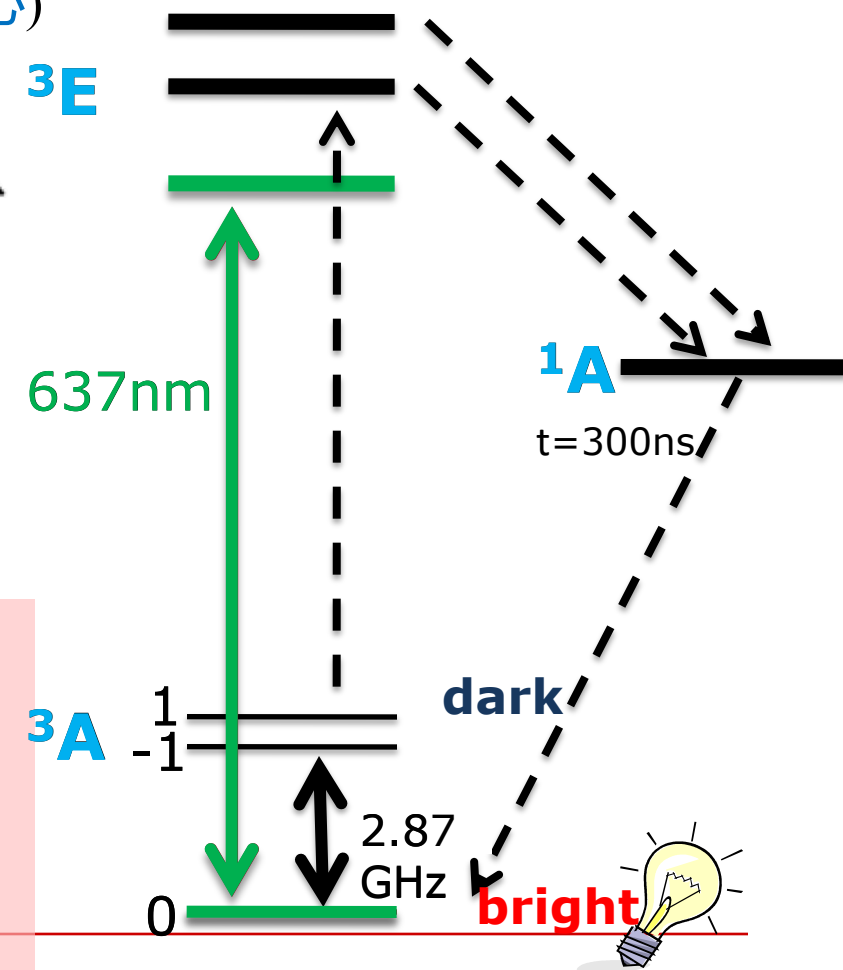
- 现有磁共振**尚不具备**对物质进行微观尺度的**灵敏探测**和**空间分辨**能力
- 在**不破坏研究对象**的前提下提供微观物质**内部三维结构信息**，对于前沿科学领域具有极其重要的意义

氮-空位缺陷中心单自旋

由一个替位的氮(Nitrogen)和一个邻位空位(Vacancy)组成(简称NV色心)



- 原子尺度：高空间分辨率
- 室温下的长量子相干时间结合动力学解耦技术：高灵敏度
- 被测磁信号可转化为自旋量子干涉仪的相位信息，光学手段读出



NV 单自旋量子传感器

$$H = D \cdot S_z^2 + E \cdot (S_x^2 - S_y^2) - \gamma_e B \cdot S + S \cdot \sum_i A_i \cdot I_i$$

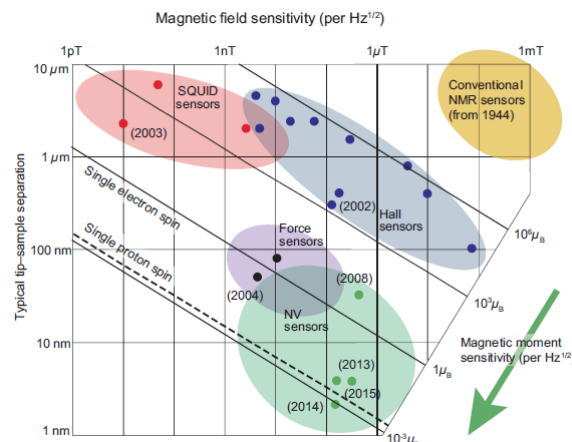
Temperature

Electric-field
stress detection

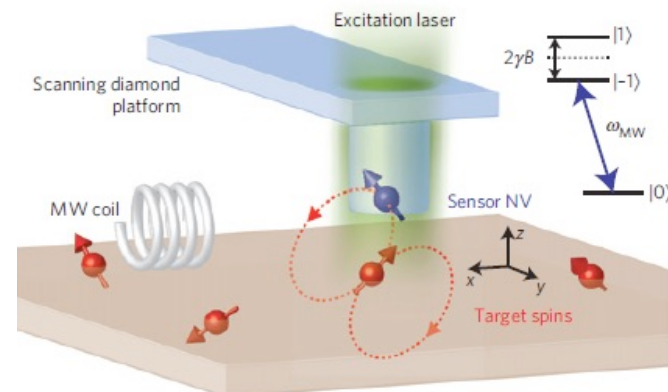
Magnetic
field

Spin-coupling
Spin-sensing

Diamond nanoscale magnetometry

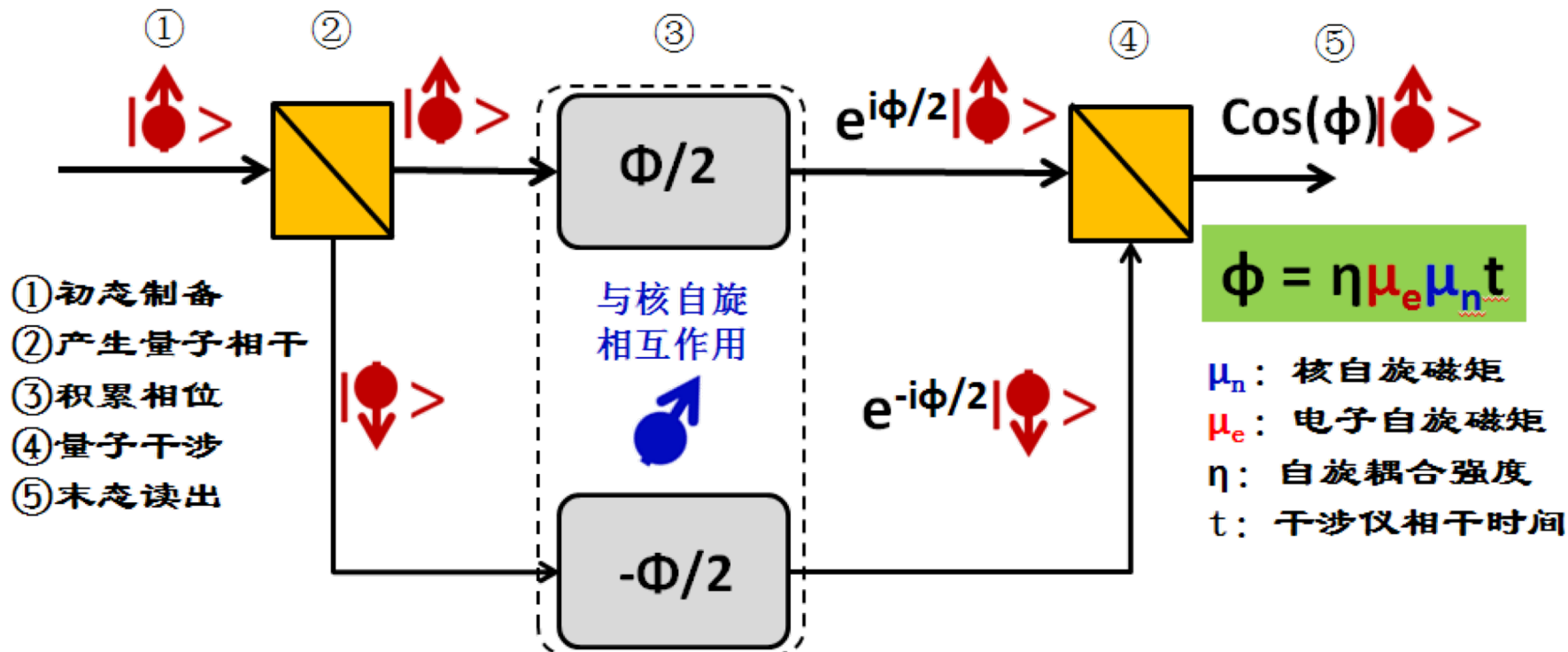


Nat. Nanotechnol. 3, 643(2008)



Nat. Phys. 9, 215 (2013)

NV 单自旋量子干涉仪



将微弱的核自旋信号 μ_n 转化为单电子量子干涉仪的相位信息，利用量子测量加以读出

Sensing using NV center

PROTEIN IMAGING

Single-protein spin resonance spectroscopy under ambient conditions

SCIENCE (2015) 347, 1135

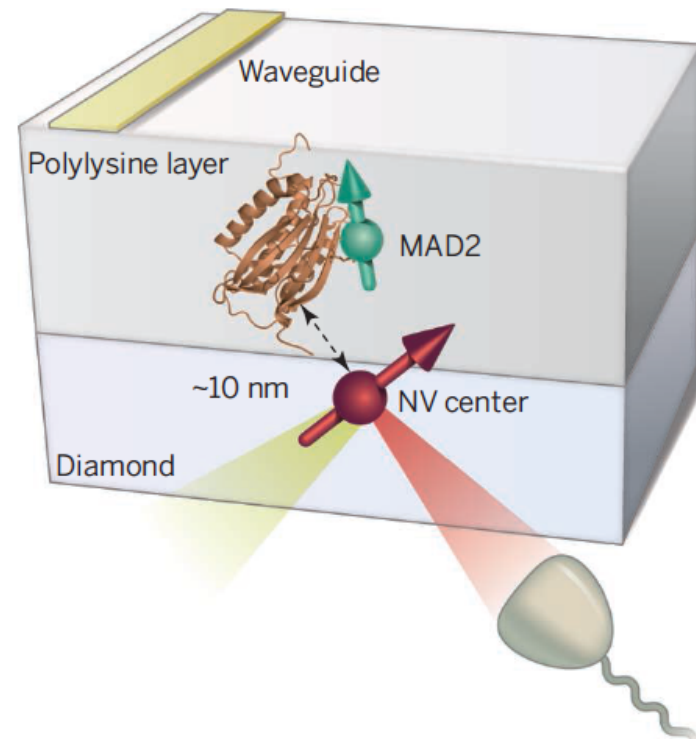
PHYSICS

Single proteins under a diamond spotlight

A diamond nanomagnetometer is used to probe conformational changes of a single protein

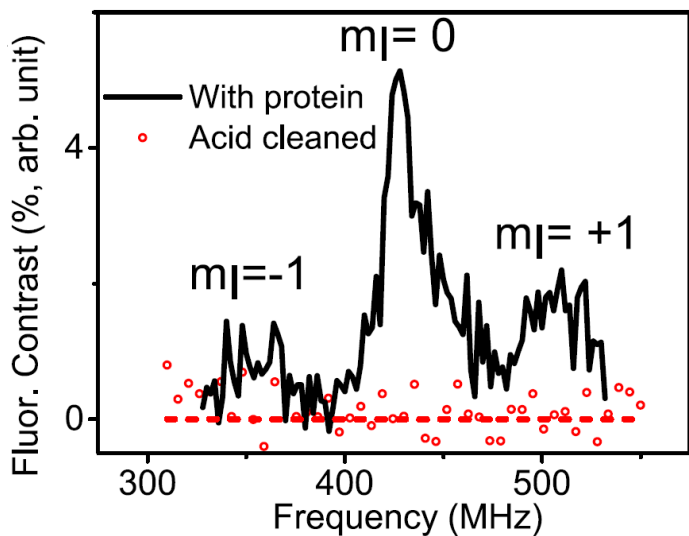
By Philip Hemmer¹ and Carmen Gomes²

| in a virus molecule down to



单蛋白质分子顺磁共振谱

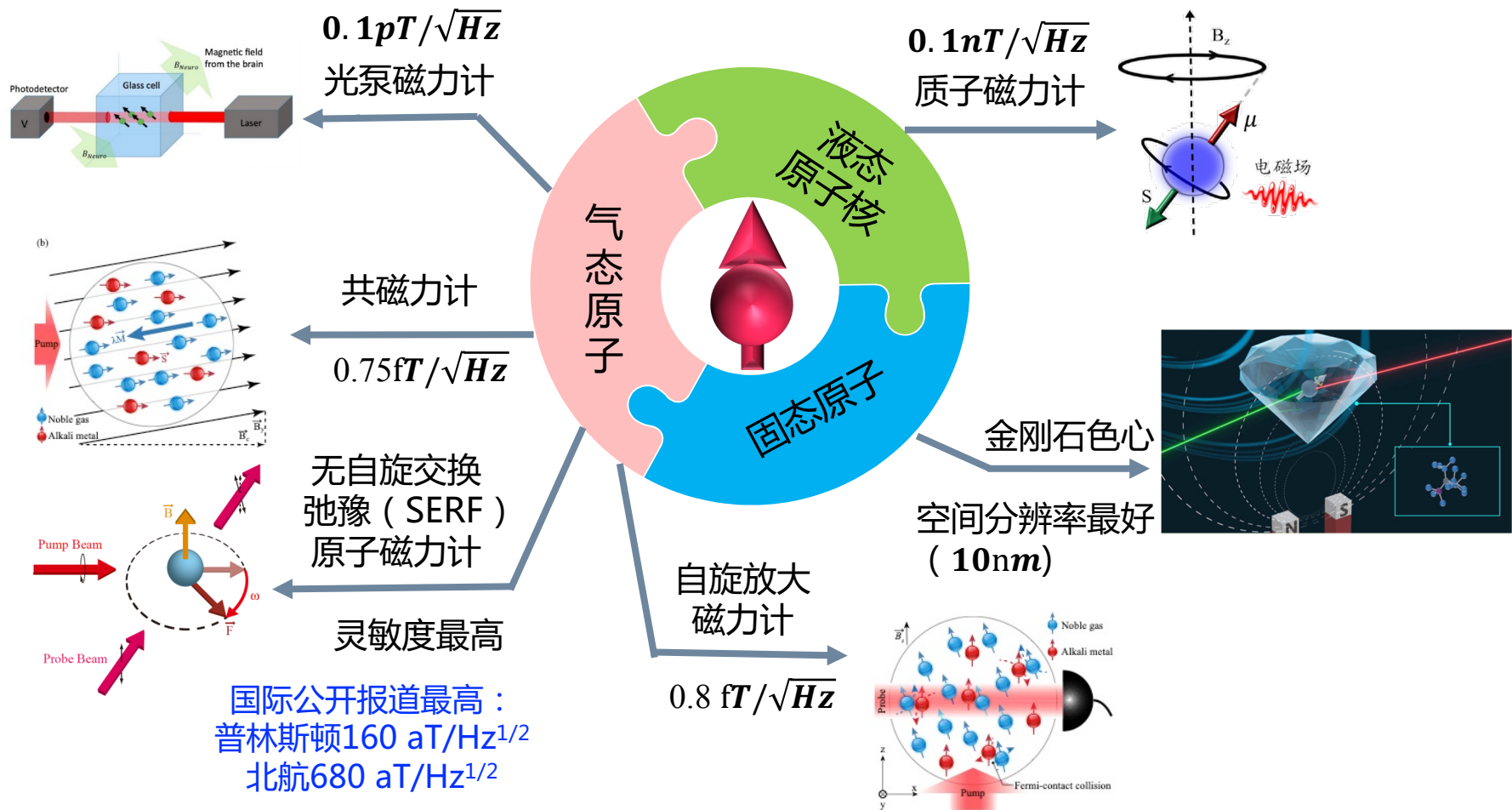
Science 347, 1135 (2015)



单蛋白质分子顺磁共振谱

- 世界上首张单分子顺磁共振谱
- 与传统电子顺磁共振相比
分辨率： 10^{-3} 米 $\rightarrow 10^{-9}$ 米
灵敏度： 10^{10} 分子 \rightarrow 单分子
- 具备室温大气的宽松实验环境，
尤为适合开展活体研究
- 与超高分辨荧光显微技术（2014
年诺贝尔奖）相比，不仅同样能
够提供纳米分辨率的空间定位信
息，还可进一步解析出单个分子
的结构信息和构象变化

原子自旋磁力计



- (1) 为什么需要测量极弱磁场？
- (2) 如何实现高精度的极弱磁场测量？
- (3) 有什么前沿科学应用？

谢 谢 !
